Mechanistic Study on Acid-Catalyzed Novel Rearrangement of Homobenzoquinone Epoxide

2010

Haruyasu Asahara

Department of Applied Chemistry
Graduate School of Engineering
Osaka University

Preface

The studies presented in this thesis have been carried out under the guidance of Professor Takumi Oshima at Osaka University during 2004–2010.

This thesis deals with the acid- and photo-reaction of small-membered ring fused quinone derivatives were focused on the fundamental studies comprised of the following points, (1) remote π-aryl participation reaction of Homobenzoquinone epoxide, (2) a prominent role of oxirane Walsh orbital, (3) rearrangement reaction of cyclobutane-fused quinone. The author hopes that this basic work described in this thesis contributes to the further development of synthesis of novel carbon skeletons, which are difficult to produce by conventional methods.

Haruyasu Asahara

Department of Applied Chemistry

Graduate School of Engineering

Osaka University

Suita, Osaka

Japan

March, 2010

Contents

General Introduction

Possessing both reactive carbonyl and olefinic bonds, quinones are powerful intermediate in organic synthesis. Consequently, quinones undergo various nucleophilic addition and cycloaddition such as Diels-Alder reaction, [2+2] photocycloaddition or addition of 1,3-dipoles (Scheme 1). Especially, the cycloaddition reaction of quinones has been the subject of extensive investigations largely,[1] due to simple reaction mechanism and the potential offered by such reactions in natural products syntheses.[2] Actually, product quinones having fused polycyclic ring systems are known as a structure component in important natural products that undergo a number of biochemical transformations [1,3,4] and the studies of their synthesis and the reactivities of these compounds have interested many organic chemists.[5]

Scheme 1. Examples of the reaction of quinone

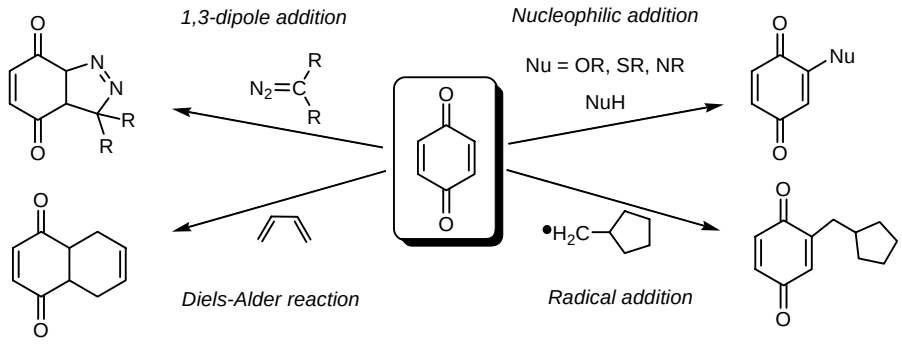

In spite of their numerous kinds and complexities, the rearrangement reaction in organic chemistry can be broken down into relatively simple steps. The chemistry of small ring compounds is replete with examples of rearrangement. The relief of ring strain is a powerful driving force in assisting ring opening and ring expansions in three- or four-membered rings under conditions where large ring compounds or aliphatic analogs retain their original carbon skeletons intact. In fact, many potential applications of cyclopropane as useful building blocks have been predicted based on regio- and stereo-controlled ring-opening reactions.[6] On the

other hand, the acid-catalyzed ring-opening reactions of epoxides have attracted a continuous interest from the synthetic and mechanistic viewpoints (Scheme 2).[7] These reactions are

Scheme 2. Examples of the reaction of epoxide

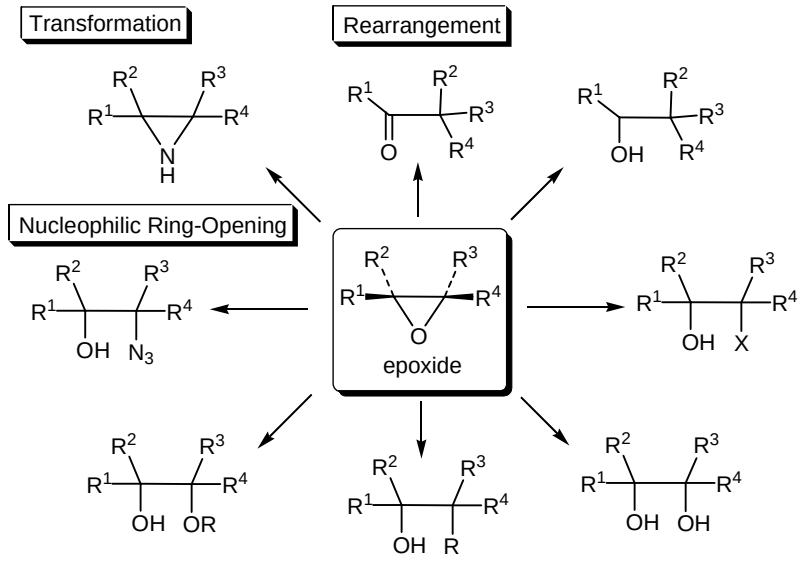

generally proceed through the regio- and stereoselective ring cleavage via a S_N2-type anti nucleophilic displacements.[8] These stereochemical features are much affected by the steric environments in the oxirane ring. Despite numerous investigations into the mechanistic aspects, a possible role of the characteristic oxirane Walsh orbital in the anti-nucleophilic ring cleavage of epoxides remains to be elucidated.

The many reviews devote only insignificant space to the interaction of small-membered ring and neighboring group. Even in the relatively well-documented field of keto-epoxides definite correlations have not been established between substrate structure, reagent, and the conditions and direction of reactions: several views are held on the mechanism which best describes such reactions.[7(a), 9] It may be said *a priori* that the direction of ring-opening will be determined by the concerted (or competing) influence of the nature of the small-membered ring, the neighboring group, and their relative arrangement (interaction). However, to determine the role of each of these factors in studying conformationally labile systems is an almost hopeless task. In fact, the nature of the electronic interactions between

three-membered ring (epoxy or cyclopropyl) and neighboring carbonyl group is usually described as conjugation resulting from orbital overlap of bent orbitals of the ring and a *p*-orbital of the carbonyl group.[10] In these systems, the maximum overlap is achieved with the planes of carbonyl group and three-membered ring parallel and the keto-group on a bisector of the ring.[11]

In the light of these situations, the author attempted to introduce the three- or four membered rings and epoxide into the quinones and investigated the acid- and photo-induced reaction of them (Figure 1). It is expected that such conformationally rigid bi- or tricyclic

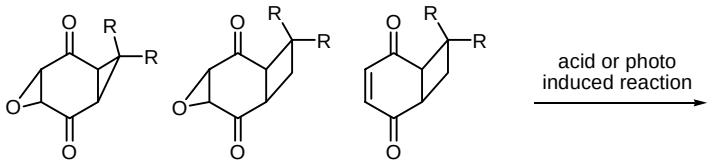

R = alkyl, aryl

Figure 1. Examples of small-membered ring-fused quinone derivatives

compounds provide insights about orbital interaction on the rearrangement reactions of small-membered ring-fused polycyclic compounds and have potential of application for regio- or stereo-controlled reactions. Furthermore, it is also anticipated that these compounds give the knowledge of very rare remote neighboring group participation in the ring-opening due to the spatial proximity between the vacant bent orbitals of small-membered ring and *p*-orbitals of remote neighboring group.

The studies in the present thesis are concerted with the development of the rearrangement reaction of small-membered ring-fused quinone derivatives. In addition, pioneering works for the revealing the mechanism of the reaction and the role of orbital interaction between small-membered ring and neighboring groups, are described. This thesis consists of general introduction, four chapters and conclusion.

In Chapter 1, is described mechanism of π-aryl participated acid-catalyzed rearrangement reaction of Homobenzoquinone epoxide (HQ-Epoxide) and a prominent role of oxirane Walsh orbital. Especially, is focused on the kinetic solvent effects on the reaction, conformational effects of ethano-bridged compound and dual pathway reaction of disubstituted HQ-Epoxide.

In Chapter 2, is described kinetic evidence for remote π-aryl participation in the reaction and η^2-type participated transition state. Kinetic substiuents effects of the acid-catalyzed reaction of HQ-Epoxide were compared with those of the analogous reaction of cyclobutene-fused homobenzoquinone. And it was found that the reaction of HQ-Epoxide exhibit the η^2 π-aryl participation with more effective contribution at the *ipso*-position.

In Chapter 3, is described the consecutive reaction of HQ-Epoxide and the rearrangement reaction of cyclobutane-fused quinone epoxides. It was found that the subsequent ring-enlargement by 1,2-migration associated with the incorporated cyclopropane ring-opening, depending on the substituent pattern and cyclobutane-fused quinone epoxide underwent the novel skeletal rearrangement.

In Chapter 4, is described the intramolecular [2+2] photocycloaddition reaction of cyclobutane-fused quinones. Cyclobutane-fused quinone underwent the intramolecular [2+2] photocycloaddition to provide the novel cage compound which has very rare diagonal conjunction of two facing cyclobutane rings.

Reference and Notes

(1) *The Chemistry of the Quinonoid Compounds, Vol. 2, Parts 1and 2*; Patai, S., Rappoport, Z., Eds.; Wiley: New York, 1988.

(2) Curruthers, W. *Cycloaddition reactions in organic synthesis,* Pergamon: New York, **1990**.

(3) (a) Thomson,R. H. In *Naturally Occurring Quinones IV*; Blackie Academic: London,1997.

(b) Lenaz, G.; Genova, M. L. *Encycl. of Biol. Chem.***2004**, *3*, 621. (c) Babula, P.; Mikelova, R.; Kizek, R.; Havel, L.; Sladky,Z. *Ceska SloVens. Farm.* **2006**, *55*, 151.

(4) For recent reviews, see: (a) Koyama, J. *Recent Patents Anti-Infect. Drug. Disco*V. **2006**, *1*, 113. (b) Babula, P.; Adam, V.; Havel, L.; Kizek, R. *Ceska Slo*V*ens. Farm.* **2007**, *56*, 114. (c) Verma, R. P. *Anti-Cancer Agents Med. Chem.* **2006**, *6*, 489.

(5) Bishop, K. J. M.; Klajn, R.; Grzybowski, B. A. *Angew. Chem., Int. Ed.* **2006**, *45*, 5348.

(6) (a) Walborsky, H. M.; Pendleton, J. F. *J. Am. Chem. Soc.* **1960**, *82*, 1405–1410. (b) Backvall, J. E.; Bjorkman, E. V.; Petterson, L.; Siegbahn, P.; Strich, A. *J. Am. Chem. Soc*. **1985**, *107*, 7408–7412. (c) Gibson, D. H.; De Puy, C. H. *Chem. Rev*. **1974**, *74*, 605–623. (d) Battiste, M. A.; Coxon, J. M. *The Chemistry of the Cyclopropyl Group*; Rappoport, Z. Ed.; Wiley & Sons, Chichester, 1987.

(7) (a) Parker, R. E.; Isaacs, N. S. *Chem. Rev*. **1959**, *59*, 737–799. (b) Rickborn, B. In *Comprehensive Organic Synthesis*; Trost, B. M., Ed.; Pergamon Press: Oxford, U. K., 1991; Vol. 3, p 733. (c) Fujita, H.; Yoshida, Y.; Kita, Y. *Yuki Gosei Kagaku Kyokaishi* **2003**, *61*, 133–143. (d) Giner, J.-L.; Li, X.; Mullins, J. J. *J. Org. Chem*. **2003**, *68*, 10079–10086.

(8) (a) Posner, G. H.; Rogers, D. Z. *J. Am. Chem. Soc*. **1977**, *99*, 8214–8218. (b) Bellucci, G.; Berti, G.; Ingrosso, G.; Mastrorilli, E. *J. Org. Chem*. **1980**, *45*, 299–303. (c) Nugent, W. A. *J. Am. Chem. Soc*. **1992**, *114*, 2768–2769. (d) Jacobsen, E. N. *Acc. Chem. Res*. **2000**, *33*, 421–431. (e) Schaus, S. E.; Jacobsen, E. N. *Org. Lett*. **2000**, *2*, 1001–1004. (f) Brandes, B. D.; Jacobsen, E. N. *Synlett*, **2001**, 1013–1015. (g) Schneider, C. *Synthesis*, **2006**, 3919–3944. (h) Hirai, A.; Tonooka, T.; Tanino, K.; Miyashita, M. *Chirality*, **2003**, *15*, 108–109.

(9) Dewar, M. J. S.; Ford, G. P. *J. Am. Chem. Soc*. **1979**, *101*, 783–791.

(10) Padawa, A.; Hamilton, L.; Norling, L. *J. Org. Chem.* **1966**, *31*, 1244–1248.

(11) Kamernitskii, A. V.; Turuta, A. M. *Russ. Chem. Rev.* **1982**, *9*, 872–886.

Chapter 1. Acid-Catalyzed Reaction of Homobenzoquinone Epoxide (HQ-Epoxide): A Prominent Role of Oxirane Walsh orbital

1-1. Introduction

The acid-catalyzed ring-opening reactions of epoxides have attracted a continuous interest from the synthetic and mechanistic viewpoints.[1] These reactions are generally proceeded through the regio- and stereoselective ring cleavage via a S_N2-type anti nucleophilic displacements.[2] These stereochemical features are much affected by the steric environments in the oxirane ring. Despite numerous investigations into the mechanistic aspects, a possible role of the characteristic oxirane Walsh orbital in the anti-nucleophilic ring cleavage of epoxides remains to be elucidated.

In order to clarify such an orbital interaction, the author has investigated the neighboring group participation which will affect the reactivity by way of the geometrically controlled through space electronic interactions with the incipient cation center (or the vacant orbital).[3] In particular, π-aryl participation is commonly recognized in the organic reactions of compounds possessing the aromatic nucleus (or nuclei) adjacent to or in the topological neighborhood, promoting reaction via a rate-determining aryl-assisted transition state.[4] In an aim of developing the new application of homobenzoquinones and revealing the the geometrical features of orbital interaction with the oxirane Walsh orbital in the transition state, the author synthesized the variously aryl-substituted homobenzoquinone epoxides **1a**-**g** and investigated the acid-catalyzed reactions (Scheme 1).

In this chapter, the author wish to describe the following three points, (1) kinetic solvent effects on the reaction of HQ-Epoxide, (2) the conformational effects of reaction of 10,11-dihydro-5*H*-dibenzo[*a*,*d*]cycloheptene spiro-linked homobenzoquinone epoxide, (3) dual pathway acid-catalyzed rearrangement reactions of disubstituted HQ-Epoxides.

Scheme 1.

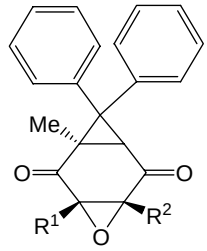

1a: R^1=H; R^2=Me
1b: R^1=Me; R^2=H

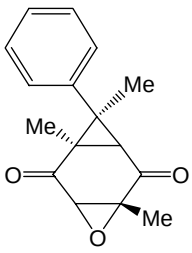

1c

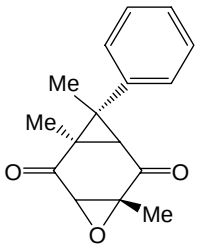

1d

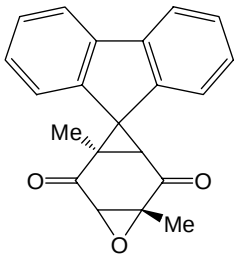

1e

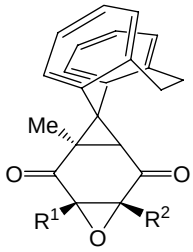

α–**1f**: R^1=H; R^2=Me
α–**1g**: R^1=Me; R^2=H

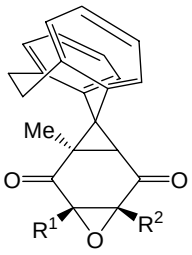

β–**1f**: R^1=H; R^2=Me
β–**1g**: R^1=Me; R^2=H

1-2. Results and Discussion

1-2-1. Conformers of Ethano-Bridged Homobenzoquinone Epoxide

Recently, 10,11-dihydro-5*H*-dibenzo[*a*,*d*]cycloheptene and its derivatives have received considerable pharmacological attention in view of a suitable subunit for drug-receptor concave-convex interaction.[5] In our previous paper, the author has reported that the reaction of 5-diazo-10,11-dihydro-5*H*-dibenzo[*a*,*d*]cycloheptene and 2,5-dimethyl-1,4-benzoquinone gave the corresponding spirohomobenzoquinone (α-**2a**) via the conformationally locked nitrogen release of the primary adduct pyrazolines.[6] The compound (α-**2a**) was found to turn out to be the more stable conformer (β-**2a**) at 100 ^{o}C by way of a complete one-way conformational inversion of the spiro-linked 10,11-dihydro-5*H* -dibenzo[*a*,*d*]cycloheptene moiety.[7] The author also found that the epoxidation of conformers (α-**2a**) and (β-**2a**) proceeded without any conformational inversion to give the corresponding epoxides (α-**1f**) and (β-**1f**), respectively (Scheme 2), but that thermal equilibration was attained at 100 ^{o}C in $CDCl_3$ with a preference for (β-**1f**) (96%, by ^{1}H NMR).

Scheme 2.

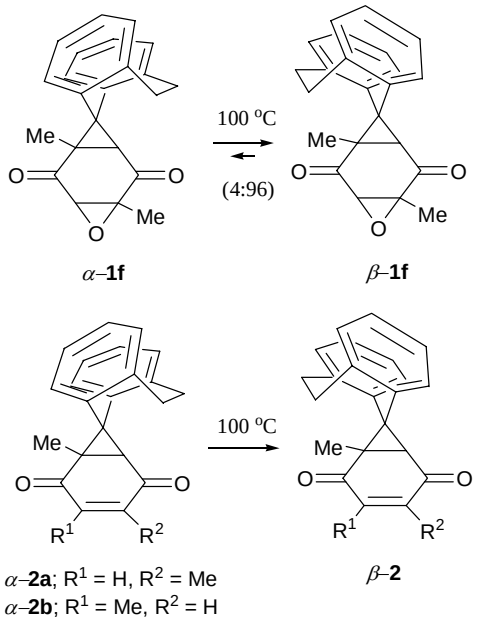

α–**1f** β–**1f**

α–**2a**; R^1 = H, R^2 = Me
α–**2b**; R^1 = Me, R^2 = H

β–**2**

As shown in Fig. 1(a), the dibenzo-fused cycloheptene ring in (α-**1f**) adopts a fairly twisted boat conformation, folding opposite to the cyclopropane Me-substituent in analogy with (α-**2a**), but the dihedral angle [θ = 33.1 (4)^o] of the –CH_2-CH_2– bridge and the intramolecular bond angle (ω = 108.9^o) centered at the spiro-carbon are slightly larger than those of the corresponding (α-**2a**) (27.3 and 107.8^o) (Table 1). For comparison, the author also listed the reference crystalline values of θ and ω (57.9 and 114.6^o) for the least strained pristine 10,11-dihydro-5*H*-dibenzo[*a*,*d*]cycloheptene[8] (**3**) together with the differential dihedral angles ($\Delta\theta = \theta_c - \theta_x$), in which θ_c and θ_x are the angles for (**3**) and the given conformer, respectively. On the other hand, as shown in Fig. 1(b), the conformationally inverted (β-**1f**) takes a more highly twisted boat conformation with θ = 63.6^o and ω = 113^o as compared with the corresponding (β-**2**) (55.5 and 111.3^o). It was also found that the ω is well

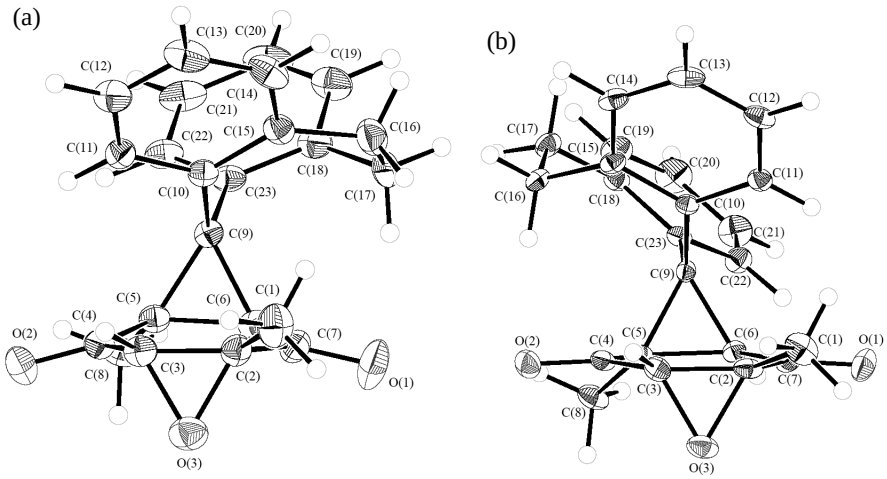

Figure 1. The molecular structures of (a) isomer (α–**1f**) and (b) isomer (β–**1f**), with the atomic numbering scheme. Displacement ellipsoids are plotted at the 35% probability level. H atoms are drawn as spheres of arbitrary radii.

correlated with the θ probably because of the constrained dibenzo-fusion; i.e., $\omega = 0.133\theta + 104$ ($n = 4$, $R = 0.99$).

Table 1. Conformational parameters of the 10,11-dihydro-5*H*-dibenzo [a,d]cycloheptene rings of crystalline (α–**2a**), (β–**2a**), (α–**1f**), (β–**1f**) as well as the reference (**3**).

Compound	θ [a] ($\Delta\theta$) [b]	ω [c]
α–**2a**	27.3 (30.6)	107.8
β–**2a**	55.5 (2.4)	111.3
α–**1f**	33.1 (24.8)	108.9
β–**1f**	63.6 (-5.7)	113.0
3	57.9 (0)	114.6

[a] Dihedral angles (°) of $-CH_2-CH_2-$briedge. [b] Values in parentheses are the differential dihedral angles $\Delta\theta$ (= $\theta_c - \theta_x$)

Assuming that the $\Delta\theta$ is a measure of the strain energy of the spiro-linked seven-membered ring, it seems that the stability difference between the epoxides (α-**1f**) and (β-**1f**) is smaller than that between (α-**2a**) and (β-**2a**). This thermodynamical consideration is consistent with the observation that the conformers (α-**1f**) and (β-**1f**) were equilibrated in preference of the latter (96%), though the parent (α-**2a**) exhibited the one-way isomerization to (β-**2a**).

A perusal of the X-ray structure of (α-**1f**) indicates that the several atoms of the dibenzo-fused seven-membered ring occupy the crowded positions almost touching the underlying quinone component as represented by the very short spatial distances; i.e., C(8)···H(20) (2.72 Å), O(1)···H(16) (2.75), and O(1)···H(14) (2.87). These unfavorable non-bonding interactions may be taken as a driving force for the conformational isomerization. However, such a van der Waals contact was also observed for the stable (β-**1f**), in particular, between the ethano-bridge hydrogen atom H(14) and the facing carbonyl oxygen atom O(2) [2.44 Å], appreciably raising the strain energy of (β-**1f**).

With respect to the structure of quinone frame, (β-**1f**) is specially characterized by the almost planar plane as represented by the dihedral angles of 177.8 and -176.1° for the bond linkages of O(2)-C(4)-C(3)-C(2) and O(1)-C(7)-C(2)-C(3), respectively, whereas the others conformers (α-**2a**), (β-**2a**) as well as (α-**1f**) adopt rather slightly folded (12~22°) boat conformations as indicated by the corresponding angles of 157.7 and -163.5° for (α-**2a**), 164.0 and -168.2° for (β-**2a**), and 164.3 and -163.8° for (β-**1f**), respectively. Further interest is that the carbon atoms of oxirane rings of (α-**1f**) and (β-**1f**) are almost planar as represented by the angles of 355° or more when the author adds three angles made by the substituents of oxirane and another carbon center. Such a geometrical planarity of oxirane carbon is commonly known for the most of oxirane derivatives compiled in the Cambridge Structural Database.[9]

1-2-2. Acid-Catalyzed Reaction of Homobenzoquinone Epoxides.

The acid-catalyzed reaction of diphenyl-substituted epoxides **1a** and **1b** in $CDCl_3$ at 30°C gave the tricyclic diketo-alcohols **4a** and **4b**, respectively, via the regioselective oxirane ring-opening[10] at the Me-substituted C-O bond and the folowing transannular cyclization of *endo*-aromatic nucleus (Scheme 3). The structures of these compounds were deduced from the ^{1}H- and ^{13}C-NMR as well as IR spectra.

Scheme 3.

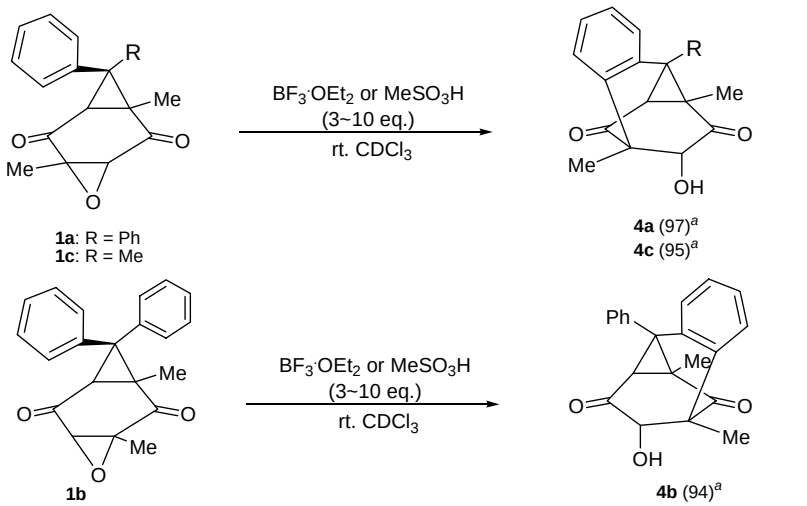

[a] Isolated yield (when BF_3·OEt_2 was used).

The *endo*-Ph-substituted **1c** also underwent the acid-catalyzed regioselective oxirane ring-cleavage to afford the similar tricyclic diketo-alcohol **2c** (Scheme 3), whereas the *exo*-Ph-substituted **1d** showed very slow complex decomposition (<5%) even on 6h standing with 20 equiv excess of BF_3 (Scheme 4). This means that the *endo*-aromatic ring plays a crucial role in the present oxirane ring-opening as the π-electron nucleophile.[11] As expected, the rigid compound **1e** bearing the spiro-linked planar fluorenylydene moiety did not display the oxirane ring-opening even on one day standing with BF_3 because of the lack of *anti* assistance of π-donor aromatic ring for the C-O bond cleavage.

Scheme 4.

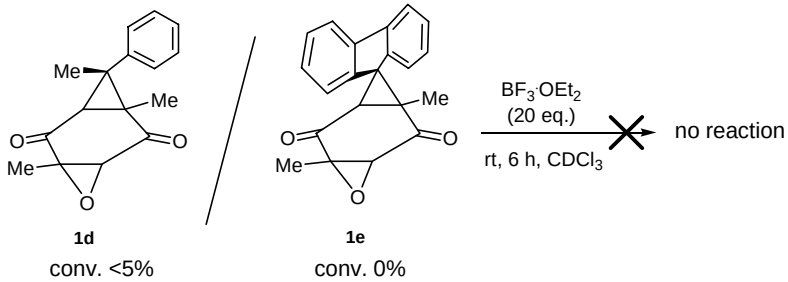

However, as shown in Scheme 5 and Table 2, the conformationally semirigid dibenzocycloheptene spiro-linked epoxides α-**1f** and α-**1g** were susceptible toward the acid-catalyzed regioselective oxirane ring-opening to produce the similar diketo-alcohol **4f** for

Scheme 5.

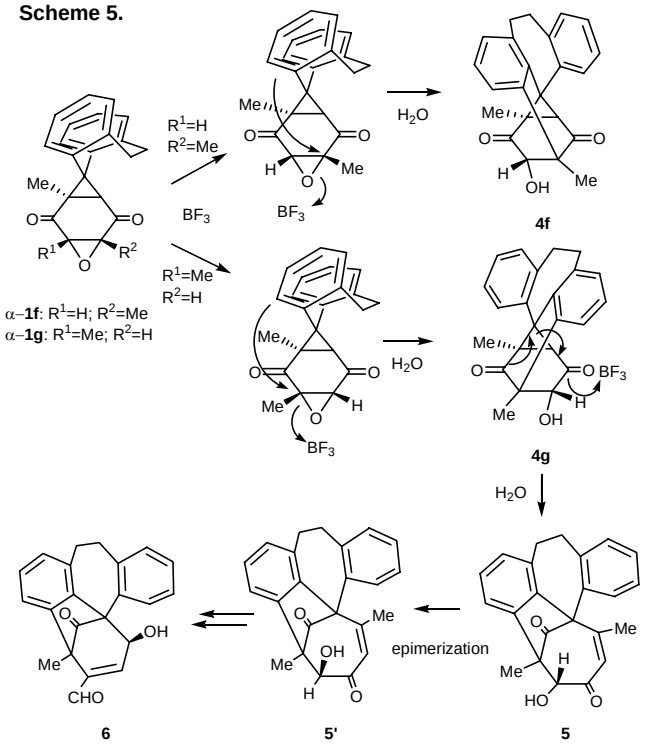

Table 2. Acid-catalysed rearrangement of α/β–**1f**,**g** (30 mM) in $CDCl_3$ at 30 °C

entry	sub.	time (h)	conv.[b] (%)	yield[a,b] (%)			
				4	**5**	**5'**	**6**
1	α–**1f**	24	90	100	0	0	0
2	α–**1g**	16	12	0	28	42	30
3	β–**1f**	24	82	90	0	0	0
4	β–**1g**	2	85	0	74	21	2

[a] Based on consumed **1**. [b] Determined by ^{1}H NMR.

the former epoxide and the secondly transformed bicyclo[4.2.1]nonaene diketo-alcohol **5** and its epimer **5'** as well as the ring-contracted **6** for the latter epoxide, respectively (further details will be described at Chapter 3). It is very noteworthy that the primary product **4g** (not detected) underwent a facile acid-catalyzed acyl migration associated with the cyclopropane ring cleavage.[12] It was found that the conformationally inverted β-**1f** and β-**1g** display the same regioselective oxirane ring-opening and the following degradation as the relevant α-**1f** and α-**1g**, affording the same products. During the BF_3-catalyzed reactions at 30 °C, conformational inversion of α-conformers into β-conformers was not observed on ^{1}H NMR measurement. However, the reactivity was much dependent on the conformational difference of the dibenzocycloheptene ring as experienced by the higher conversion (though shorter reaction time) of β-**1g** compared to the conformational isomer α-**1g** (entries 2 and 4). The structures of **4f** , **5'** and **6** were confirmed by X-ray crystallographic analyses.[13]

1-2-3. Kinetic Solvent Effects.

To clarify the reaction mechanisms, the kinetic solvent effects provide a useful mechanistic information on the transition state in such a way that the more polar the solvent is, the more stabilized the polar transition state is, with the rate being largely accelerared like in the S_N1 reactions.[14] The author has measured the rate constants for the $MeSO_3H$-catalyzed oxirane ring-opening of the parent unsubstituted diphenylhomobenzoquinone epoxide **1a** by monitoring its first-order decay in various less basic solvents (Figure. 2).

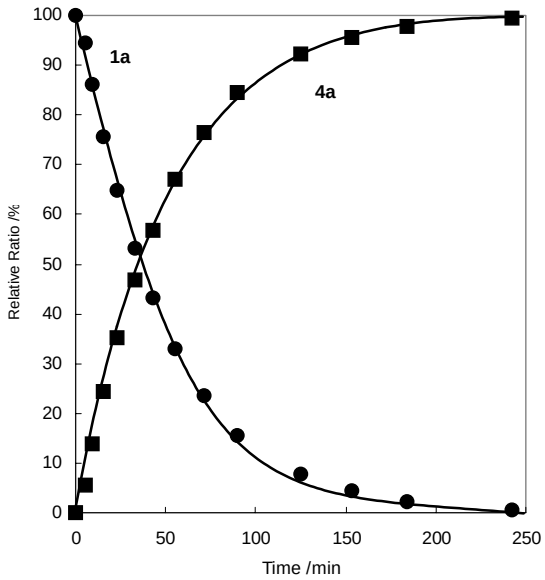

Figure 2. A representative time course of the $MeSO_3H$ ([30 mM])-catalyzed rearrangement of **1a** into **4a** in $CDCl_3$ (650 μl) at 30°C.

The rate constants in a wide range of solvents at 30°C are summarized along with the solvent polarity parameter $E_T(30)$[15] (Table 3). The total variation of k_2 amounts to only a factor of 3 over a wide range of solvent polarities investigated. The very poor kinetic solvent

Table 3. Rate constants for $MeSO_3H$-catalyzed ring-opening of epoxide **1a** in various solvents at 30 °C

Solvent	$E_T(30)$	k_2[a] (10^3, $M^{-1}s^{-1}$)	k_{rel}[b]
1,2-Dichloroethane	41.3	1.15	3.0
Dichloromethane	40.7	1.17	3.1
Chloroform-*d*	39.0	0.979	2.6
o-Dichlorobenzene	38.0	0.280	0.73
Fluorobenzene	37.0	0.380	0.99
Chlorobenzene	36.8	0.297	0.77
Benzene	34.3	0.384	1.0

[a] The second-order rate constants k_2 were obtained by diving the pseudo-first-order rate constants k_{obs} by the catalyst concentration ([0.030 M])
[b] Relative ratio of acid-catalyzed reaction of **1a** in various solvents.

effects strongly support a concerted mechanism involving a less polar transition state in which the charge is highly dispersed on the π-aryl participated aromatic nucleus as well as on the breaking oxirane carbon atom. In such a S_N2-like transition state, it is conceived that the

orbital interaction between the HOMO of the π-electron donating aromatic group and the Walsh-type LUMO of oxirane ring[16] plays a crucial role in the cleavage of the relevant C-O bond as depicted in Scheme 3. The aryl participation in the ring opening of oxiranes is scarcely reported but has been put forwarded in order to explain the *syn*-stereochemistry in the acid-induced ring opening of a particular case of oxiranes bearing aryl groups directry or indirectry linked to the epoxide ring such as stilbene epoxides[17] and spiro-linked 2-phenyl-1,2-epoxid[18] or 1-benzyl-1,2-epoxides[11] in which the well-documented phenonium ion intermediates are invoked.

1-2-4. Conformational Analysis in π-Aryl Participation.

As described above, acid-catalyzed reaction of these α- and β-conformers of epoxides **1f** and **1g** resulted in the regioselective oxirane ring opening at the Me-substituted C-O bonds. The following intramolecular nucleophilic attack (transannular cyclization) by the *endo*-aromatic nucleus (S_E2-Ar reaction) afforded the identical tricyclic diketoalcohols **4f**,**g** as the primary products (Scheme 5). Here, it is noted that the α-**1f** and β-**1g** were subjected to the whole inversion of the twist-boat form in these reactions, as represented by X-ray crystal structure of **4f**. Due to the appreciable thermal stability, the α- and β-conformers of epoxides **1f** and **1g** take advantage of evaluating the conformational effects (i.e., stereoelectronic effects) on the possible anti- π-aryl participation in the oxirane ring-cleavage. Therefore, the author has made a kinetic investigation of acid-catalyzed rearrangement of each conformer of **1f** and **1g** in comparison with the reference epoxides **1a-c** (Scheme 1).

First, to assess the conformational stability of the less stable α-conformers of **1f**,**g**,**2a**,**b** the author carried out a kinetic study of the non-mediated thermal interconversion into the corresponding β-isomers by ^{1}H NMR in $CDCl_3$ at 80 ^{o}C in a sealed tube. Only the epoxide **3**α established the equilibration (α:β = 4:96), whereas the other α–conformers were completely transformed into the corresponding β-isomers. The first-order rate constants k_1/s^{-1} thus obtained were given in Table 4. The estimated energy barriers from the k_1 values for $\alpha \rightarrow \beta$ conversion are 108–109 and 117–125 kJ mol^{-1} at 80 ^{o}C for **1f**,**g** and **2a**,**b**, respectively. These values are high enough to prevent the conformational interconversion at ordinary temperature, although the epoxidation slightly reduced the energy barriers by ~17 kJ mol^{-1}. Thus the thermal stability increases in the order of α-**2b** > α-**2a** > α-**1f** > α-**1g**. The conformational locking for the intrinsically flexible parent dibenzocycloheptene ring[19] can be ascribed to the repulsive van der Waals interaction between (A) the peri-hydrogen atom of *endo*-aromatic ring and the quinone plane as well as (B) the peri-hydrogen atom of *exo*-aromatic ring and the cyclopropane Me substituent.

Keeping this in mind, the author next investigated the kinetics of acid-catalyzed reactions of the α- and β- families of the conformationally locked **1f** and **1g** as well as the mobile **1a-c**. The representative kinetic run was performed at 30 ^{o}C in a NMR tube containing epoxide (0.03 M) and $BF_3 \cdot OEt_2$ (0.30 M) in $CDCl_3$ (0.65 mL) by following the decay of the diagnostic Me group of the relevant epoxide (TMS as an internal standard) over the second-half lives. During all kinetic runs, no indication of the conformational isomerization $\alpha \rightarrow \beta$ was found by the NMR measurement, in accordance with the significant thermal stability of these α-conformers. The observed pseudo-first-order rate constants (k_{obs}/s^{-1}) were divided by the concentration of the acid to obtain the second-order rate constants $k_2/s^{-1}\ M^{-1}$. The values of k_2 thus obtained are listed along with the relative rate constants k_2^{rel} (vs the reference **1a**) in Table 4.

Table 4. Rate constants for the conformational inversion and BF_3-catalyzed ring-opening of homobenzoquinone epoxides at 30^{o}C in $CDCl_3$.

		inversion	ring-opening of epoxide	
entry	compd.	$10^5 k_1$ / s^{-1}	$10^4 k_2$[a] / $M^{-1}s^{-1}$	k_2^{rel}
1	α–**2a**	4.05[b]	-	
2	α–**2b**	0.27[b]	-	
3	α–**1f**	59.5[c]	6.98	1.4
4	β–**1f**	2.72[d]	1.84	0.4
5	α–**1g**	89.3[b]	3.99	0.8
6	β–**1g**	-	98.0	19.0
7	**1a**	-	5.16	1.0
8	**1b**	-	15.1	2.9
9	**1c**	-	4.64	0.9

[a] The second-order rate constants were obtained by dividing the pseudo-first-order rate constants kobs (at 30 ^{o}C in CDCl[3]) by the catalyst concentration ([0.30 M]). [b] Completery inverted into the corresponding β–isomer. [c] The k values at different temperature (60 and 70 ^{o}C) are 7.66 and 23.2 (x 10^{-5} s^{-1}), respectively, and give the extrapolated k values of 2.18 (x 10^{-6} s^{-1}) at 30 ^{o}C as well as the activation parameters ($\Delta H^{\ddagger}$ = 97.9 kJ/mol, $\Delta S^{\ddagger}$ = –35.3 J/K·mol, $\Delta G^{\ddagger}$ = 108.6 kJ/mol at 80 ^{o}C). [d] Calculated from the equilibrium constant (K = 2.1 at 80 ^{o}C) for α to β.

Table 4 indicates that the rates were accelerated or decelerated depending on the conformation (α or β) of the dibenzocycloheptene moiety and on the substitution pattern (*p* or *m*) of quinone dimethyl substituents. The most striking feature of the reactions of the **1f** and **1g** is a reversal of the relative reactivity of α and β-conformers. Thus, for **1f**, the less stable α-conformer was ca 4 times more reactive than the stable β-one (entries 3 and 4), whereas for **1g** the stable β-conformer was ca 25 times more reactive than the less stable α-one (entries 5 and 6) Additionally, the noticeable points are as follows; (1) the conformationally locked **1f** and **1g** (except β-**1g**) exhibited the reactivity comparable to that for the related **1a** and **b**; (2) the *m*-dimethyl-substituted **1g** and **1b** tended to react faster than the *p*-dimethyl-substituted **1f** and **1a** (entries 3-8).

These appreciable conformational effects can be explained by assuming that the present acid-catalyzed regioselective oxirane ring-opening occurs via a S_N2 like concerted mechanism. Indeed, the concerted mechanism was strongly supported by the poor kinetic solvent effects in the $MeSO_3H$-mediated reaction of epoxide **1a** as well as the appreciable kinetic substituent effects.[20] Specifically, it can be envisaged that the reaction proceeds through the stereoelectronically controlled π-aryl participated rate-determining transition state with the aid of the vacant oxirane Walsh orbital (LUMO)[16] as depicted in Figure 3. Here, the author can

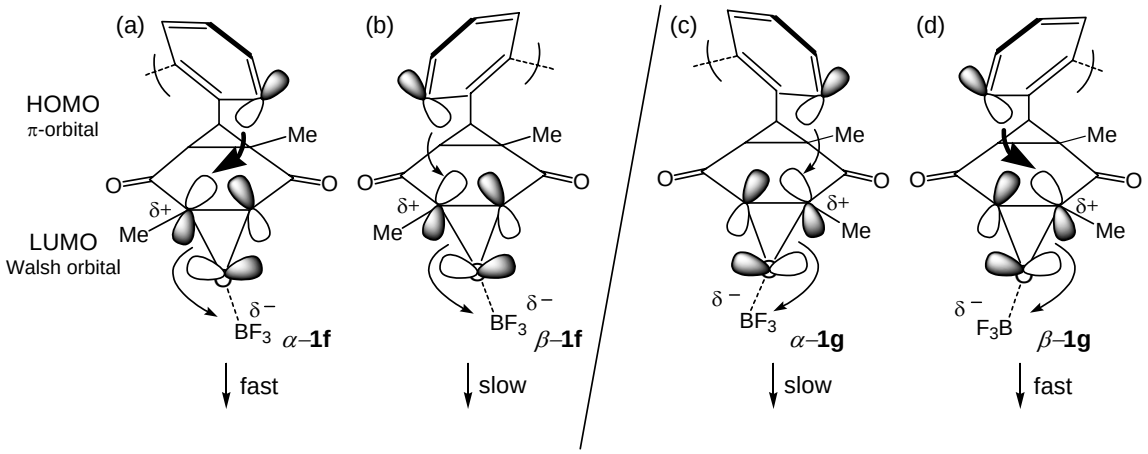

Figure 3. Orbital interaction between HOMO (aromatic ring) and LUMO (Walsh orbital) in transition state.

also imagine that the π-aryl participation would be significantly intensified in the conformers in which the approaching aromatic π-orbital (HOMO) performs the ideal head-to-head orbital overlapping with the oxirane Walsh orbital. Such a through space orbital interaction is favorably achieved for the conformers *α*-**1f** and *β*-**1g** (Figure 3a and d), overriding the high inversion energy cost (> 108 kJ mol^{-1}). This is a reason for the higher reactivity of *α*-**1f** and *β*-**1g** than the corresponding isomers *β*-**1f** and *α*-**1g**, respectively. By contrast, the corresponding orbital interaction for the less reactive conformers *β*-**1f** and *α*-**1g** is considerably reduced due to the rather insufficient orthogonal orbital interaction (Figure 3b and c), thus lowering the reactivity irrespective of requiring no conformational inversion.

Accordingly, the 25-fold higher reactivity of the stable *β*-**1g** compared with *α*-**1g** can be taken as a strong evidence for the occurrence of favored π-electron donating interaction with the oxirane vacant Walsh orbital as depicted in Figure 3d. As to *α*-**1f**, however, the rather diminished 3.5-fold higher lability than the *β*-isomer may be due to the additional steric interaction between the cyclopropane Me substituent and the *exo*-aromatic ring (B). As a result, the rates of epoxide ring-opening of **1f** and **1g** are goverened by the critical balance between the attractive π-aryl participated orbital interaction and the repulsive van der Waals congestion associated with the conformational inversion of dibenzocycloheptene ring.

Incidentally, alternative S_N1 like two-step mechanism may contradict the present kinetic results because the more reactive conformers *α*-**1f** and *β*-**1g** have the capturing aryl orbital

unfavorably reacting across the ring system to engage the carbocation p-orbital (rehybridized from the Walsh orbital), whereas the less reactive β-**1f** and α-**1g** enjoy the capture on the same side of the ring system. This would predict the result opposite to that deduced from the consideration of Walsh orbital.

1-2-5. Dual Pathway Acid-Catalyzed Reaction of Disubstituted HQ-Epoxide

Next, on the basis of the results descrived above, the author felt that an appropriately *p*-substituted diphenylhomobenzoquinone epoxide **1** might allow to provide a possible *ipso*-product from the π-aryl participated transition state. Herein, the author wishes to report the mechanistic evidence for the very rare π-aryl-assisted oxirane ring opening in the BF_3-catalyzed reaction of bis(*p*-chlorophenyl)homobenzoquinone epoxide **1i**. The acid-induced reaction of *p*,*p*'-dimethyl-, unsubstituted, and *p*,*p*'-dichloro-substituted **1a**,**h** and **i** (0.02 mmol) was carried out in the presence of BF_3 (0.40 mmol) in $CDCl_3$ (0.62 ml) at ordinary temperature.[21] The reaction proceeded in a regioselective oxirane ring-opening at the Me substituted C-O bond and on treatment with water gave the common *o*-phenylene bridged tricyclic diketo-alcohols **4a**, **h**, and **i** (for **4i**, as a mixture of small amount of its epimer **4'i**) and 2,5-cyclohexadien-4-one spiro-linked tricyclic diketo-alcohol **7i** (47%) for only the

Scheme 6.

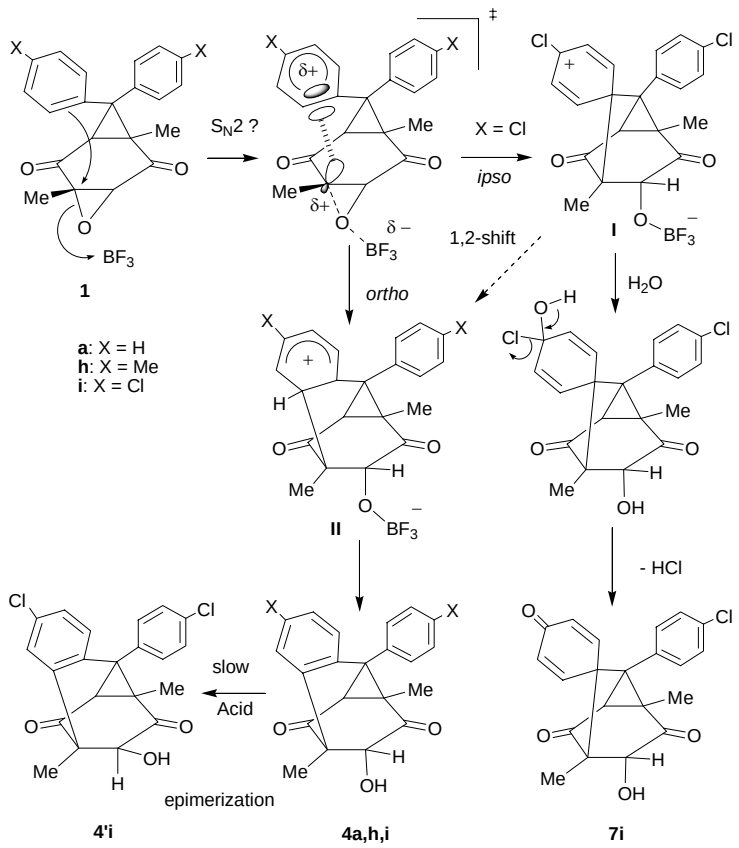

chloro-substituted **1i** in almost quantitative total yields based on the consumed **1** (Scheme 6). Unfortunately, we could not isolate **4i** and **4'i** in pure form.

The structures of compounds **7i**, **4h, i** and **4'i** were deduced from their ^{1}H- and ^{13}C-NMR spectra and the **7i** was confirmed by the X-ray crystal analysis (Figure 4).

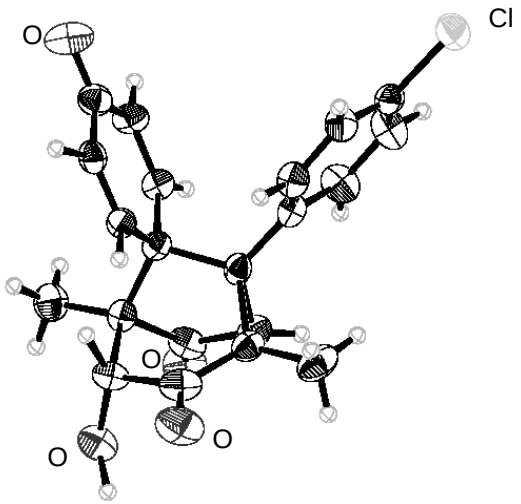

Figure 4. ORTEP drawing of compound **7i**. Displacement ellipsoids are plotted at the 50% probability level. H atoms are drawn as spheres of arbitrary radii.

As shown in Scheme 6, the formation of **7i** and **4a,h,i** can be rationalized by the occurrence of the competitive *ipso*- and *ortho*- S_E2-Ar reaction via aryl bridged benzenonium ions, i.e., σ-complexes I and II, respectively. Although the intermediate II easily undergoes a rearomatization to afford **4a,h,i** via a proton migration, the formation of compound **7i** can be explained by the capture of the intermediate I with some water followed by the loss of HCl. Thus, the isolation of **7i** and **4i** is taken as a strong evidence for the appearance of both the σ-complexes, I and II. These schematic considerations prompted us to further examine the following mechanistic questions about the transition state leading to the above σ-complexes[22] as well as the marked substituent effects on the product distributions.

Why does the *p*-chloro-substituted **1i** provide the dual *ipso*/*ortho* conjunct products in contrast to the *p*,*p*'-dimethyl-substituted **1h** and the unsubstituted **1a**?

This question can be easily solved by considering the characteristic electronic properties of *p*-Cl substituent as exhibiting the electron-donating resonance effect as well as the good leaving ability which would stabilize the adjoining positive center of I and then facilitate the release of HCl (Scheme 6). In view of the *ipso*-attack, the *p*-tolyl group would allow such a reaction more favorably than the *p*-chlorophenyl group due to the electron density at the ipso aromatic carbon. However, even if such an *ipso* σ-complex is formed for **1a** and **1h** and undergoes the attack of water at the *p*-position, the lack of the leaving ability of Me group (including H) will cause the transformation into the *ortho* σ-complex via a facile 1,2-shift on the aromatic ring.

1-3. Conclusion

In summary, the acid-catalyzed rearrangement of homobenzoquinone epoxides possessing *endo*-aromatic ring displayed a new synthesis of polycyclic compounds involving a regioselective oxirane ring-opening and a crucial transannular cyclization as well as the subsequent ring-enlargement by 1,2-acyl migration associated with the incorporated cyclopropane ring-opening, depending on the substitution pattern of the quinone methyl groups. These findings provide the useful information on the rearrangements of polycyclic epoxides and the design of more extended framework compounds. Additionally, based on the kinetics and conformational effects in acid-catalysed reactions of the present homobenzoquinone epoxides, the author has found that the π-aryl participated electron-donating interaction with the vacant oxirane Walsh orbital plays a prominent role in the epoxide ring-opening. Moreover, the dual pathway for **1i** as well as the kinetic solvent effects is likely to prove that the acid-catalyzed ring-opening of diarylhomobenzoquinone epoxides **1** occurs via a concerted manner involving a very rare remote (*δ*-located) π-aryl participated transition state. The present findings will provide very useful insights into the mechanistic understanding of the acid-catalyzed ring-opening of epoxides.

1-4. Experimental Section

General procedures for the synthesis of homobenzoquinone epoxides. To a mixture of homobenzoquinone (0.5 mmol) and 30% H_2O_2 (0.75 mmol) in DMSO (1 mL) was added dropwisely (10 min) a solution of Bu_4NF (1M solution in THF, 0.5 mmol) at room temperature. After the addition of the reagent the reaction mixture was stirred for 2h. Then, the epoxide **1** was extracted with ethyl acetate (3 mL × 3). The organic layer was washed with water (3 mL × 3) and dried over magnesium sulfate. The solvent was evaporated *in vacuo*. The epoxide **1** was purified by column chromatography on silica gel (benzene as an eluent) and recrystallization from hexane-ether or hexane-benzene. The structures of all epoxides were deduced from the ^1H and ^{13}C NMR, and IR spectra and the compounds *α*-**1f**, *β*-**1f**, *α*-**1g** were also confirmed by the X-ray crystallographic analyses.

General procedures for acid-catalyzed reaction of homobenzoquinone epoxides. To a $CDCl_3$ solution (670 μl) of **1** (0.02 mmol) in a NMR tube was added the requisite amount of $BF_3{\cdot}OEt_2$ at room temperature by using a micro syringe. The progress of reaction was monitored by ^1H NMR. After a period of requisit time, the reaction solution was transferred into a separate funnel, diluted with chloroform (10 mL) and then washed with water (3 mL × 3). The aqueous layer was extracted with chloroform (5 mL × 2). The combined organic

layer was washed with water (3 mL × 3), then dried over calcium chloride. After the evaporation of the solvent *in vacuo*, the residue was submitted for a ^{1}H NMR analysis to determine the product distribution. The column chromatographic treatment of the reaction mixtures on silica gel gave **5**, **5'**, and **6** with a mixture of hexane-ethyl acetate as an elurnt. The other compounds **4a-c**, **f** and **h** were purified by recrystallization from hexane-ether. The structures of all products were deduced from the ^{1}H and ^{13}C NMR, and IR spectra. The structures of **4f**, **5** and **5'** were also confirmed by the X-ray crystallographic analyses.

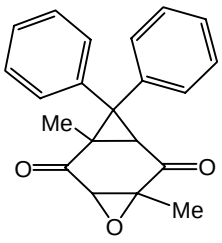

1a

1,5-Dimethyl-8,8-diphenyl-4-oxa-tricyclo[5.1.0.0^{3,5}]octane-2,6-dione (**1a**): mp. 123.5^{o}C (from chloroform/*n*-hexane); ^{1}H NMR(270 MHz, $CDCl_3$) δ 0.92 (s, 3H), 1.18 (s, 3H), 2.81 (s, 1H), 2.82 (s, 1H), 7.17-7.32 (m, 8H), 7.37-7.40 (m, 2H); ^{13}C NMR (67 MHz, $CDCl_3$) δ13.7, 16.9, 37.6, 39.7, 49.6, 60.1, 60.3, 127.5, 127.9, 128.2, 128.9, 129.1, 129.5, 138.1, 139.9, 198.1, 200.3; *Anal* Calcd for $C_{21}H_{18}O_3$: C, 79.22; H, 5.70, Found : C, 79.10; H, 5.86.

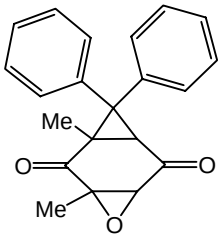

1b

1,3-Dimethyl-8,8-diphenyl-4-oxa-tricyclo[5.1.0.0^{3,5}]octane-2,6-dione (**1b**): mp. 229.4-229.8^{o}C (from chloroform/*n*-hexane); ^{1}H NMR(270 MHz, $CDCl_3$) δ 0.99 (s, 3H), 1.23 (s, 3H), 2.75 (d, 1H, *J* = 1.15 Hz), 2.78 (d, 1H, *J* = 1.15 Hz), 7.18-7.27 (m, 6H), 7.30-7.33 (m, 2H), 7.39 (m, 2H); ^{13}C NMR (67 MHz, $CDCl_3$) δ 14.3, 17.4, 36.9, 40.0, 49.5, 60.0, 60.4, 127.6, 127.9, 128.3, 128.9, 129.1, 129.5, 138.1, 140.0, 198.2, 200.3; IR (KBr): 3378, 3082, 3056, 3031, 2999, 2938, 1958, 1897, 1698, 1597, 1580, 1493, 1447, 1372, 1344, 1294, 1278, 1235, 1198, 1159, 1083, 1060, 1026, 1011, 990, 974, 935, 906, 884, 863 cm$^-$1; *Anal.* Calcd for $C_{21}H_{18}O_3$: C, 79.22; H, 5.70, Found : C, 79.52; H, 5.69.

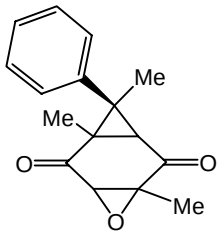

1c

***endo*-1,5,8-trimethyl-8-phenyl-4-oxa-tricyclo[5.1.0.0^{3,5}]octane-2,6-dione** (**1c**): mp. 136.8-138.0^{o}C (from chloroform/*n*-hexane); ^{1}H NMR(270 MHz, $CDCl_3$) δ 0.94 (s, 3H), 1.54 (s, 6H), 2.16 (s, 1H), 2.62 (s, 1H), 7.11-7.15 (m, 2H), 7.22-7.33 (m, 3H); ^{13}C NMR (67 MHz, $CDCl_3$) δ 13.7, 15.0, 26.4, 37.6, 41.7, 42.2, 59.6, 59.7, 127.8, 129.0, 139.1, 199.0, 200.6; IR (KBr): 3455, 2982, 2936, 1740, 1691, 1599, 1488, 1441, 1381, 1277, 1227, 1162, 1139, 1092, 1031, 940, 919, 836, 801 cm$^-$1; *Anal* Calcd for $C_{16}H_{16}O_3$: C, 74.98; H, 6.29, Found : C, 74.71; H, 5.97.

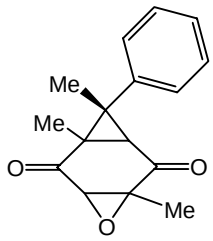

1d

***exo*-1,5,8-trimethyl-8-phenyl-4-oxa-tricyclo[5.1.0.0^{3,5}]octane-2,6-dione** (**1d**): ^{1}H NMR(270 MHz, $CDCl_3$) δ 1.01 (s, 3H), 1.27 (s, 3H), 1.55 (s, 3H), 2.26 (s, 1H), 3.49 (s, 1H), 7.26-7.37 (m, 5H); ^{13}C NMR (67 MHz, $CDCl_3$) δ 14.0, 17.4, 20.6, 34.6, 35.7, 39.1, 63.3, 63.4, 127.3, 128.2, 128.6, 140.9, 199.6, 202.1; IR (KBr): 2964, 1695, 1496, 1445, 1387, 1332, 1262, 1165, 1068, 985, 865, 849 cm^{-}1; *Anal* Calcd for $C_{16}H_{16}O_3$: C, 74.98; H, 6.29, Found : C, 75.02; H, 6.42.

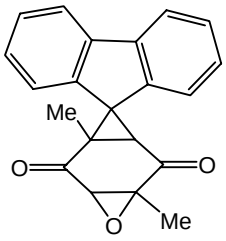

1e

***spiro*-[9H-fluorene-9,8'-1,5-dimethyl-4-oxa-tricyclo[5.1.0.0^{3,5}]octane-2,6-dione] (1e)**: mp. 134.4-135.0 ^{o}C (from chloroform / *n*-hexane); ^{1}H NMR(270 MHz, $CDCl_3$) δ 1.65 (s, 3H), 1.69 (s, 3H), 2.88 (s, 1H), 3.73 (s, 1H), 6.57 (d, 1H, *J* = 7.91), 7.10－7.17 (m, 2H), 7.25－7.43 (m, 3H), 7.75－7.80 (m, 2H); ^{13}C NMR (67 MHz, $CDCl_3$) δ 14.0, 15.9, 37.6, 38.5, 44.9, 63.9, 64.9, 120.3, 120.6, 121.6, 122.7, 126.5, 126.9, 127.5, 127.8, 139.5, 140.9, 141.2, 141.4, 198.2, 201.5; IR (KBr): 3394, 3053, 3006, 2973, 2933, 1705, 1482, 1449, 1396, 1378, 1310, 1241, 1198, 1144, 1112, 1101, 1084, 1064, 1003, 941, 901, 855, 830, 792, 783, 772, 760 cm^{-1}; *Anal* Calcd for $C_{21}H_{16}O_3$: C, 79.73; H, 5.10, Found : C, 79.48; H, 5.33.

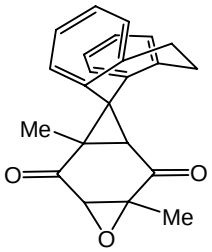

α-**1f**

***exo*-spiro-[10,11-Dihydro-dibenzo[a,d]cycloheptane-5,8'-1,5-dimethyl-4-oxatricyclo[5.1.0.0^{3,5}]octane-2,6-dione] (*α*-1f) :** mp. 185.3-186.2^{o}C (from chloroform/*n*-hexane) ; ^{1}H NMR(270 MHz, $CDCl_3$) δ 0.78 (s, 3H), 1.60 (s, 3H), 2.44 (s, 1H), 2.81－2.96 (m, 2H), 3.00 (s, 1H), 3.30－3.41 (m, 1H), 4.08－4.17(m, 1H), 6.95－6.99(m, 2H), 7.00－7.26 (m,6H); ^{13}C NMR(67 MHz, $CDCl_3$) δ 13.4, 18.5, 29.8, 31.6, 38.0, 44.9, 48.1, 59.7, 60.6, 125.8, 126.3, 126.5, 126.9, 128.1, 128.1, 130.2, 132.2, 134.9, 138.6, 139.2, 140.4, 197.4, 201.0; IR (KBr): 3385, 3051, 3034, 2967, 2940, 2896, 1933, 1700, 1601, 1486, 1460, 1445, 1373, 1330, 1261, 1229, 1206, 1177, 1153, 1099, 1084, 1073, 1053, 1019, 994, 958, 914, 874, 858, 806, 793, 779, 759 cm^{-1}; *Anal* Calcd for $C_{23}H_{20}O_3$: C, 80.21; H, 5.85, Found : C, 79.94; H, 5.88.

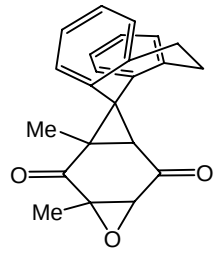

α-**1g**

***exo*-spiro-[10,11-Dihydro-dibenzo[a,d]cycloheptane-5,8'-1,3-dimethyl-4-oxatricyclo[5.1.0.0^{3,5}]octane-2,6-dione] (α-1g) :** mp. 120.0-121.0^{o}C (from hexane-chloroform); ^{1}H NMR (270 MHz, $CDCl_3$) δ 1.33 (s, 3H), 1.62 (s, 3H), 2.37 (d, 1H, *J* = 1.07), 2.81 (d, 1H, *J*= 1.07), 2.85-2.93 (m, 2H), 3.33-3.45 (m, 1H), 4.14-4.27 (m, 1H), 6.93-6.98 (t, 2H), 7.04-7.23 (m, 6H); ^{13}C NMR (67 MHz, $CDCl_3$) δ 15.1, 19.4, 29.8, 31.6, 36.5, 44.1, 47.0, 60.3, 60.7, 125.5, 126.2, 126.4, 127.3, 128.0, 128.1, 130.2, 132.4, 134.6, 138.6, 139.4, 140.6, 197.3, 201.5; IR (KBr): 3061, 2992, 2938, 2895, 1693, 1601, 1487, 1460, 1375, 1345, 1279, 1195, 1089, 1058, 1038, cm^{-1}; *Anal* Calcd for $C_{23}H_{20}O_3$: C, 80.21; H, 5.85, Found : C, 79.95; H, 5.59.

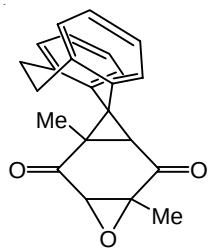

β-**1f**

***endo*-spiro-[10,11-Dihydro-dibenzo[a,d]cycloheptane-5,8'-1,5-dimethyl-4-oxatricyclo[5.1.0.0^{3,5}]octane-2,6-dione] (β-1f) :** mp. 117.2-118.5 ^{o}C (from hexane-chloroform); ^{1}H NMR (270 MHz, $CDCl_3$) δ 1.21 (s, 3H), 1.34 (s, 3H), 2.70-2.95 (m, 2H), 2.73 (s, 1H), 2.97 (s, 1H), 3.43-3.66 (m, 2H), 7.02-7.20 (m, 7H), 7.34-7.37 (m, 1H); ^{13}C NMR (67 MHz, $CDCl_3$) δ 14.6, 16.3, 30.3, 32.2, 37.9, 39.4, 48.8, 60.1, 61.0, 126.1, 126.2, 126.8, 127.2, 128.1, 128.7, 130.2, 131.6, 135.5, 136.8, 138.4, 140.9, 199.0, 199.4; IR (KBr): 3389, 3047, 2983, 2969, 2917, 1956, 1707, 1690, 1488, 1445, 1426, 1384, 1358, 1327, 1252, 1210, 1158, 1110, 1085, 1064, 1020, 952, 930, 865, 837, 804, 795, 775, 762, 739 cm^{-1}; *Anal* Calcd for $C_{23}H_{20}O_3$: C, 80.21; H, 5.85, Found : C, 79.91; H, 5.83.

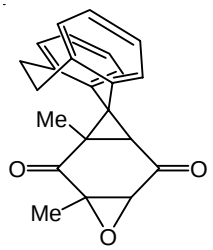

β-**1g**

***endo*-spiro-[10,11-Dihydro-dibenzo[a,d]cycloheptane-5,8'-1,3-dimethyl-4-oxatricyclo[5.1.0.0^{3,5}]octane-2,6-dione] (β-1g) :** mp. 136-137^{o}C (from hexane-chloroform); ^{1}H NMR (270 MHz, $CDCl_3$) δ 0.67 (s, 3H), 1.22 (s, 3H), 2.71-2.78 (m, 1H), 2.87-3.04 (m, 1H), 2.97 (d, 1H, *J*= 0.98), 3.03 (d, 1H, *J*= 0.98), 3.42-3.56 (m, 2H), 7.04-7.21 (m, 8H); ^{13}C NMR (67 MHz, $CDCl_3$) δ 13.6, 16.2, 30.3, 32.2, 39.1, 40.0, 49.6, 59.6, 61.0, 126.3, 126.5, 126.5, 127.3, 128.2, 128.6, 130.1, 131.7, 135.2, 137.2, 138.4, 141.1, 198.7, 198.9; IR (KBr): 3436, 3060, 3020, 2934, 1694, 1487, 1444, 1338, 1315, 1281, 1197, 1112, 1059, 1019, 973, 905, 862, 826 cm^{-1}; *Anal* Calcd for $C_{23}H_{20}O_3$: C, 80.21; H, 5.85, Found : C, 80.00; H, 5.59.

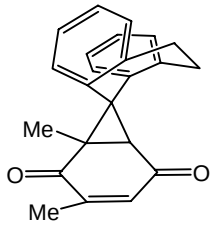

α-**2b**

***exo*-spiro[10,11-Dihydro-5H-dibenzo[a,d]cycloheptene-5,7'-1,3-dimethyl-bicyclo[4,1,0]hept-3-ene-2,5-dione]** (α-**2**b): mp. 170-171 ^{o}C (from chloroform / *n*-hexane); ^{1}H NMR (270 MHz, $CDCl_3$) δ 1.71 (s, 3H), 1.78 (d, 3H, *J* = 1.48 Hz), 2.63 (s, 1H), 2.65-2.94 (m, 2H), 3.27-3.36 (m, 1H), 3.98-4.12 (m, 1H), 6.03 (q, 1H, *J* = 1.48 Hz), 6.85-6.90 (m, 4H), 7.02-7.36 (m, 4H); ^{13}C NMR (67.5 MHz, $CDCl_3$) δ 16.7, 19.0, 30.0, 31.1, 39.5, 48.3, 50.5, 125.5, 126.1, 126.4, 127.5, 127.7, 127.9, 130.3, 131.9, 134.8, 136.2, 138.6, 138.6, 140.9, 149.9, 194.2, 198.1; IR (KBr): 3059, 3016, 2979, 2941, 2895, 1672, 1657, 1628, 1601, 1484, 1460, 1358, 1307, 1285, 1221, 1202, 1177 cm^{-}1; HRMS: Calculated for $C_{23}H_{20}O_2$, 328.1463, found 328.1461

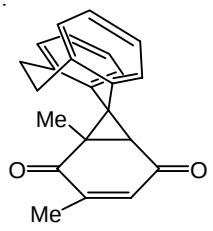

β-**2b**

***endo*-spiro[10,11-Dihydro-5H-dibenzo[a,d]cycloheptene-5,7'-1,3-dimethyl-bicyclo[4,1,0]hept-3-ene-2,5-dione]** (β-**2b**): mp. 138-139 ^{o}C (from chloroform / *n*-hexane); ^{1}H NMR(270 MHz, $CDCl_3$) δ 1.28 (s, 3H), 1.50 (d, 3H, *J* = 1.48 Hz), 2.64-2.71 (m, 1H), 2.91-2.96 (m, 1H), 3.21 (s, 1H), 3.41-3.49 (m, 2H), 6.23 (q, 1H, *J* = 1.48), 6.89-6.90 (m, 1H), 6.96-7.25 (m, 6H), 7.33-7.37 (m, 1H); ^{13}C NMR (67.5 MHz, $CDCl_3$) δ 16.0, 16.6, 29.9, 32.5, 41.5, 42.2, 51.4, 126.2, 126.3, 126.8, 127.9, 128.0, 128.6, 129.6, 131.8, 135.7, 136.1, 137.5, 138.4, 140.3, 149.2, 195.5, 196.6; IR (KBr): 3058, 3006, 2967, 2890, 1684, 1655, 1618, 1477, 1380, 1368, 1300, 1283, 1255, 1241, 1111 cm^{-}1; HRMS : Calculated for $C_{23}H_{20}O_2$, 328.1463, found 328.1461

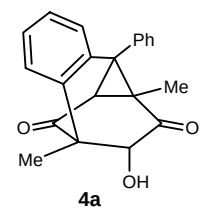

4a

(1R*,8R*,9S*,10R*,12S*)-12-Hydroxy-1,10-dimethyl-8-phenyl-tetracyclo-[6.4.1^{1,9}.0^{2,7}.0^{8,13}]trideca-2(7),3,5-triene-11,13-dione (**4a**): ^{1}H NMR (270 MHz, $CDCl_3$) δ 1.27 (s, 3H), 1.64 (s, 3H), 2.73 (s, 1H), 3.02 (d, 1H, *J*= 4.59, OH), 3.86 (d, 1H, *J*= 4.59), 6.82 (dd, 1H, *J*= 1.32, 7.91), 7.09 (ddd, 1H, *J*= 1.65, 7.25, 7.91), 7.20 (ddd, 1H, *J*= 1.32, 7.25, 7.58), 7.26-7.30 (m, 2H), 7.36-7.46 (m, 4H); ^{13}C NMR (67 MHz, $CDCl_3$) δ 14.5, 19.3, 41.8, 47.3, 52.6, 53.7, 85.5, 125.6, 127.8, 127.9, 128.1, 128.2, 128.5, 129.9, 130.1, 131.8, 136.1, 136.2, 136.5, 205.0, 205.4; IR (KBr): 3457, 3008, 2935, 1744, 1685, 1488, 1442, 1378, 1307, 1235, 1151, 1054, 940, 912, 834, 793, 758 cm^{-1}

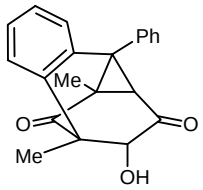

4b

(1R*,8R*,9S*,10R*,12S*)-12-Hydroxy-1,9-dimethyl-8-phenyl-tetracyclo-[6.4.1^{1,9}.0^{2,7}.0^{8,13}]trideca-2(7),3,5-triene-11,13-dione (**4b**): mp. 74.8-75.2 ^{o}C (from hexane-chloroform): ^{1}H NMR (270 MHz, $CDCl_3$) δ 1.14 (s, 3H), 1.68 (s, 3H), 2.35 (s, 1H, OH), 3.05 (d, 1H, J=1.35 Hz, OH), 3.78 (d, 1H, J=1.35 Hz), 6.53 (dd, 1H), 6.56-7.50 (m, 8H); ^{13}C-NMR (67 MHz, $CDCl_3$) δ 15.0, 15.3, 29.8, 37.9, 49.8, 52.6, 84.1, 125.3, 127.9, 128.1, 128.3, 128.9, 128.9, 129.0, 129.2, 129.9, 131.0, 136.7, 136.9, 203.2, 206.3; IR (KBr): 3348, 3060, 3018, 2932, 2902, 2832, 1766, 1694, 1595, 1486, 1443, 1376, 1360, 1161, 1092, 1060, 1016, 973, 866 cm^{-1}

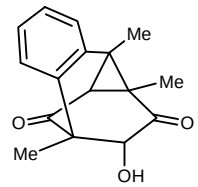

4c

(1R*,8R*,9S*,10R*,12S*)-12-Hydroxy-1,8,10-trimethyl-tetracyclo-[6.4.1^{1,9}.0^{2,7}.0^{8,13}]trideca-2(7),3,5-triene-11,13-dione (**4c**): mp. 161.1-162.0 ^{o}C (from hexane-chloroform): ^{1}H NMR (270 MHz, $CDCl_3$) δ 1.52 (s, 3H), 1.57 (s, 3H), 1.73 (s, 3H), 2.26 (s, 1H), 2.76 (br, 1H, OH), 3.70 (br, 1H), 7.24-7.34 (m, 3H), 7.39-7.41 (m, 1H); ^{13}C NMR (67 MHz, $CDCl_3$) δ 14.2, 16.2, 19.7, 42.6, 43.6, 47.1, 53.6, 85.2, 125.3, 126.2, 127.8, 128.3, 136.7, 137.0, 205.2, 205.3; IR (KBr): 3464, 2925, 1715, 1698, 1559, 1541, 1508, 1489, 1457, 1387, 1204, 1034, cm^{-1}

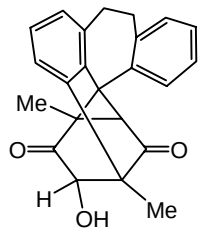

4f

(**4f**): mp. 164.5-165.0 ^{o}C (from hexane-chloroform): ^{1}H NMR (270 MHz, $CDCl_3$) δ 1.05 (s, 3H), 1.64 (s, 3H), 2.64 (d, 1H, *J*= 3.54, OH), 2.77-2.85 (m, 1H), 2.96 (s, 1H), 2.90-3.17 (m, 2H), 3.27-3.3.8 (m, 1H), 3.59 (d, 1H, *J*= 3.54), 6.95-6.99 (m, 1H), 7.10-7.11 (m, 2H), 7.13-7.31 (m, 4H); ^{13}C NMR (67 MHz, $CDCl_3$) δ 14.3, 15.5, 31.2, 36.3, 40.4, 49.6, 50.5, 54.8, 86.3, 122.5, 126.5, 126.7, 126.9, 129.1, 129.6, 131.9, 132.3, 135.7, 138.3, 140.6, 144.9, 204.5, 205.0; IR (KBr): 3380, 3037, 2928, 1708, 1598, 1542, 1482, 1446, 1381, 1325, 1278, 1156, 1040, 953, 930, 867, 836, cm^{-1}

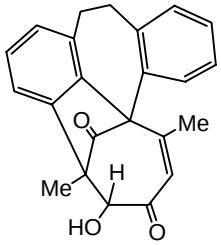

5

(**5**): ^{1}H NMR (270 MHz, $CDCl_3$) δ 1.62 (s, 3H), 1.80 (d, 3H, *J*= 1.40), 2.83-2.96 (m, 3H, OH), 3.14-3.30 (m, 2H), 4.15 (d, 1H, *J*= 8.01), 5.93 (q, 1H, *J*= 1.40), 7.02-7.05 (m, 1H), 7.13-7.30 (m, 5H) 7.74-7.78 (m, 1H); ^{13}C NMR (67 MHz, $CDCl_3$) δ 17.1, 24.1, 32.3, 32.4, 57.7, 65.3, 90.1, 120.9, 126.4, 126.7, 127.4, 128.2, 129.0, 129.8, 131.0, 136.6, 137.0, 140.6, 140.7, 141.5, 154.4, 200.1, 210.3; IR (KBr): 3432, 2963, 1743, 1706, 1489, 1444, 1377, 1262, 1098, 1027, 867, cm^{-1}

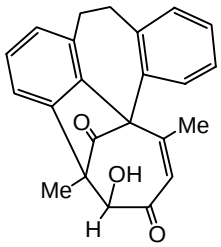

5'

(**5'**): mp. 112.2-112.6^{o}C (from hexane-chloroform): ^{1}H NMR (270 MHz, $CDCl_3$) δ 1.72 (s, 3H), 1.82 (d, 3H, *J*= 1.32), 2.82-2.92 (m, 2H), 3.13-3.24 (m, 2H), 3.94 (d, 1H, *J*= 4.37, OH), 4.40 (d, 1H, *J*= 4.37), 6.08 (q, 1H, *J*= 1.32), 6.96-6.99 (m, 1H), 7.11-7.28 (m, 5H) 7.83-7.87 (m, 1H); ^{13}C NMR (67 MHz, $CDCl_3$) δ 16.6, 24.6, 31.8, 32.1, 63.5, 64.1, 86.3, 121.6, 126.0, 126.4, 127.3, 128.1, 128.2, 129.5, 130.9, 135.9, 137.2, 139.8, 140.6, 141.0, 157.1, 200.2, 207.3; IR (KBr): 3454, 2935, 1739, 1688, 1440, 1381, 1227, 1092, 1030, 918, 800, cm^{-1}

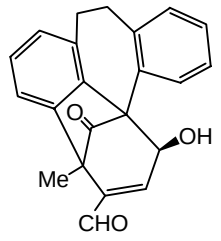

6

(**6**): mp. 238.3-238.8 ^{o}C (from hexane-chloroform): ^{1}H NMR (270 MHz, $CDCl_3$) δ 1.86 (s, 3H), 2.91-3.02 (m, 2H), 3.10-3.29 (m, 2H), 5.09 (s, 1H), 5.28 (s, 1H, OH), 6.75 (s, 1H), 7.03-7.08 (m, 1H), 7.18-7.33 (m, 5H), 7.76-7.79 (m, 1H) 9.43 (s, 1H); ^{13}C NMR (67 MHz, $CDCl_3$) δ 11.7, 33.7, 36.0, 51.8, 64.9, 77.2, 118.7, 121.5, 125.5, 127.4, 128.0, 128.3, 130.9, 132.7, 140.4, 141.9, 143.0, 145.6, 146.2, 149.4, 190.1, 207.2; IR (KBr): 3568, 2925, 2851, 1772, 1684, 1571, 1542, 1386, 1185, 1117, 915, 857, cm^{-1}

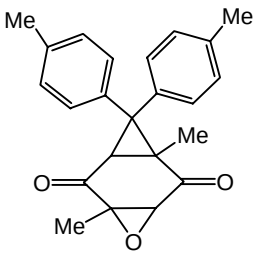

1h

1,3-Dimethyl-8,8-ditolyl-4-oxa-tricyclo[5.1.0.0^{3,5}]octane-2,6-dion e (**1h**): mp 139.9-140.8 ^{o}C, colorless prisms (chloroform/pentane); ^{1}H NMR(270 MHz, $CDCl_3$) δ 0.94 (s, 3H), 1.17 (s, 3H), 2.24 (s, 3H), 2.27 (s, 3H), 2.77 (s, 1H), 2.81 (s, 1H), 7.02-7.14 (m, 6H), 7.22-7.26 (m, 2H); ^{13}C-NMR (67 MHz, $CDCl_3$) δ 13.8, 16.9, 21.1, 21.1, 37.7, 39.8, 49.3, 60.1, 60.4, 128.0, 129.2, 129.5, 129.7, 135.3, 137.3, 137.3, 137.6, 198.4, 200.5; IR (KBr) 1702 (C=O) cm^{-1}. HRMS: Calcd for $C_{23}H_{22}O_3$: 346.1569. Found: 346.1572.

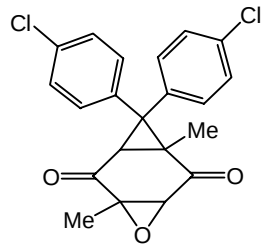

1i

1,5-dimethyl-8,8-bis(4-chlorophenyl)-4-oxa-tricyclo[5.1.0.0^{3,5}]octane-2,6-dione (1i): mp 142.7-143.5 ^{o}C, colorless prisms (chloroform/pentane); ^{1}H-NMR(270 MHz, $CDCl_3$) δ 1.01 (s, 3H), 1.19 (s, 3H), 2.75 (s, 1H), 2.89 (s, 1H), 7.14-7.19 (m, 2H), 7.22-7.27 (m, 2H), 7.29 (s, 4H); ^{13}C NMR (67 MHz, $CDCl_3$) δ 13.8, 17.0, 37.2, 39.2, 47.4, 60.4, 129.3, 129.4, 129.6, 130.8, 133.9, 134.3, 136.1, 138.0, 197.8, 200.0; IR (KBr): 1702 (C=O) cm^{-1}. HRMS: Calcd for $C_{21}H_{16}Cl_2O_3$: 386.0476. Found: 386.0479.

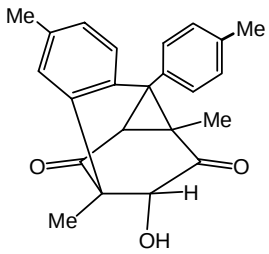

4h

(1R*,8R*,9S*,10R*,12S*)-12-Hydroxy-5-methyl-1,10-dimethyl-8-tolyl-tetracyclo-[6.4.1^{1,9}.0^{2,7}.0^{8,13}]trideca-2(7),3,5-triene-11,13-dione (**4h**): mp. 237.5-238.4 ^{o}C (from chloroform/*n*-hexane); ^{1}H NMR(270 MHz, $CDCl_3$) δ 1.24 (s, 3H), 1.61 (s, 3H), 2.13 (s, 3H), 2.41 (s, 3H), 2.68 (s, 1H), 3.09 (d, 1H, *J* = 3.63 Hz), 3.81 (d, 1H, *J* = 3.63) 6.64 (d, 1H, *J* = 1.65 Hz), 6.97-7.00 (m, 1H), 7.13-7.16 (m, 2H), 7.22-7.33 (m, 3H); ^{13}C NMR (67 MHz, $CDCl_3$) δ 14.5, 19.3, 21.2, 21.3, 42.0, 47.4, 52.5, 53.3, 85.6, 125.5, 128.4, 128.6, 129.1, 129.9, 130.4, 131.6, 133.1, 133.4, 136.1, 137.9, 138.0, 205.5, 205.9; IR (KBr): 3357, 2921, 1707, 1493, 1458, 1393, 1327, 1069, 1041, 942cm-1.

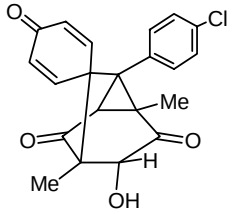

7i

Spiro[cyclohexa-2,5-dienone-4,8'-7-(4-chlorophenyl)-1,4-dimethyl-3-hydroxy-tricyclo[2.2.2.0^{6,7}]octane-2,5-dione] (**7i**): mp 206.6-206.9 ^{o}C (from chloroform/*n*-hexane); ^{1}H NMR(270 MHz, $CDCl_3$) δ 1.00 (s, 3H), 1.08 (s, 3H), 2.75 (s, 1H), 2.93 (s, 1H), 4.00 (s,1H), 6.17 (dd, 1H, *J* = 1.81, 10.4 Hz), 6.52 (dd, 1H, *J* = 1.81, 10.2 Hz), 6.54 (dd, 1H, *J* = 3.13, 10.4 Hz), 6.82 (dd, 1H, *J* = 3.13, 10.2 Hz), 7.00-7.10 (m, 2H), 7.25-7.26 (m, 2H); ^{13}C NMR (67 MHz, $CDCl_3$) δ10.9, 14.8, 29.8, 43.1, 46.0, 52.8, 56.0, 75.4, 128.9, 129.7, 130.5, 131.3, 134.4, 135.3, 142.7, 147.5, 184.0, 203.0, 204.0; IR (KBr): 3417, 2925, 1745, 1664, 1261, 1091, 801 cm-1.

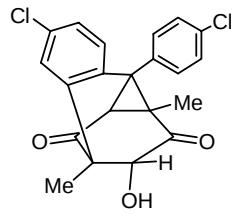

4i

(1R*,8R*,9S*,10R*,12S*)-12-Hydroxy-5-chloro-1,10-dimethyl-8-(4-chlorophenyl)-tetracyclo-[6.4.1^{1,9}.0^{2,7}.0^{8,13}]trideca-2(7),3,5-triene-11,13-dione (**4i**):^{1}H NMR(270 MHz, $CDCl_3$) δ 1.33 (s, 3H), 1.65 (s, 3H), 2.67 (s, 1H), 4.09 (s, 1H), 6.76 (d, 1H, *J* = 1.65 Hz), 7.17-7.31 (m, 3H), 7.34-7.56 (m, 3H).

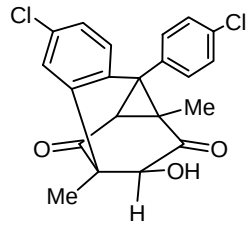

4'i

(1R*,8R*,9S*,10R*,12R*)-12-Hydroxy-5-chloro-1,10-dimethyl-8-(4-chlorophenyl)-tetracyclo-[6.4.1^{1,9}.0^{2,7}.0^{8,13}]trideca-2(7),3,5-triene-11,13-dione (**4'i**):^{1}H NMR(270 MHz, $CDCl_3$) δ 1.70 (s, 3H), 1.83 (s, 3H), 3.15 (s, 1H), 6.40 (s, 1H), 6.93 (d, 1H, *J* = 1.81 Hz), 6.93-7.34 (m, 4H), 7.55 (d, 2H, *J* = 8.74 Hz).

X-ray Crystal structure Determination of α-1f: $C_{23}H_{20}O_3$, M = 344.41, monoclinic, space group $P2_1/a$ with *a* = 12.517(1), *b* = 10.206(1), *c* = 14.704(2) Å, *β* = 11.747(7)°, *V* = 1744.7(4) Å ^{3}, *Z* = 4, *Dcalc* = 1.311 g/cm^3, *R* = 0.136 and *Rw* = 0.188 for 3922 reflections with *I*>2.0σ(*I*).

X-ray Crystal structure Determination of β-1f: $C_{23}H_{20}O_3$, M = 344.41, orthorhombic, space group Pbca with *a* = 9.4653(3), *b* = 14.6974(4), *c* = 25.3890(9) Å, *V* = 3532.0(2) Å ^{3}, *Z* = 8, *Dcalc* = 1.295 g/cm^3, *R* = 0.100 and *Rw* = 0.176 for 3955 reflections with *I*>2.0σ(*I*).

X-ray Crystal structure Determination of 1d: $C_{17}H_{17}O_2$, M = 253.32, orthorhombic, space group $Pna2_1$ with *a* = 16.1082(4), *b* = 11.8925(4), *c* = 7.0686(2) Å, *V* = 1354.11(7) Å ^{3}, *Z* = 4, *Dcalc* = 1.242 g/cm^3, *R* = 0.127 and *Rw* = 0.142 for 13581 reflections with *I*>2.0σ(*I*).

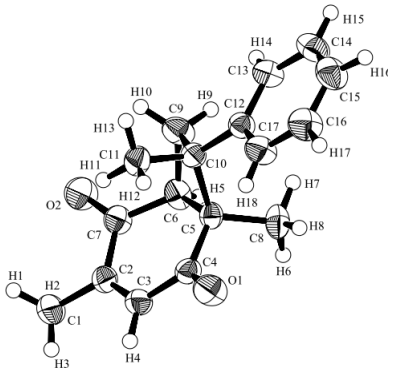

Figure 5. ORTEP drawing of **1d**.

X-ray Crystal structure Determination of 4f: $C_{23}H_{22}O_4$, M = 362.42, orthorhombic, space group $P2_12_12_1$ with *a* = 7.7719(6), *b* = 12.712(1), *c* = 18.431(2) Å, *V* = 1821.0(3) Å ^{3}, *Z* = 4, *Dcalc* = 1.322 g/cm^3, *R* = 0.074 and *Rw* = 0.155 for 2263 reflections with *I*>2.0σ(*I*).

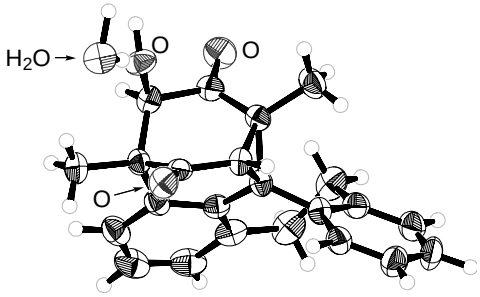

Figure 6. ORTEP drawing of **4f**.

X-ray Crystal structure Determination of 7i: $C_{21}H_{17}O_4Cl$, M = 368.82, monoclinic, space group $P2_1/a$ with *a* = 11.4880(7), *b* = 12.525(1), *c* = 13.3085(6) Å, *β* = 114.312, *V* = 1754.1(2) Å ^{3}, *Z* = 4, *Dcalc* = 1.404 g/cm^3, *R* = 0.141 and *Rw* = 0.203 for 2516 reflections with *I*>2.0σ(*I*).

1-5. Reference and Notes

(1) (a) Parker, R. E.; Isaacs, N. S. *Chem. Rev*. **1959**, *59*, 737–799. (b) Rickborn, B. In *Comprehensive Organic Synthesis*; Trost, B. M., Ed.; Pergamon Press: Oxford, U. K., 1991; Vol. 3, p 733. (c) Fujita, H.; Yoshida, Y.; Kita, Y. *Yuki Gosei Kagaku Kyokaishi* **2003**, *61*, 133–143. (d) Giner, J.-L.; Li, X.; Mullins, J. J. *J. Org. Chem*. **2003**, *68*, 10079–10086.

(2) (a) Posner, G. H.; Rogers, D. Z. *J. Am. Chem. Soc*. **1977**, *99*, 8214–8218. (b) Bellucci, G.; Berti, G.; Ingrosso, G.; Mastrorilli, E. *J. Org. Chem*. **1980**, *45*, 299–303. (c) Nugent, W. A. *J. Am. Chem. Soc*. **1992**, *114*, 2768–2769. (d) Jacobsen, E. N. *Acc. Chem. Res*. **2000**, *33*, 421–431. (e) Schaus, S. E.; Jacobsen, E. N. *Org. Lett*. **2000**, *2*, 1001–1004. (f) Brandes, B. D.; Jacobsen, E. N. *Synlett*, **2001**, 1013–1015. (g) Schneider, C. *Synthesis*, **2006**, 3919–3944. (h) Hirai, A.; Tonooka, T.; Tanino, K.; Miyashita, M. *Chirality*, **2003**, *15*, 108–109.

(3) Isaacs, N. S. *Physical Organic Chemistry*, 2nd Ed.; Longman Scientific & Technical, Essex, U.K., 1995, Chaper 13, p 643.

(4) (a) Lancelot, C. J.; Cram, D. J.; Scheyer, P. v. R. *Carbenium Ions*; Olah, G. A.; Scheyer, P. v. R. Eds., Wiley-Interscience, New York, 1972, Vol. 3, Chapter 27, p 1347. (b) Smith, M. B.; March, J. *March's Advanced Organic Chemistry*, Wiley, New York, 2001, Chapter 10, p 407. (c) Peeran, M.; Wilt, J. W.; Subramanian, R.; Crumrine, D. S. *J. Org. Chem*. **1993**, *58*, 202–210. (d) Kevill, D. N.; D'Souza, M. J. *J. Chem. Soc., Perkin Trans. 2*, **1997**, 257–263. (e) Fujio, M.; Goto, N.; Dairokuno, T.; Goto, M.; Saeki, Y.; Okusaka, Y.; Tsuno, Y. *Bull. Chem. Soc. Jpn*., **1992**, *65*, 3072–3079. (f) Nagumo, S.; Ono, M.; Kakimoto, Y.; Furukawa, T.; Hisano, T.; Mizukami, M.; Kawahara, N.; Akita, H. *J. Org. Che*m. **2002**, *67*, 6618–6622. (g) Río, E. d.; Menéndez, M. I.; López, R.; Sordo, T. L. *J. Am. Chem. Soc*., **2001**, *123*, 5064–5068.

(5) Burger, A. *A Guide to the Chemical Basis of Drug Design*, Wiley, New Tork. **1983**.

(6) Oshima, T.; Nagai, T. *J. Chem. Soc., Chem. Commun*. **1994**, 2787–2788.

(7) Oshima, T.; Fujii, S.; Takatani, T.; Kokubo, K.; Kawamoto, T. *J. Chem. Soc., Perkin Trans. 2*, **1999**, 1783–1789.

(8) Reboul, P. J. P.; Cristau, B. *Acta Cryst.* **1981**. *B37*, 394–398.

(9) Oki, M.; Toyofuku, Y.,; Sakaue, T.; Hirose, T.; Asakura, M.; Morita, N.; Toyota, S. *Russ. J. Org. Chem*., **2003**, *39*, 542–553; see also *The Cambridge Structural Database, Version 5.22*, January 2002, Cambridge Crystallographic Data Center, 12, Union Road. Cambridge. CB2 1EZ. UK.

(10) Overman, L. E.; Renhowe, P. A. *J. Org. Chem*. **1994**, *59*, 4138–4142.

(11) (a) Costantino, P.; Crotti, P.; Ferretti, M.; Macchia, F. *J. Org. Chem*. **1982**, *47*, 2917–2923. (b) Crotti, P.; Ferretti, M.; Macchia, F.; Stoppioni, A. *J. Org. Chem*. **1984**, *49*, 4706–4711. (c) Crotti, P.; Ferretti, M.; Macchia, F.; Stoppioni, A. *J. Org. Chem*. **1986**, *51*, 2759–2766.

(12) We could not detect **2g** by ^{1}H NMR even for shorter rection time (10 min, 30% conversion) under the same condition.

(13) Crystallographic data for the structure of **2f, 4** and **5** have been deposited with the Cambridge Crystallographic Data Center as supplementary publication number CCDC 650017, 650018 and 650209. Copies of the data can be obtained, free of charge, on application to the CCDC, 12 Union Road, Cambridge CB2 1EZ, UK. Fax: +44-1233-336033. E-mail: deposit@ccdc.cam.ac.uk.

(14) C. Reichard, "Solvents and Solvent Effects in Organic Chemistry" Wiley-VCH Verlag GmbH & Co. KGaA, Weinheim, 2003, ch.5, pp147–328.

(15) Reichardt, C. *Chem. Rev*. **1994**, *94*, 2319–2358.

(16) (a) Mollere, P. D.; Houk, K. N. *J. Am. Chem. Soc*., **1977**, *99*, 3226–3233. (b) Iwamura, H.; Sugawara, T.; Kawada, Y.; Tori, K.; Muneyuki, R.; Noyori, R. *Tetrahedron Lett.*, **1979**, *20*, 3449–3452. (c) Bach, R. D.; Wolber, G. J. *J. Am. Chem. Soc*., **1984**, *106*, 1410–1415.

(17) Parker, R. E.; Isaacs, N. S. *Chem. Rev*. **1959**, *59*, 737–799.

(18) Kita, Y.; Furukawa, A.; Futamura, J.; Higuchi, K.; Ueda, K.; Fujioka, H. *Tetrahedron*, **2001**, *57*, 815–825.

(19) Weissensteiner, W.; Hofer, O.; Wagner, U. G. *J. Org. Chem*., **1988**, *53*, 3988–3996.

(20) A preliminary kinetic study indicated that the introduction of *p,p'*-dimethyl or *p,p'*-dichloro substituents results about 11-fold increase or 33-fold decrease in the rate of the parent epoxide **5**; further details will be described at Chapter 2.

(21) The conversions of **1a**, **1h**, and **1i** were >99% (for 4h), 100 (0.5h), and 82 (20h), respectively.

(22) Structure and dynamics of σ- and π-complexes are described in detail for the electrophilic aromatic substitutions, see Hubig, S. M.; Kochi, J. K. *J. Org. Chem*., **2000**, *65*, 6807–6818.

Chapter 2. Kinetic Evidence for η^2 π-Aryl Participation in Acid-Catalyzed Reaction of HQ-Epoxide

2-1. Introduction

π-Aryl participation is one of the most sophisticated physicochemical phenomena that control the reactivity of substrates and sometimes govern the reaction mechanism.[1] These effects are generally derived from (ascribed to) the through-space electronic stabilization of the transition states by the direct π-electronic donation (not by resonance) from the contained aryl groups to the reaction center (usually, but not necessarily an incipient carbocation).[2] A large number of studies have been made of the π-aryl assisted solvolyses of β-aryltosylates and brosylates from the kinetic[3] and stereochemical[4] point of view. In these adjacent β-aryl-substituted substrates, the kinetic substituent effects as well as the product analyses clearly indicated that the π-aryl participation occurs at the proximal *ipso*-carbon and hence the phenonium ion (σ-complex) can be formed as an intermediate. By contrast, little is known for the anchimeric assistance of the aryl group located in the γ-position or further away from the reaction site.[5] However, the remote π-aryl participation is of continuous theoretical interest because a detailed understanding of the physical origin and scope of such interactions has become one of the major goals of physical organic chemistry. Compared to the more conventional π-aryl participation at the *ipso*-position, the elucidation of the steric and electronic factors controlling the remote electron-donation and knowing which positions of the aromatic ring are responsible for such phenomenon, are of prime importance.

Very recently, the author reported that the unsubstituted and *p*-substituted diphenylhomobenzoquinone epoxides **1** (X, Y = H, Me and Cl) show a remote π-aryl participated transannular S_E2-Ar cyclization of *endo*-phenyl group associated with the acid-catalyzed regioselective oxirane ring-cleavage to give the *ortho*-carbon bound tricyclic diketo-alcohols **2** and the *ipso*-carbon bound 2,5-cyclohexadien-4-one spiro-linked tricyclic diketo-alcohol **3** (only for the π-resonating *p*-Cl substituted entity) as shown in Scheme 1a.[6] This observation raises a question as to which positions of the aromatic ring and how the aryl group interacts with the vacant oxirane Walsh orbital.[7]

Herein, aiming at obtaining physicochemical information on the π–aryl participated transition state, the author has conducted kinetic studies of the BF_3-catalyzed transannular cyclization of variously *endo*/*exo m*- and *p*-substituted diarylhomobenzoquinone epoxides **1a-k** in $CDCl_3$ at 30 °C. Based on the kinetic substituent effects, the author has found that the dihapto (η^2)-type coordination (through *ipso* and *ortho*) of *endo*-aromatic ring occurs in the rate-determining oxirane ring-cleavage. A modified Hammett treatment indicated that the *ipso*/*ortho* contribution ratio (=1.6) is considerably higher than that (0.89) of the similar

S_E2-Ar transannular cyclization of cyclobutene-fused diarylhomobenzoquinones **4** into the *ortho*-carbon bound tetracyclic keto-alcohols **5** (Scheme 1b).[8] These results were explained in terms of the stereoelectronic effects in the orbital interaction between the π-donor aromatic rings (HOMO) and the vacant *anti*-bonding orbitals of the cleaved oxirane and cyclobutene rings (LUMO).

Scheme 1.

a) Epoxide ring-opening

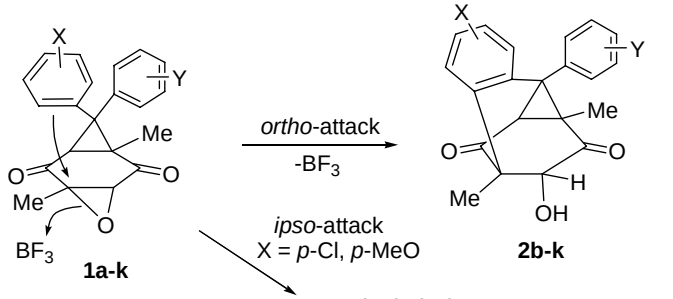

	X	Y
endo/exo-**1a**	*p*-MeO / H	H / *p*-MeO
1b	*p*-Me	*p*-Me
1c	*m*-MeO	*m*-MeO
endo/exo-**1d**	*m*-MeO / H	H / *m*-MeO
endo/exo-**1e**	*p*-Me / H	H / *p*-Me
endo/exo-**1f**	*m*-Me / H	H / *m*-Me
1g	H	H
endo/exo-**1h**	*p*-Cl / H	H / *p*-Cl
endo/exo-**1i**	*m*-Cl / H	H / *m*-Cl
1j	*p*-Cl	*p*-Cl
endo/exo-**1k**	*p*-CF_3 / H	H / *p*-CF_3

b) Cyclobutene ring-opening

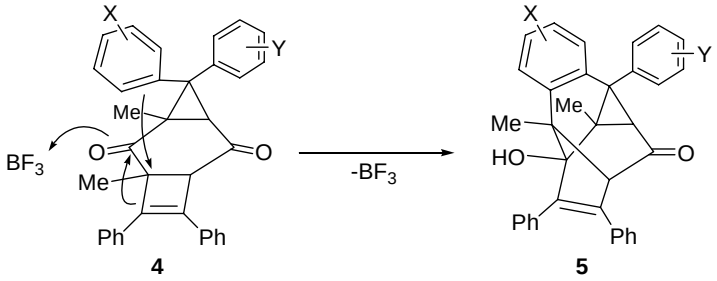

2-2. Results and Discussion

2-2-1. Synthesis and Structural Characteristics of Epoxides

The *endo*/*exo*-substituted diarylhomobenzoquinone epoxides **1a-k** were prepared by the epoxidation of diarylhomobenzoquinones[9] derived from 1,3-dipolar cycloaddition of the corresponding *m*- and *p*-substituted diphenyldiazomethanes with 2,5-dimethyl-1,4-benzoquinone.[10] For the mono-substituted diphenyldiazomethanes, a mixture of *endo*/*exo*-substituted isomers was formed and separated by careful column chromatography and recrystallization. The *m*-chloro-substituted **1i**, however, could not be

isolated due to the very similar *endo*/*exo* adsorbability on silicagel. The structures of **1a-k** were deduced as the *cis-transoid-cis* tricyclic dione frame from the representative X-ray

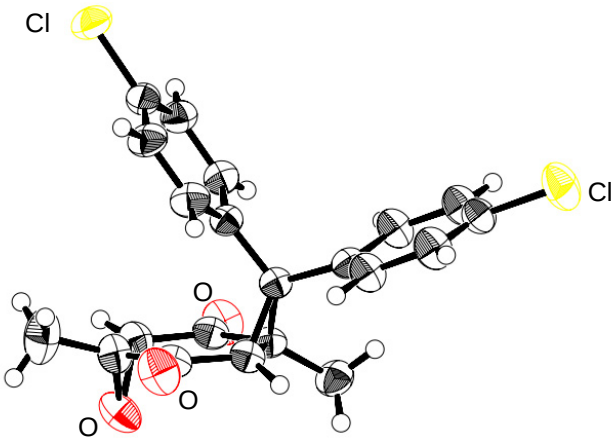

Figure 1. ORTEP drawing of bis(*p*-chlorophenyl) homobenzoquinone epoxide **1j** with 50% ellipsoid probability.

crystal structural analysis of bis(*p*-chlorophenyl)-substituted **1j** (Figure 1).[11] The original quinone frame was found to adopt an appreciable pseudo-boat conformation with a slight deformation opposite to the *endo*-aromatic ring. This deformation results in an overhang of *endo*-aryl ring above the quinone plane and a pseudoaxial flipping of the conjunct planar oxirane ring as noted by the average dihedral angle (95.4°) between the epoxide ring and the fused quinone plane. The very short spatial distance (3.21 Å) between the *endo*-aromatic *ipso*-carbon and the cleaved epoxide tertiary carbon seems to allow the π-electron donation to the underlying acid-activated oxirane ring. However, the corresponding distance (4.74 Å) with the outside *exo*-aromatic *ipso*-carbon is long enough to inhibit the through-space π-electron donation. Such π-electron participation becomes very important if the present epoxide ring-opening reaction proceeds through an S_N2 type intramolecular transannular cyclization. As a result, the geometrical features of **1** can take advantage of π-anchimeric assistance in the present acid-catalyzed ring-opening.

2-2-2. Kinetic Substituent Effects

The observed pseudo-first-order rate constants k_{obs}(**1**) were divided by the concentration of BF_3 to provide the second-order rate constants k(**1**). The values for k(**1**) and the relative rate constants k_{rel}(**1**) (vs the unsubstituted **1g**) are collected in Table 1. For comparison, Table 1 also includes the relative rate constants k_{rel}(**4**) (vs the unsubstituted entity) for the previous BF_3-catalyzed reactions of similarly *endo*/*exo* *m*- and *p*-substituted analogous cyclobutene-fused diarylhomobenzoquinones **4a-k**.[8]

A perusal survey of Table 1 indicated some noticeable differences between the epoxides **1a-k** and the cyclobutene-fused **4a-k**: (1) for the *endo*-substituted series, the rates were

increased more effectively in **1** ($k^{p\text{-MeO}}/k^{p\text{-CF3}}$ = 8200) than in **4** (= 5600)[12]; (2) by contrast, the same substituent change brought about only a small increase for the *exo*-substituted **1 (**2-fold) and for **4** (11-fold); (3) of particular interest is that the *endo*-*p*-substituted **1** (X = MeO, Me, Cl) reacted faster than the *endo*-*m*-substituted isomer, whereas the *endo*-*m*-substituted **4** exhibited rather higher reactivity than the *endo*-*p*-substituted isomer; (4) on the other hand,

Table 1. Rate constants *k* and the relative rate ratios k_{rel}(**1**) for BF_3-catalyzed rearrangements of **1** along with the relative rate ratios k_{rel}(**4**) for the reaction of **4** in $CDCl_3$ at 30°C

entry	compoud	substituent		10^3k^a(**1**) /$M^{-1}s^{-1}$	k_{rel}(**1**)	$k_{rel}{}^b$(**4**)
		X	Y			
1	*endo*-**1a**	*p*-MeO	H	18.7	37	17
2	**1b**	*p*-Me	*p*-Me	5.25	11	5.3
3	**1c**	*m*-MeO	*m*-MeO	3.90	8.0	-
4	*endo*-**1d**	*m*-MeO	H	3.70	7.6	22
5	*endo*-**1e**	*p*-Me	H	3.11	6.4	4.9
6	*endo*-**1f**	*m*-Me	H	1.36	2.8	5.6
7	**1g**	H	H	0.486	1.0	1.0[c]
8	*endo*-**1h**	*p*-Cl	H	0.122	0.25	0.017
9	*endo*-**1i**	*m*-Cl	H	0.0213	0.044	0.078
10	**1j**	*p*-Cl	*p*-Cl	0.0154	0.032	0.015
11	*endo*-**1k**	*p*-CF_3	H	0.00217	0.0045	0.0040
12	*exo*-**1a**	H	*p*-MeO	0.602	1.2	3.2
13	*exo*-**1d**	H	*m*-MeO	0.456	0.94	0.94
14	*exo*-**1e**	H	*p*-Me	0.523	1.1	1.2
15	*exo*-**1f**	H	*m*-Me	0.478	0.98	0.70
16	*exo*-**1h**	H	*p*-Cl	0.420	0.86	0.39
17	*exo*-**1i**	H	*m*-Cl	0.345	0.71	0.33
18	*exo*-**1k**	H	*p*-CF_3	0.278	0.57	0.30

[a] The second-order rate constants *k* were obtained by dividing the pseudo-first-order rate constant k_{obs} by the concentration of BF_3. The *k* values are the average of at least two measurements. Error limit of *k* is ±2%.
[b] The relative rate constant of cyclobutene ring-opening reaction of analogous homobenzoquinones **4**.
[c] The second-order rate constant *k*(**4g**) = 1.25 x 10^{-3} $M^{-1}s^{-1}$(cf ref 8).

exo-*m*/*p*-substituted couples showed the usual substituent effects for both the **1** and **4**.

Since the *endo*-aromatic ring is located at the δ-position with respect to the epoxide carbon atom, the notable rate-acceleration by electron-donating *m*- and *p*-substituents can not be ascribed to the direct inductive or the resonance stabilization of a rate-determining transition state. Indeed, the *exo*-aromatic substituents lacked the drastic effects on the rates. Accordingly, the remarkable rate dependency on the *endo*-substituents must be explained by considering the through-space electron donation of the overhanging aromatic nucleus to the acid-activated oxirane ring. In order to evaluate the degree to which the present acid-catalyzed ring-opening reactions respond to the *meta* and *para* substituent changes of **1,** the author

applied a linear free energy relationships analysis for k_{rel}(**1**). As a consequence, it was found that the usual Hammett treatment for the *endo*-X substituted series by using σ or σ^+ one parameter[13] provided rather poor correlations; log k_{rel}^{endo}(**1**) = – 4.5σ + 0.35 (r^2 = 0.89, n = 8) and – 2.8σ^+ – 0.09 (r^2 = 0.77, n = 8) respectively.[14] These unsatisfactory correlations with the normal single parameter apparently indicate that the π-aryl participation of *endo*-aromatic ring must be performed not only at the *ipso*- but also at the *ortho*-carbon atom. This simultaneous binding seems to be responsible for the formation of the *ortho*- and the *ipso*-carbon bound products, **2j** and **3j**, from the bis(*p*-chlorophenyl)-substituted **1j** (Scheme 1a).[6]

Based on these findings, the author thought that the transannular S_E2-Ar cyclization of *endo*-aryl groups of **1** involves a dihapto (η^2) π-aryl participated transition state through the *ipso* and the *ortho* carbon atom. Although the *m*-substituted aromatic nucleus has two different *ortho*-positions with respect to the *ipso*-carbon, the less congested *ortho*-position, that is to say *para* to the introduced *m*-substituent, is expected to participate in the product formation (vide infra). Accordingly, the author attempted to correlate the log k_{rel}^{endo}(**1**) with the combination of newly defined two site-dependent substituent parameters σ^{ipso} and σ^{ortho} which display the substituent effects on the *ipso*- and *ortho*-aromatic carbon atoms, respectively. Thus, the substituent constant σ^{ipso} is related to the *ipso*-participation by using σ_p^+ for *p*-X and σ_m for *m*-X substituent.[13] On the other hand, the other σ^{ortho} refers to the *ortho*-participation by using, specifically, σ_m for *p*-X and σ_p^+ for the *m*-X substituent,

$$\log k_{rel}^{endo}(\mathbf{1}) = -2.49\sigma^{ipso} - 1.62\sigma^{ortho} - 0.108 \quad (R^2 = 0.98,\ n = 8) \quad (1)$$

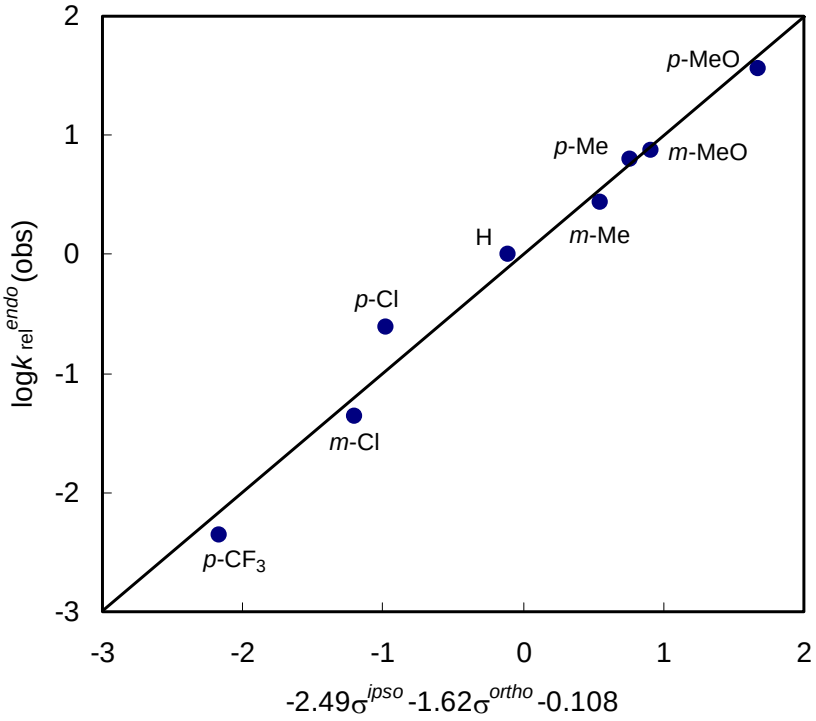

Figure 2. Plots of the observed log k_{rel}^{endo}(**1**)(obs) vs the caluculated log k_{rel}^{endo}(**1**)(calc) according to eq. 1 for BF_3-catalyzed rearrangements of unsubstituted **1g** and *endo*-substituted **1a, d-f, h, i,** and **k** in $CDCl_3$ at 30 °C.

respectively. As expected, a very sufficient regression was obtained by considering such η^2-type coordination of *endo*-aromatic ring through the *ipso* and *ortho*-positions (eq. 1 and Figure 2). Here, it is noteworthy that the η^2-binding of aromatic ring is more effectively performed at the *ipso*-carbon than the *ortho*-one as indicated by the percent contribution of the parameter σ^{ipso} (61%) and σ^{ortho} (39%).

As to the *exo*-Y substituted series, the author observed only 2-fold rate-acceleration irrespective of the wide range of *p*-MeO/*p*-CF_3 substituent variation. These *exo*-isomers provided a good linear free energy relationship when used Yukawa-Tsuno (Y-T) equation,[15,3(d)] where σ^0 is the normal substituent constant and $\Delta\bar{\sigma}_R^+$ is the resonance substituent constant defined by ($\sigma^+ - \sigma^0$) (eq. 2). The present reaction yielded a small negative

$$\log k_{rel}^{exo} = -0.912(\sigma^0 + 0.237\Delta\bar{\sigma}_R^+) \quad (R^2 = 0.96, n = 8) \quad (2)$$

reaction constant ($\rho = -0.912$) and a small resonance parameter ($r = 0.237$). These very low values are certainly due to the reduced *exo*-substituent effects on the far more remote acid-activated oxirane-ring (δ-position through the intervened cyclopropane and carbonyl function). Incidentally, the well-known acetolyses of β-aryltosylates and brosylates at 75-115 °C also displayed the Y-T equations with larger ρ values of –3.3 ~ –4.0 and *r* values of 0.54 ~ 0.63.[16] The enhanced substituent effects of these reactions can be explained by the formation of phenonium ion intermediates via the π-aryl participation at the *ipso*-carbon.

In the later section, the author will discuss these kinetic substituent effects from the mechanistic viewpoints in comparison with those of the analogous S_E2-Ar transannular cyclization of **4a-k**.

2-2-3. Mechanistic Considerations

(a) π-Aryl Participation in S_N2 type Ring-Opening of Epoxide. The acid-catalyzed cleavage of the oxirane C-O bond preferentially occurs in such a way that the substituent of the oxirane ring further stabilizes the developing positive charge by both, electron donation and the conjugation.[17] Accordingly, the reaction features are highly dependent on the substituents on the oxirane ring as well as the nucleophiles. Mechanistically, the nucleophilic displacement of epoxides can be rationalized by either concerted attack of a nucleophile on the acid activated oxirane ring (S_N2 mechanism) or by stepwise attack of a nucleophile on a pre-formed carbocation intermediate (S_N1 mechanism). [17(b),(e),18] Most of the reactions are generally known to proceed through the regio- and stereoselective ring cleavage under the S_N2 anti nucleophilic assistance.[19] However, the S_N1 mechanism is reported for the reaction of epoxides bearing strongly electron-releasing and conjugated substituents in the high polar solvents.[20]

Since the present epoxide ring is substituted by two electron-withdrawing quinone carbonyl groups, the acid-catalyzed ring-cleavage of **1** seems to obey the S_N2 process in the less polar $CDCl_3$.[21] Under these conditions, the overhanging *endo*-aromatic ring is apt to behave as an effective internal π-nucleophile. Indeed, the author has obtained very poor kinetic solvent effects ($k^{\text{dichloroethane}}/k^{\text{benzene}}$ =3.0) regardless of the appreciable change of solvent polarity (as indicated by the polarity parameter; $E_T(30)$ = 41.3 for 1,2-dichloroethane and 34.3 for benzene)[22] for the same transannular cyclization of **1g** by protic acid $MeSO_3H$.[6] The negligible solvent effects can be taken as a conclusive mechanistic criterion for the concerted process involving the less polar transition state.[21]

The mechanistic evidence for the concertedness was also obtained for the above mentioned dual *ipso*/*ortho* transannular S_E2-Ar reactions of bis(*p*-chlorophenyl)homobenzoquinone epoxide **1j**.[6] The common π-aryl participated transition state leads to the *ortho*-linked product **2** via σ-complex **I** and competitively to the *ipso*-linked product **3** via the π-resonating σ-complex **II** followed by the hydrolysis with residual water (Scheme 2). The present *p*-anisyl- and *p*-chloro-substituted *endo*-**1a** and

Scheme 2.

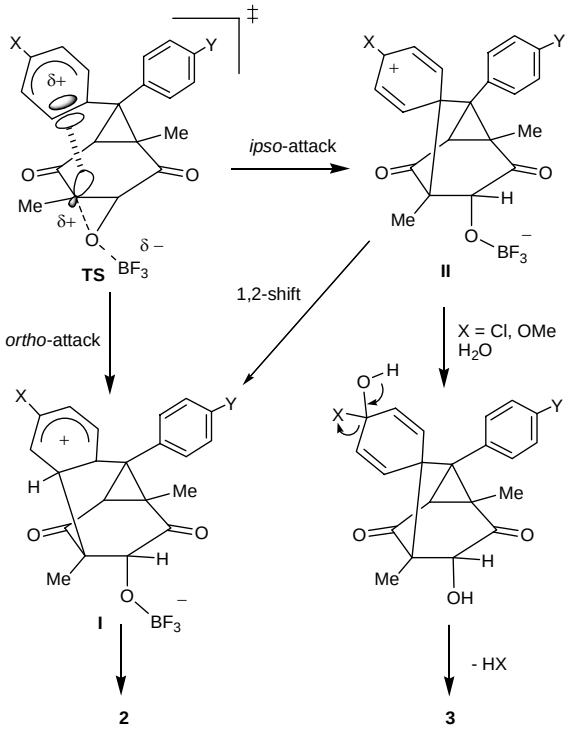

endo-**1h** also provided **3a** (~100 %) and **3h** (80%) along with **2h** (20%), respectively. Quantitative formation of **3a** for the reaction of *endo*-**1a** may be explained in view of the reaction pathways on which the common transition state TS would prefer the very facile degradation into the π-resonating and water sensitive intermediate **II** rather than the less stabilized **I**. By contrast, other *para*-substituents (including H) brought about the exclusive formation of **2** via the *ortho*-linked σ-complex **I**. This is probably because the possible *ipso*-linked σ-complex **II** can not be transformed into the stable **3** via the nucleophilic

displacement by residual water, but rather underwent the facile 1,2-shift to the *ortho*-linked **I** reading to **2**. Thus, it is not suprising that the percent contribution of the σ^{ipso} and σ^{ortho} in the transition state stabilization can not be directly reflected on the product distributions which are dependent on the following channels to the respective **I** and **II** as well as the contaminant water. The author also found that the transannular cyclization of *endo m*-X-substituted aromatic ring occurs exclusively at the less congested *ortho*-position (i.e., *para*-position with respect to the *m*-X) as confirmed by the representative reaction of *endo m*-MeO-substituted **1d**. A significant steric hindrance of *m*-MeO with the oxirane Me group probably inhibits the alternative π-aryl participation at the adjacent *ortho*-position.

(b) Prominent Role of Oxirane Walsh Orbital. In the acid-catalyzed intramolecular S_E2-Ar reactions of **1a-k**, the vacant oxirane Walsh orbital seems to play a crucial role in the initial epoxide ring-opening with the aid of *endo*-aromatic ring.[23] However, the aryl participation in the ring opening of epoxides is scarcely reported but has been put forward in the acid-induced ring opening of a particular case of epoxides bearing aryl groups directly or indirectly linked to the oxirane ring. For instance, the well-documented phenonium ion intermediates via the aryl participated transition states are invoked in the reactions of stilbene oxides[17(a)] and spiro-linked 2-phenyl-1,2-epoxide[24] or 1-benzyl-1,2-epoxides.[25] In our previous study using the ethano-bridged diphenylhomobenzoquinone epoxides, the author has found that the rate of the acid-catalyzed transannular cyclization is highly dependent on the rigid conformation of *endo*-aryl ring.[23] The author rationalized the conformational effects on the basis of the π-aryl participated orbital interaction with the vacant oxirane Walsh orbital. Keeping this in mind, the author will later interpret the present kinetic substituent effects in terms of the geometrically restricted orbital interaction in the S_N2-type epoxide ring-opening.

The author has previously found that the analogous cyclobutene-fused *endo*/*exo m*- and *p*-substituted diarylhomobenzoquinones **4** exhibited the similar π-aryl participated transannular S_E2-Ar cyclization under BF_3 acid conditions (Scheme 1b).[6] This cyclobutene ring-opening reaction involves the formal vinyl-anion migration to the adjacent acid-activated carbonyl carbon associated with the concerted S_N2 transannular cyclization of *endo*-aryl group.[26] Accordingly, the vacant cyclobutene *anti*-bonding orbital activated by the adjoining BF_3-complexed carbonyl group will accept the π-electrons of the *endo*-aryl group and facilitate the σ-bond cleavage. Therefore, a comparison between the epoxide and the cyclobutene ring-opening reactions will provide a very useful insight into the stereoelectronic effects in the π-aryl participated orbital interaction.

2-2-4. Stereoelectronic Effects in Dihapto(η^2) π-Aryl Participation

As previously reported, the author has obtained the excellent two parameter regression using the σ^{ipso} and σ^{ortho} parameters for the BF_3-catalyzed transannular cyclization of cyclobutene-fused *endo m*- and *p*-substituted diarylhomobenzoquinones **4** (eq. 3).[6] This

equation also manifested the η^2-coordination in the π-aryl participated transition state (Figure 3b). The percent contribution of σ^{ipso} (47%) is slightly smaller than that of σ^{ortho} (53%). This is in contrast to the reaction of epoxides **1**, where the σ^{ipso} contributed 1.6 times more effectively than σ^{ortho} (eq. 1).

$$\log k_{rel}^{endo}(\mathbf{4}) = -2.07\sigma^{ipso} - 2.33\sigma^{ortho} - 0.172 \quad (R^2 = 0.99, n = 8) \quad (3)$$

Why does the *endo*-**4** undergo the slightly enhanced substituent effects on the *ortho*-carbon atom, but the *endo*-**1** the more significant substituent effects on the *ipso*-carbon atom? To answer this question, the author must recall that the acid-catalyzed S_N2-type nucleophilic displacement of **1** and **4** involves the π-aryl participated transition states. The π-electron donation should occur onto the vacant oxirane Walsh orbital of **1** and the

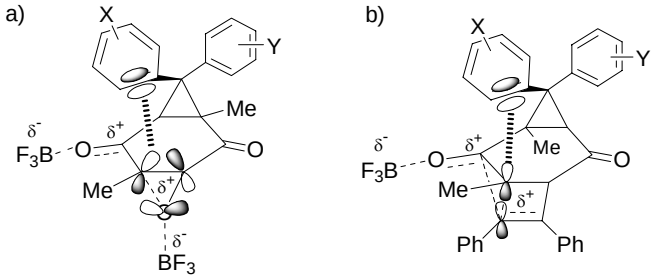

Figure 3. a) Representative lowest unoccupied Walsh orbital of epoxides **1** and b) the unoccupied orbital (in part) of cyclobutene ring of **4**.

cyclobutene anti-bonding σ^* orbital of **4**, respectively. Since the lowest unoccupied Walsh orbital (LUMO) is trigonally bent, the geometrical orbital interaction with the *endo*-aromatic ring (HOMO) may be represented in Figure 3. Thus, the dihapto π-aryl participation of **1** can be more effectively performed at the *ipso*-carbon rather than the *ortho*-one (Figure 3a). By contrast, such a stereoelectronic preference for the *ipso*-position should be considerably reduced for **4** because the vector of the relevant four-membered cyclobutene σ^*-bond deviates from the vertical plane through the *ipso*- and *para*-position of the aromatic ring (Figure 3b). Indeed, a theoretical calculation by DFT B3LYP/6-31G* method[27] apparently showed the similar geometrical characteristics for the relevant vacant orbitals of epoxide and cyclobutene

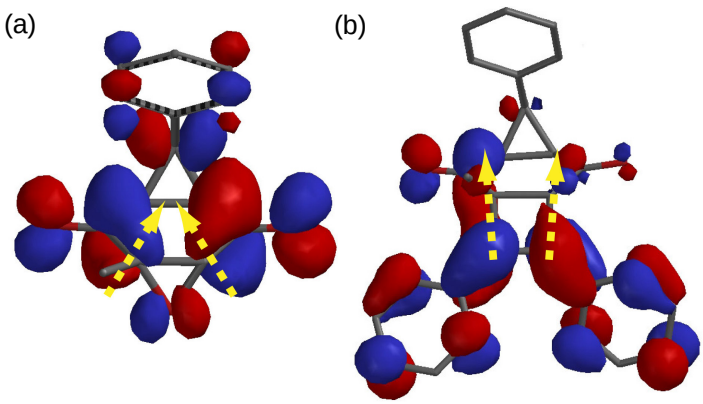

Figure 4. LUMO orbitals of (a) epoxide **1g** and (b) cyclobutene-fused analogue **4g** optimized by B3LYP/6-31G* method (*exo*-aromatic ring is omitted for clarity).

ring moieties (Figure 4). The vacant Walsh orbital of **1g** at the carbon corner is conjugated with the carbonyl π*-orbital but is rather directed to the aromatic *ipso*-carbon (as yellow dotted arrow in Figure 4a). On the other hand, the vector of vacant cyclobutene orbital of **4g** is essentially perpendicular (yellow dotted arrow) to the quinone plane and is expected to enjoy the ideal *ipso*/*ortho* η^2 coordination with the faced *endo*-aromatic nucleus (Figure 4b). This is because the epoxides **1g** display more effective *ipso*-contribution in the η^2 π-aryl participation than the cyclobutene-cleaved **4g**.

$$\log k_{rel}^{exo} = -0.794(\sigma^0 + 0.904\Delta\bar{\sigma}_R^+) \qquad (R^2 = 0.96, n = 8) \quad (4)$$

As to the *exo*-Y substituted **4**, the author previously obtained the Y-T equation (eq. 4) with a larger *r* value of 0.904 than the similar equation for *exo*-**1** (*r* = 0.237, eq. 2).[6] The larger resonance parameter *r* means that the π-delocalization of *exo*-aryl substituents of **4** can appreciably stabilize the developing positive charge on the acid-activated γ-located carbonyl carbon atom. Such an activation of carbonyl π*-orbital results in the acceleration of the concerted vinyl anion migration responsible for the S_E2-Ar transannular cyclization of **4**. By contrast, as seen in the Y-T equation 2, the reduced resonance stabilization by the *exo*-aryl substituents of **1** may be due to the change in the reaction mechanism. The epoxide ring-opening is substantially facilitated by the binding of BF_3 not at the carbonyl oxygen but at the epoxide oxygen atom. Even if the carbonyl function is activated by BF_3 like in **4**, it would rather deactivate the ring-opening because of the destabilization of the developing positive charge on the epoxide carbon atom.

2-3. Conclusion

In summary, the author has performed a kinetic study of the BF_3-catalyzed ring-opening reactions of *endo*/*exo m*- and *p*-substituted diarylhomobenzoquinone epoxides **1**. These reactions proceeded through two types of S_E2-Ar transannular cyclizations to give tricyclic diketo-alcohols and cyclohexadienone spiro-linked tricyclic diketo-alcohols, respectively. The rates were significantly accelerated by the through-space π-aryl participation of electron-donating *endo*-aromatic rings, but negligibly influenced by the through-bond electronic effects of *exo*-aromatic rings. The Hammett treatment using modified site-dependent substituent parameters σ^{ipso} and σ^{ortho} indicated that the *ipso*/*ortho* dihapto(η^2) π–aryl participation occurs for the *endo*-aryl groups. Kinetics substituent effects of these reactions were compared with those of the analogous acid-catalyzed transannular cyclization of the cyclobutene-fused diarylhomobenzoquinones **4**. It was found that the present epoxides **1** exhibit the η^2 π-aryl participation with the 1.6-times more effective contribution at the *ipso*-position, whereas the cyclobutene-fused homologues **4** with almost comparable *ipso*/*ortho* contribution. These results were interpreted in terms of the geometrical

features of the π-electron accepting vacant orbital of oxirane and cyclobutene ring. The physicochemical information obtained in the present study will provide a very important insight into the understanding of the π-aryl participation as well as the mechanistic aspects in the acid-catalyzed ring-opening reaction of epoxides.

2-4. Experimental Section

Materials. Deuterated Chloroform ($CDCl_3$) was purchased from Aldrich Chemicals Ltd. and used without further purification. All epoxides **1a-k** were prepared according to the previous methods by the epoxidation of the corresponding diarylhomobenzoquinones.[6] The *endo*/*exo* isomeric mixtures were separated by a column chromatography on silica gel with a mixture of hexane/ethyl ether as an eluent and purified by recrystallization from chloroform/pentane. The analytical data are collected below. Unfortunately, we could not obtain the pure *endo*-**1e**, *endo*/*exo*-**1i** because of the contamination of the respective isomers. The assignment of the *endo*/*exo* stereochemistry of **1a**, **d-f**, **h**, and **k** failed because of the complexity in their ^{1}H-NMR spectra. Thus, the stereochemistry was tentatively deduced from their kinetic behaviors; i.e., the more reactive isomers of **1a** and **d-f** are *endo* but the more reactive isomers of **1h**, **i**, and **k** are *exo*.

Kinetic Measurements. The kinetic data were obtained by at least duplicate measurements according to the NMR spectroscopic methods. The solution of epoxide **1** (0.02 mmol, $CDCl_3$, 0.67 mL) for kinetic experiments was prepared in a stoppered NMR tube and preheated at 30°C (±0.1) in a thermostated bath. The reaction was initiated by the quick addition of the requisite volume of catalyst $BF_3{\cdot}OEt_2$ (0.3 M) and submitted for the NMR measurements at 30°C (±0.1) in a thermostated tube holder. For the reactive **1a**, the introduced amount of $BF_3{\cdot}OEt_2$ was reduced to 1/10 and 1/5 (0.03 and 0.06 M). For the less or least reactive *endo*-**1h**, **1j** and *endo*-**1k**, the NMR tube was sealed with a gas burner. The progress of reactions was followed by requisite interval monitoring the relative signal intensity of the diagnostic methy groups on cyclopropane (0.91 ~ 1.01 ppm) and oxirane ring (1.17 ~ 1.22) of **1** over 75% conversion with respect to the internal standard TMS. For the least reactive *endo*-**1k**, the measurements were performed at requisite time interval by taking the sealed NMR tube out of a thermostated bath (30°C (±0.1)). The natural logarithmic plots of the relative amounts of **1** with respect to the measurement starting point (t = 0) gave the correlation line against time. The obtained first-order rate constants (slope) were divided by the concentration of catalyst to provide the second-order rate constants. The first-order decay plots and the logarithmic plots for the most reactive *endo*-**1a**, the unsubstituted **1g**, and the least reactive *endo*-**1k** are represented in SI.

Acid-Catalyzed Reaction of 1a-k. The acid-induced reactions of epoxides **1a-k** (0.02 mmol) were carried out in the presence of $BF_3{\cdot}OEt_2$ (0.30 M) in $CDCl_3$ (0.67 mL) at room temperature. After the completion of reactions, the reaction solution was transferred into a separate funnel, diluted with chloroform (10 mL) and then washed with water (3 mL × 3). The aqueous layer was extracted with chloroform (5 mL × 2). The combined organic layer was washed with water (3 mL × 3), then dried over calcium chloride. After the evaporation of the solvent *in vacuo*, the residue was submitted for the ^{1}H NMR analysis to determine the product distributions. The reactions were found to give the *ortho*-carbon bound tricyclic diketo-alcohols **2b-k** together with the *ipso*-carbon bound 2,5-cyclohexadien-4-one spiro-linked tricyclic diketo-alcohol **3a** (~100%), **3h** (the same as **3a**, 80), and **3j** (81) for *endo*-**1a**, *endo*-**1h**, and **1j**, respectively, in almost quantitative total yields based on the consumed **1**. Except for the representative reactions of *endo*-**1a**, **1b**, *endo*-**1d**, *endo*-**1h**, and **1j**, no further detailed analyses of products were carried out. The analytical data of the products **2b**, **2g**, **2j**, **3j** have been already described elsewhere.[6,28] The new compounds **3a** and *endo*-**2d** were isolated by column chromatography on silica gel with a mixture of hexane/ethyl acetate as an eluent.

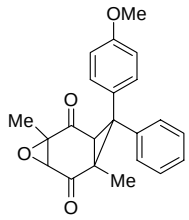

***Endo*-1,5-dimethyl-8-phenyl-8-(4-anisyl)-4-oxa-tricyclo[5.1.0.0^{3,5}]octane-2,6-dione** (*endo*-**1a**): mp 116.5-117.5 ^{o}C, colorless prisms (chloroform/pentane); ^{1}H-NMR (270 MHz, $CDCl_3$) δ 0.91 (s, 3H), 1.19 (s, 3H), 2.78 (s, 1H), 2.80 (s, 1H), 3.75 (s, 3H), 6.80-6.84 (m, 2H), 7.18-7.30 (m, 7H); ^{13}C-NMR (67 MHz, $CDCl_3$) δ 13.6, 16.7, 37.9, 40.0, 49.2, 55.3, 60.1, 60.4, 114.4, 127.8, 129.2, 129.5, 129.6, 132.3, 138.7, 159.0, 198.5, 200.6; IR (KBr) 1705 (C=O) cm^{-1}. *Anal* Calcd for $C_{22}H_{20}O_4$: C, 75.84; H, 5.79; O, 18.37. Found: C, 75.69; H, 5.72; O, 18.59.

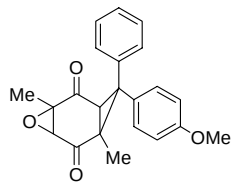

***Exo*-1,5-dimethyl-8-(4-anisyl)-8-phenyl-4-oxa-tricyclo[5.1.0.0^{3,5}]octane-2,6-dione** (*exo*-**1a**): mp 105.8-106.8 ^{o}C, colorless prisms (chloroform/pentane); ^{1}H-NMR (270 MHz, $CDCl_3$) δ 0.99 (s, 3H), 1.17 (s, 3H), 2.79 (s, 1H), 2.86 (s, 1H), 3.73 (s, 3H), 6.76-6.79 (m, 2H), 7.16-7.37 (m, 7H); ^{13}C-NMR (67 MHz, $CDCl_3$) δ 13.8, 16.8, 37.5, 39.5, 48.9, 55.3, 60.3, 60.5, 114.5, 127.5, 128.2, 129.0, 130.2, 130.8, 140.5, 159.1, 198.6, 200.8; IR (KBr) 1695 (C=O) cm^{-1}. *Anal* Calcd for $C_{22}H_{20}O_4$: C, 75.84; H, 5.79; O, 18.37. Found: C, 75.69; H, 5.72; O, 18.59.

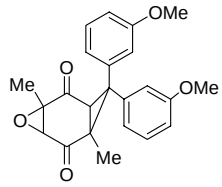

1,5-dimethyl-8,8-bis(3-anisyl)-4-oxa-tricyclo[5.1.0.0^{3,5}]octane-2,6-dione (**1c**): mp 194.5-195.1 ^{o}C, colorless prisms (chloroform/pentane); ^{1}H-NMR (270 MHz, $CDCl_3$) δ 0.97 (s, 3H), 1.20 (s, 3H), 2.78 (s, 1H), 2.84 (s, 1H), 3.74 (s, 3H), 3.78 (s, 3H), 6.71-7.36 (m, 8H); ^{13}C-NMR (67 MHz, $CDCl_3$) δ 13.8, 16.7, 37.6, 49.5, 55.3, 60.1, 60.3, 112.7, 113.8, 114.6, 115.1, 120.7, 121.8, 130.0, 130.2, 139.5, 141.2, 159.8, 198.3, 200.5; IR (KBr) 1698 (C=O) cm^{-1}. *Anal* Calcd for $C_{23}H_{22}O_5$: C, 73.00; H, 5.86; O, 21.14. Found: C, 72.97; H, 5.85; O, 21.18.

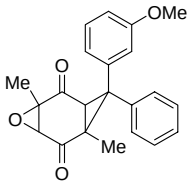

***Endo*-1,5-dimethyl-8-(3-anisyl)-8-phenyl-4-oxa-tricyclo[5.1.0.0^{3,5}]octane-2,6-dione**(*endo*-**1d**): mp 165.6-166.6 ^{o}C, colorless prisms (chloroform/pentane); ^{1}H-NMR (270 MHz, $CDCl_3$) δ 0.98 (s, 3H), 1.18 (s, 3H), 2.80 (s, 1H), 2.85 (s, 1H), 3.74 (s, 3H), 6.72-6.86 (m, 3H), 7.14-7.41 (m, 6H); ^{13}C-NMR (67 MHz, $CDCl_3$) δ 13.8, 16.8, 37.6, 39.7, 49.6, 55.3, 60.1, 60.3, 113.8, 115.1, 121.8, 127.7, 128.4, 128.9, 130.3, 139.6, 139.8, 159.8, 198.4, 200.5; IR (KBr) 1699 (C=O) cm^{-1}. *Anal* Calcd for $C_{22}H_{20}O_4$: C, 75.84; H, 5.79; O, 18.37. Found: C, 75.72; H, 5.75; O, 18.53.

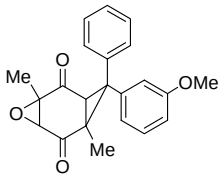

***Exo*-1,5-dimethyl-8-(3-anisyl)-8-phenyl-4-oxa-tricyclo[5.1.0.0^{3,5}]octane-2,6-dione**(*exo*-**1d**): mp 168.8-169.8 ^{o}C, colorless prisms (chloroform/pentane); ^{1}H-NMR (270 MHz, $CDCl_3$) δ 0.91 (s, 3H), 1.21 (s, 3H), 2.80 (s, 1H), 2.80 (s, 1H), 3.78 (s, 3H), 6.73-6.76 (m, 1H), 6.90-6.96 (m, 2H), 7.19-7.26 (m, 6H); ^{13}C-NMR (67 MHz, $CDCl_3$) δ 13.6, 16.8, 37.6, 39.7, 49.5, 55.3, 60.1, 60.4, 112.7, 114.6, 120.6, 128.0, 129.2, 129.7, 130.0, 138.2, 141.5, 159.9, 198.3, 200.6; IR (KBr) 1699 (C=O) cm^{-1}. *Anal* Calcd for $C_{22}H_{20}O_4$: C, 75.84; H, 5.79; O, 18.37. Found: C, 75.72; H, 5.75; O, 18.53.

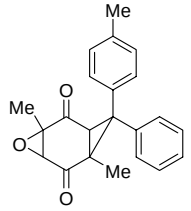

***Endo*-1,5-dimethyl-8-phenyl-8-(4-tolyl)-4-oxa-tricyclo[5.1.0.0^{3,5}]octane-2,6-dione** (*endo*-**1e**): (This compound could not be obtained in pure form because of the contamination of small amount of *exo*-**1e**). ^{1}H-NMR (270 MHz, $CDCl_3$) δ 0.95 (s, 3H), 1.18 (s, 3H), 2.25 (s, 3H), 2.80 (s, 1H), 2.83 (s, 1H), 7.39-6.86 (m, 3H), 7.14-7.39 (m, 9H); ^{13}C-NMR (67 MHz, $CDCl_3$) δ 13.7, 16.8, 21.0, 37.5, 39.6, 49.4, 60.1, 60.4, 127.6, 128.3, 128.9, 129.4, 129.8, 135.2, 137.9, 140.3, 198.5, 200.7. *Anal* Calcd for $C_{22}H_{20}O_3$: C, 79.50; H, 6.06; O, 14.44. Found: C, 79.50; H, 6.05; O, 14.45.

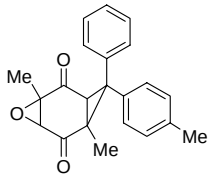

***Exo*-1,5-dimethyl-8-(4-tolyl)-8-phenyl-4-oxa-tricyclo[5.1.0.0^{3,5}]octane-2,6-dione** (*exo*-**1e**): mp 143.9-144.9 ^{o}C, colorless prisms (chloroform/pentane); ^{1}H-NMR (270 MHz, $CDCl_3$) δ 0.91 (s, 3H), 1.19 (s, 3H), 2.28 (s, 3H), 2.79 (s, 1H), 2.80 (s, 1H), 7.10-7.28 (m, 9H); ^{13}C-NMR (67 MHz, $CDCl_3$) δ 13.6, 16.8, 21.0, 37.8, 39.8, 49.5, 60.1, 60.3, 127.9, 128.2, 129.2, 129.6, 129.7, 137.1, 137.5, 138.5, 198.5, 200.7; IR (KBr) 1708 (C=O) cm^{-1}. *Anal* Calcd for $C_{22}H_{20}O_3$: C, 79.50; H, 6.06; O, 14.44. Found: C, 79.50; H, 6.05; O, 14.45.

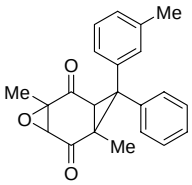

***Endo*-1,5-dimethyl-8-phenyl-8-(3-tolyl)-4-oxa-tricyclo[5.1.0.0^{3,5}]octane-2,6-dione** (*endo*-**1f**): mp 137.1-138.1 ^{o}C, colorless prisms (chloroform/pentane); ^{1}H-NMR (270 MHz, $CDCl_3$) δ 0.93 (s, 3H), 1.18 (s, 3H), 2.27 (s, 3H), 2.79 (s, 1H), 2.80 (s, 1H), 6.99-7.41 (m, 9H); ^{13}C-NMR (67 MHz, $CDCl_3$) δ 13.6, 16.8, 21.2, 37.6, 39.8, 49.7, 60.0, 60.2, 126.6, 127.6, 128.4, 128.7, 129.0, 129.1, 130.2, 138.2, 139.1, 140.1, 198.4, 200.5; IR (KBr) 1700 (C=O) cm^{-1}. *Anal* Calcd for $C_{22}H_{20}O_3$: C, 79.50; H, 6.06; O, 14.44. Found: C, 79.33; H, 5.97; O, 14.70.

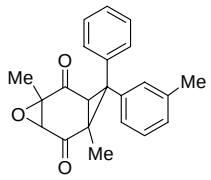

***Exo*-1,5-dimethyl-8-(3-tolyl)-8-phenyl-4-oxa-tricyclo[5.1.0.0^{3,5}]octane-2,6-dione** (*exo*-**1f**) mp 116.2-117.2 ^{o}C, colorless prisms (chloroform/pentane); ^{1}H-NMR (270 MHz, $CDCl_3$) δ 0.92 (s, 3H), 1.19 (s, 3H), 2.32 (s, 3H), 2.80 (s, 1H), 2.81 (s, 1H), 7.02-7.27 (m, 9H); ^{13}C-NMR (67 MHz, $CDCl_3$) δ 13.6, 16.8, 21.4, 37.6, 39.7, 49.7, 60.1, 60.3, 125.4, 127.9, 128.5, 128.8, 128.9, 129.2, 129.6, 138.4, 138.8, 139.9, 198.5, 200.7; IR (KBr) 1703 (C=O) cm^{-1}. *Anal* Calcd for $C_{22}H_{20}O_3$: C, 79.50; H, 6.06; O, 14.44. Found: C, 79.33; H, 5.97; O, 14.70.

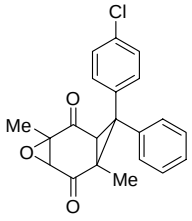

***Endo*-1,5-dimethyl-8-phenyl-8-(4-chlorophenyl)-4-oxa-tricyclo[5.1.0.0^{3,5}]octane-2,6-dione** (*endo*-**1h**): mp 126.2-127.2 ^{o}C, colorless prisms (chloroform/pentane); ^{1}H-NMR (270 MHz, $CDCl_3$) δ 1.01 (s, 3H), 1.19 (s, 3H), 2.81 (s, 1H), 2.89 (s, 1H), 7.18-7.38 (m, 9H); ^{13}C-NMR (67 MHz, $CDCl_3$) δ 13.6, 16.8, 37.4, 39.3, 48.3, 60.3, 60.4, 127.9, 128.3, 129.1, 129.4, 131.0, 134.2, 136.8, 139.7, 198.2, 200.5; IR (KBr) 1695 (C=O) cm^{-1}. *Anal* Calcd for $C_{21}H_{17}ClO_3$: C, 71.49; H, 4.86; Cl, 10.05; O, 13.60. Found: C, 71.20; H, 4.87; Cl, 10.23; O, 13.70.

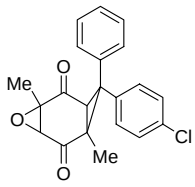

***Exo*-1,5-dimethyl-8-(4-chlorophenyl)-8-phenyl-4-oxa-tricyclo[5.1.0.0^{3,5}]octane-2,6-dione** (*exo*-**1h**): mp 173.7-174.7 ^{o}C, colorless prisms (chloroform/pentane); ^{1}H-NMR (270 MHz, $CDCl_3$) δ 0.92 (s, 3H), 1.19 (s, 3H), 2.77 (s, 1H), 2.82 (s, 1H), 7.21-7.34 (m, 9H); ^{13}C-NMR (67 MHz, $CDCl_3$) δ 13.6, 16.8, 37.3, 39.5, 48.6, 60.2, 60.3, 128.2, 129.2, 129.3, 129.6, 129.7, 133.7, 137.8, 138.6, 198.1, 200.3; IR (KBr) 1705 (C=O) cm^{-1}. *Anal* Calcd for $C_{21}H_{17}ClO_3$: C, 71.49; H, 4.86; Cl, 10.05; O, 13.60. Found: C, 71.20; H, 4.87; Cl, 10.23; O, 13.70.

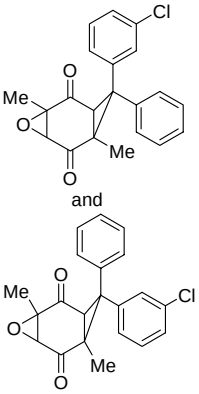

***Endo/exo*-1,5-dimethyl-8-phenyl-8-(3-chlorophenyl)-4-oxa-tricyclo[5.1.0.0^{3,5}]octane-2,6-dione** (*endo/exo*-**1i**): (These compounds could not be separated); ^{1}H-NMR (270 MHz, $CDCl_3$) δ 0.93 (s, 3H), 1.01 (s, 3H), 1.19 (s, 3H), 1.20 (s, 3H), 2.78 (s, 1H), 2.81 (s, 1H), 2.81 (s, 1H), 2.87 (s, 1H), 7.14-7.40 (m, 18H); ^{13}C NMR (67 MHz, $CDCl_3$) δ 13.6, 13.6, 16.8, 16.8, 37.3, 37.5, 39.4, 39.5, 48.5, 48.7, 60.2, 60.2, 60.2, 60.3, 126.6, 127.8, 128.0, 128.0, 128.3, 128.3, 128.4, 128.5, 129.1, 129.3, 129.7, 129.7, 130.3, 130.5, 134.8, 135.0, 137.5, 139.3, 140.2, 141.9, 198.0, 198.0, 200.2, 200.2; IR (KBr): 1703 (C=O) cm^{-1}. *Anal* Calcd for $C_{21}H_{17}ClO_3$: C, 71.49; H, 4.86; Cl, 10.05; O, 13.60. Found: C, 71.43; H, 4.83; Cl, 10.00; O, 13.74.

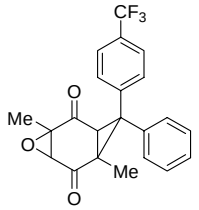

***Endo*-1,5-dimethyl-8-phenyl-8-(4-trifluoromethylphenyl)-4-oxa-tricyclo[5.1.0.0^{3,5}]octane-2,6-dione** (*endo*-**1k**): mp 158.8-159.8 ^{o}C, colorless prisms (chloroform/pentane); ^{1}H-NMR (270 MHz, $CDCl_3$) δ 0.96 (s, 3H), 1.22 (s, 3H), 2.85 (s, 1H), 2.87 (s, 1H), 7.24-7.55 (m, 9H); ^{13}C-NMR (67 MHz, $CDCl_3$) δ 13.5, 14.0, 16.9, 37.3, 39.3, 48.4, 60.2, 60.3, 123.6 (q, J_{CF} = 272.1 Hz), 126.1 (q, J_{CF} = 3.91 Hz), 128.1, 128.4, 129.2, 130.1, 130.3 (q, J_{CF} = 33.0 Hz), 139.1, 142.3, 198.1, 200.4; IR (KBr) 1704 (C=O) cm^{-1}. *Anal* Calcd for $C_{22}H_{17}F_3O_3$: C, 68.39; H, 4.43; F, 14.75; O, 12.42. Found: C, 68.27; H, 4.39; F, 14.84; O, 12.50.

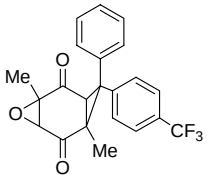

***Exo*-1,5-dimethyl-8-(4-trifluoromethylphenyl)-8-phenyl-4-oxa-tricyclo[5.1.0.0^{3,5}]octane-2,6-dione** (*exo*-**1k**): mp 157.8-158.8 ^{o}C, colorless prisms (chloroform/pentane); ^{1}H-NMR (270 MHz, $CDCl_3$) δ 0.94 (s, 3H), 1.20 (s, 3H), 2.81 (s, 1H), 2.84 (s, 1H), 7.23-7.60 (m, 9H); ^{13}C-NMR (67 MHz, $CDCl_3$) δ 13.6, 16.9, 37.1, 39.3, 48.6, 60.2, 60.3, 123.8 (q, J_{CF} = 272.1 Hz), 126.1 (q, J_{CF} = 3.91 Hz), 128.4, 128.9, 129.4, 129.5 (q, J_{CF} = 33.0Hz), 129.6, 137.3, 143.8, 197.9, 200.1; IR (KBr) 1701 (C=O) cm^{-1}. *Anal* Calcd for $C_{22}H_{17}F_3O_3$: C, 68.39; H, 4.43; F, 14.75; O, 12.42. Found: C, 68.27; H, 4.39; F, 14.84; O, 12.50.

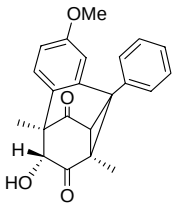

(1R*,8R*,9S*,10R*,12S*)-12-Hydroxy-5-methoxy-1,10-dimethyl-8-phenyl-tetracyclo-[6.4.1^{1,9}.0^{2,7}.0^{8,13}]trideca-2(7),3,5-triene-11,13-dione (**2d**) : mp 164.4-165.1 ^{o}C, colorless prisms (chloroform/pentane); ^{1}H-NMR (270 MHz, $CDCl_3$) δ 1.14 (s, 3H), 1.24 (s, 3H), 2.63 (br, 1H), 3.05 (s, 1H), 3.58 (s, 3H), 3.65 (s, 1H), 6.06 (d, 1H, *J* = 2.64 Hz), 6.68 (dd, 1H, *J* = 2.64, 8.24 Hz), 6.97 (d, 1H, *J* = 8.24 Hz), 7.14-7.16 (m, 1H), 7.38-7.42 (m, 2H), 7.48-7.50 (m, 2H); ^{13}C-NMR (67 MHz, $CDCl_3$) δ 14.5, 21.1, 38.2, 49.7, 54.0, 55.1, 60.6, 81.3, 112.0, 115.8, 125.0, 128.5, 128.8, 129.3, 130.1, 131.1, 136.5, 138.3, 159.6, 203.2, 205.6; IR (KBr) 3330 (-OH), 1714, 1698 (C=O) cm^{-1}; HRMS : Calculated for $C_{22}H_{20}O_4$, 348.1362, Found: 348.1356

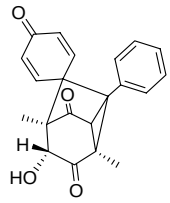

Spiro[cyclohexa-2,5-dienone-4,8'-7-phenyl-1,4-dimethyl-3-hydroxy-tricyclo[2.2.2.0^{6,7}]octane-2,5-dione] 3a (same as **3h)**: mp 97.3-98.1 ^{o}C, colorless prisms (chloroform/pentane); ^{1}H-NMR (270 MHz, $CDCl_3$) δ 1.00 (s, 3H), 1.07 (s, 3H), 2.79 (s, 1H), 3.06 (s, 1H), 4.01 (s, 1H), 6.13 (dd, *J* = 1.98, 10.22 Hz), 6.51 (dd, *J* = 1.98, 10.22 Hz), 6.58 (dd, *J* = 3.30, 10.22 Hz), 6.86 (dd, *J* = 3.30, 10.22 Hz), 7.07 (br, 2H), 7.29 (br, 3H); ^{13}C-NMR (67 MHz, $CDCl_3$) δ 10.8, 14.7, 43.2, 46.2, 53.0, 53.6, 56.0, 75.5, 128.6, 129.0, 129.2, 129.4, 131.2, 131.2, 134.2, 143.2, 148.1, 184.4, 203.7, 204.6; IR (KBr) 3411 (-OH), 1747, 1712, 1664 (C=O) cm^{-1}; HRMS : Calculated for $C_{23}H_{22}O_3$, 334.1205, found 334.1197

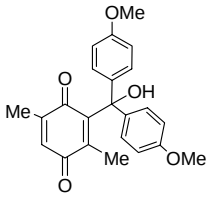

6-(hydroxybis(4-methoxyphenyl)methyl)-2,5-dimethylcyclohex-2-ene-1,4-dione (**6**): mp 173.4-174.1 ^{o}C; ^{1}H-NMR (270 MHz, $CDCl_3$) δ 1.36 (s, 3H), 2.02 (d, 3H, *J* = 1.89 Hz), 3.80 (s, 3H), 3.80 (s, 3H), 5.39 (s, 1H), 6.64 (q, 1H, *J* = 1.62 Hz), 6.84-6.88 (m, 4H), 7.14-7.25 (m, 4H); ^{13}C-NMR (67 MHz, $CDCl_3$) δ 14.4, 15.9, 55.3, 81.6, 113.7, 128.5, 133.0, 137.1, 143.4, 146.7, 147.1, 159.2, 187.7, 191.4; IR (KBr) 3447 (O—H) cm^{-1}; *Anal* Calcd for $C_{23}H_{22}O_5$: C, 73.00; H, 5.86; O, 21.14, found C, 72.83; H, 5.75; O, 21.42.

Kinetic data.

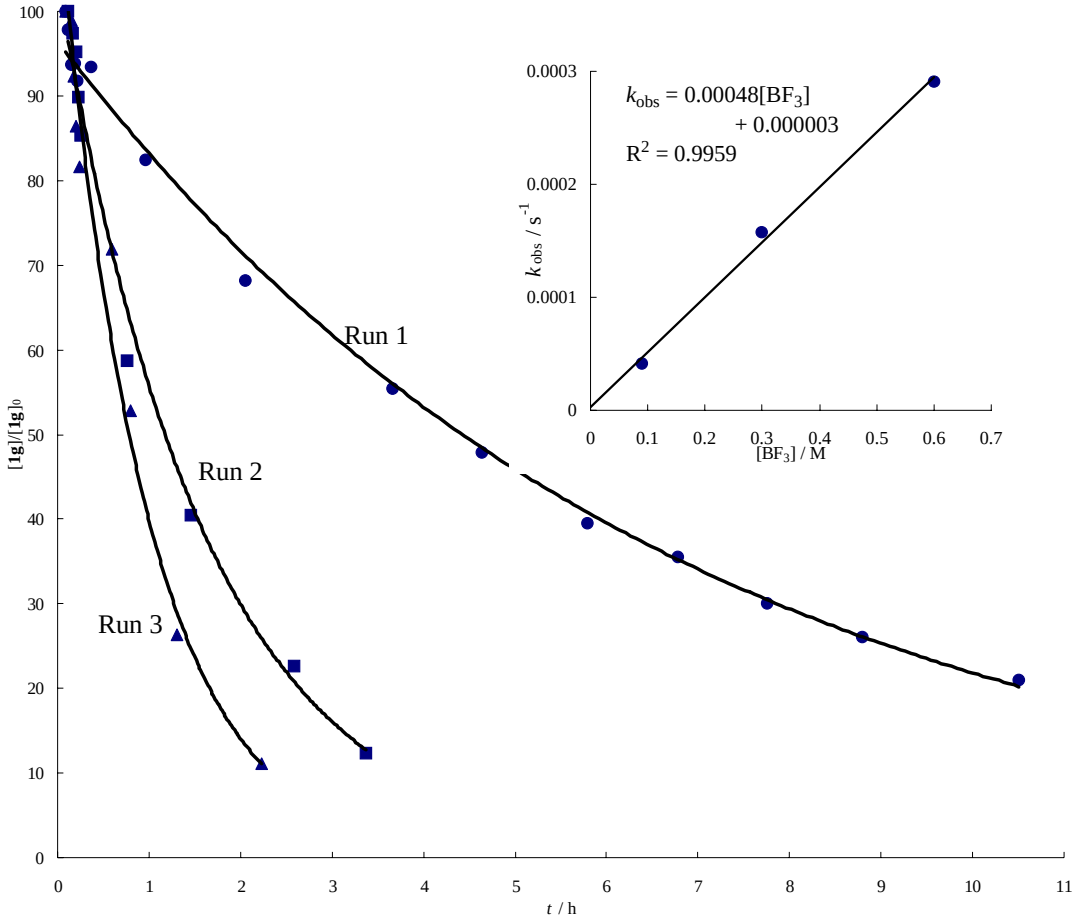

Figure 5. First-order decay plots of the relative ratio of **1g** against time for the reaction at 30°C in $CDCl_3$ with various catalyst concentration [BF_3] (= 0.090 M for Run 1; 0.30 for Run 2; 0.60 for Run 3, respectively). The first-order rate constants k_{obs} were calculated by natural logarithmic plots of the relative ratio of **1g** vs time and the second-order rate constants k were obtained by dividing the k_{obs} by [BF_3]. Inset: a linear dependency of k on [BF_3].

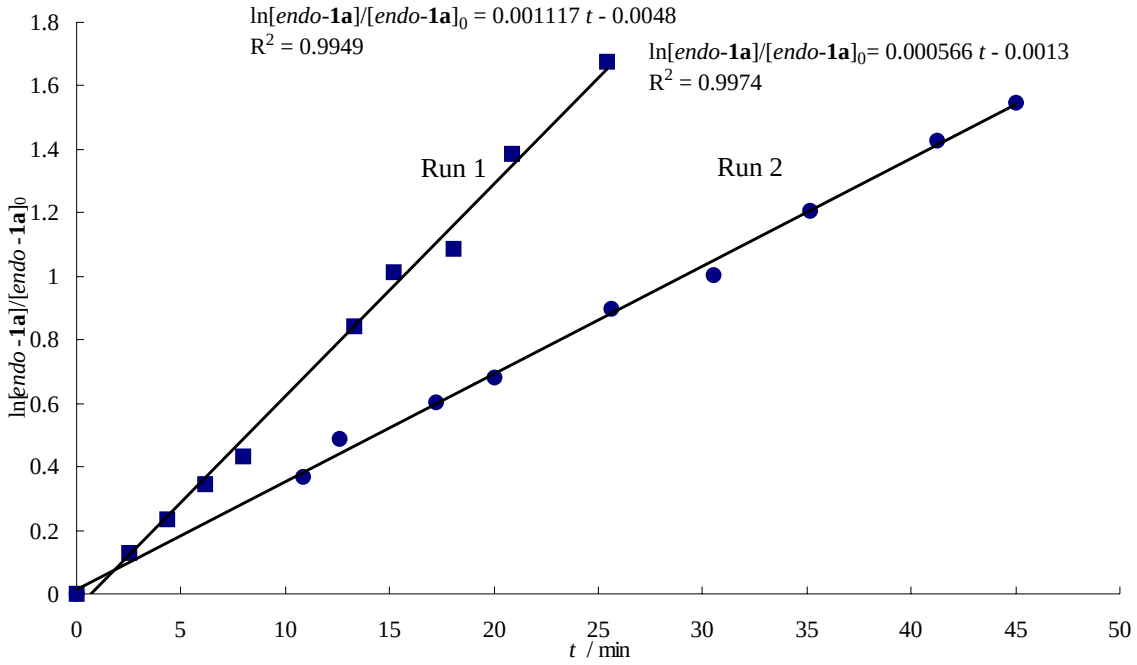

Figure 6. Logarithmic plots of the [*endo*-**1a**]/[*endo*-**1a**]$_0$ vs time for the reaction at 30°C in $CDCl_3$ with various catalyst concentration ([BF_3] = 0.060 M for Run 1 and 0.030 for Run 2, respectively).

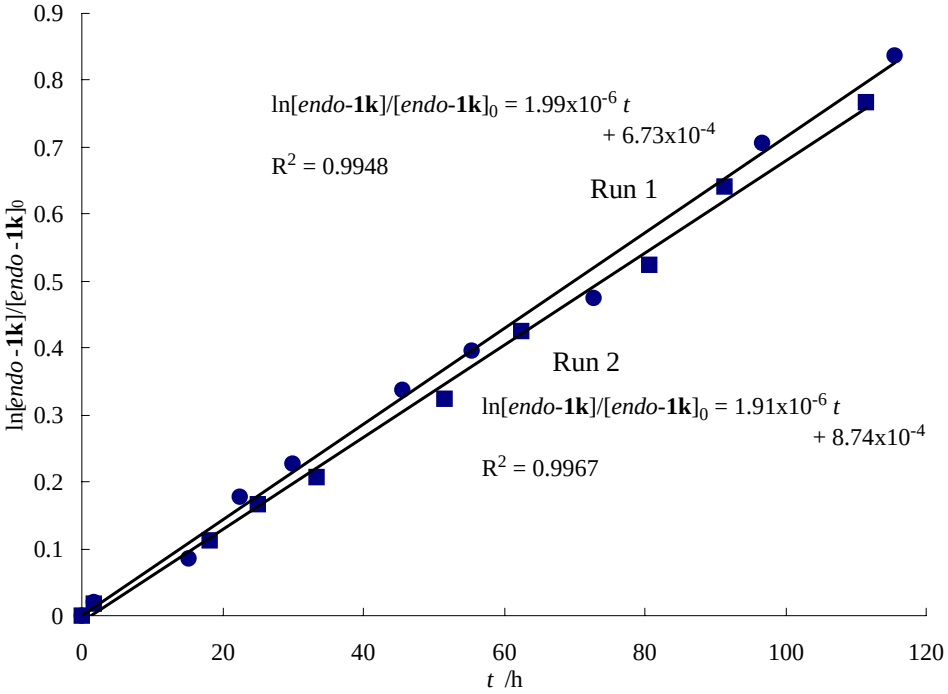

Figure 7. Logarithmic plots of the relative [*endo*-**1k**]/[*endo*-**1k**]$_0$ vs time for the duplicate reactionsat 30°C in $CDCl_3$ with catalyst concentration [BF_3] (= 0.90 M).

Calculation Procedure. All calculations were executed by PC SPARTAN'04 on a general Windows PC (Intel Celeron 2.8GHz, 2GB RAM). Geometries of 1g and 4g were optimized by density functional theory calculation (B3LYP/6-31G* level). The optimized energies were –650526.028 kcal/mol (**1g**) and –942075.871 kcal/mol (**4g**).

X-ray Crystal Structure Determination of 1j: $C_{21}H_{16}Cl_2O_3$, M = 387.26, monoclinic, space group $P2_1/n$ with a = 13.6787(3), b = 15.7928(3), c = 17.9803(4) Å, β = 107.2044(11)°, V = 3710.40(13) Å ^{3}, Z = 8, $Dcalc$ = 1.386 g/cm^3, R = 0.0959 and Rw = 0.2478 for 7111 reflections with $I>2.0\sigma(I)$.

X-ray Crystal Structure Determination of 6: $C_{23}H_{22}O_5$, M = 378.42, monoclinic, space group Pn with a = 8.9422(2), b = 10.7454(3), c = 10.7371(3) Å, β = 110.3428(14)°, V = 967.35(4) Å ^{3}, Z = 2, $Dcalc$ = 1.299 g/cm^3, R = 0.0487 and Rw = 0.1220 for 3310 reflections with $I>2.0\sigma(I)$.

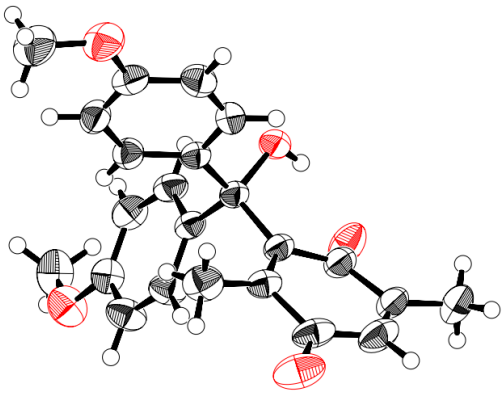

Figure 8. ORTEP drawing of **6**.

2-5. Reference and Notes

(1) (a) Lancelot, C. J.; Cram, D. J.; Scheyer, P. v. R. *Carbenium Ions*, Olah, G. A. and Scheyer, P. v. R., Eds., Wiley-Interscience, New York, 1972, Vol. 3, Chapter 27, p 1347–1483. (b) Smith, M. B.; March, J. *March's Advanced Organic Chemistry*, Wiley, New York, 2007, Chapter 11, p 657–751. (c) Peeran, M. J.; Wilt, W.; Subramanian, R.; Crumrine, D. S. *J. Org. Chem.* **1993**, *58*, 202–210. (d) Kevil, D. N.; D'Souza, M. J. *J. Chem. Soc. Perkin Trans. 2* **1997**, 257–263. (e) Fujio, M.; Goto, N.; Dairokuno, T.; Goto, M.; Saeki, Y.; Okusaka, Y.; Tsuno, Y. *Bull. Chem. Soc. Jpn*. **1992**, *65*, 3072–3079. (f) Nagumo, S.; Ono, M.; Kakimoto, Y.; Furukawa, T.; Hisano, T.; Mizukami, M.; Kawahara, N.; Akita, H. *J. Org. Chem*. **2002**, *67*, 6618–6622. (g) del Río, E.; Menéndez, M. I.; López, R.; Sordo, T. *J. Am. Chem. Soc*. **2001**, *123*, 5064–5068.

(2) Isaacs, N. S. *Physical Organic Chemistry*, Longman Science & Technical, Essex, 1995, Chapter 13, p 643–700.

(3) (a) Fujio, M.; Funatsu, K.; Goto, M.; Mishima, M.; Tsuno, Y. *Tetrahedron* **1987**, *43*, 307–316. (b) Fujio, M.; Goto, M.; Mishima M.; Tsuno, Y. *Bull. Chem. Soc. Jpn*. **1990**, *63*, 1121–1128. (c) Okamura, M.; Hazama, K.; Ohta, M.; Kato, K.; Horaguchi, T.; Ohno, A. *Chem. Lett*. **1997**, *26*, 973–974. (d) Tsuno, Y.; Fujino, M. *Advances in Physical Organic Chemistry*; Bethell, D., Ed.; Academic Press; London, 1999, Vol 32, p 267–385.

(4) (a) Cram, D. J. *J. Am. Chem. Soc*. **1952**, *74*, 2129–2137, (b) Cram, D. J. *J. Am. Chem. Soc*. **1952**, *74*, 2137–2148; (c) Streitwieser, A. Jr.; Walsh, T. D.; Wolfe, J. R. *J. Am. Chem. Soc*. **1965**, *87*, 3686–3691; (d) Cram, D. J.; Thompson, J. A. *J. Am. Chem. Soc*. **1967**, *89*, 6766–6768; (e) Thompson, J. A.; Cram, D. J. *J. Am. Chem. Soc*. **1969**, *91*, 1778–1789.

(5) (a) Jackman, L. M.; Haddon, V. R. *J. Am. Chem. Soc*. **1974**, *96*, 5130–5138; (b) Gates, M.; Frank, D. L.; Felten, W. C. *J. Am. Chem. Soc*. **1974**, *96*, 5138–5143; (c) Ando, T.; Yamawaki, J.; Saito, Y. *Bull. Chem. Soc. Jpn*. **1978**, *51*, 219–224.

(6) Oshima, T.; Asahara, H.; Koizumi, T.; Miyamoto, S. *Chem. Commun*. **2008**, *15*, 1804–1806.

(7) (a) Mollere, P. D.; Houk, K. N. *J. Am. Chem. Soc*. **1977**, *99*, 3226–3333; (b) Iwamura, H.; Sugawara, T.; Kawada, Y.; Tori, K.; Muneyuki R.; Noyori, R. *Tetrahedron Lett*. **1979**, *20*, 3449–3452; (c) Bach, R. D.; Wolber, G. J. *J. Am. Chem. Soc*. **1984**, *106*, 1410–1415.

(8) Koizumi, T.; Harada, K.; Mochizuki, E.; Kokubo, K.; Oshima, T. *Org. Lett*. **2004**, *6*, 4081–4084.

(9) Miyashita, M.; Suzuki, T.; Yoshikoshi, A. *Chem. Lett*. **1987**, 285–288.

(10) Oshima, T.; Nagai, T. *Bull. Chem. Soc. Jpn*. **1988**, *61*, 2507–2512.

(11) Crystallographic data for this compound have been deposited at the Cambridge Crystallographic Data Centre. These data can be obtained free of charge via www.ccdc.cam.ac.uk/data-request/cif, by emailing data_request@ccdc.cam.ac.uk, or by contacting The Cambridge Crystallographic Data Centre, 12 Union Road, Cambridge CB2 1EZ, UK; fax: +44 1223336033. CCDC 749514.

(12) Our attempt to follow the rate of the reaction of di(*p*-anisyl)homobenzoquinone epoxide by NMR was failed because of the very fast degradation. Interestingly, this reaction gave neither **2** nor **3** type product, but yielded di(anisyl)methyl-substituted benzoquinone derivative **6** which seems to arise from the cyclopropane ring-cleavage as well as the loss of oxygen atom. The structure of **6** was determined by the X-ray crystal structural analysis. CCDC 750112.

(13) Williams, A. *Free Energy Relationships in Organic and Bio-organic Chemistry*, The Royal Society of Chemistry, Cambridge, 2003.

(14) The author obtained rather worse correlations when the author assumed the π-aryl participation occurs only at the ortho carbon; log k_{rel}*exo*(**1**) = –0.38σ –0.01 (R^2 = 0.96, n = 8) and –0.24σ^+ –0.05 (R^2 = 0.82, n = 8).

(15) (a) Yukawa, Y.; Tsuno, Y. *Bull. Chem. Soc. Jpn*. **1959**, *32*, 971-981. (b) Shorter, J.; *Correlation Analysis in Chemistry. Recent Advances*; Chapman, N. B.; Shorter, J., Ed.; Plenum Press; New York, 1978, Chapter 4, p 119–173.

(16) (a) Fujio, M.; Funatsu, K.; Goto, M.; Mishima, M.; Tsuno, Y. *Tetrahedron* **1987**, *43*, 307–316. (b) Fujio,

M.; Goto, M.; Mishima, M.; Tsuno, Y. *Bull. Chem. Soc. Jpn*. **1990**, *63*, 1121−1128. (c) Fujio, M.; Goto, N.; Dairokuno, T.; Goto, M.; Saeki, Y.; Okusako, Y.; Tsuno, Y. *Bull. Chem. Soc. Jpn*. **1992**, *65*, 3072−3079.

(17)(a) Parker, R. E.; Issaacs, N. S. *Chem. Rev*. **1959**, *59*, 737−799. (b) Rickborn, B. *In Comprehensive Organic Synthesis*; Trost, B. M., Ed.; Pergamon Press: Oxford, U.K., 1991; Vol. 3, pp 733−771. (c) Fujita, H.; Yoshida, Y.; Kita, Y. *Yuki Gosei Kagaku Kyokaishi.* **2003**, *61*, 133−143. (d) Giner, J.-L.; Li, X.; Mullins, J. J. *J. Org. Chem*. **2003**, *68*, 10079−10086. (e) Whalen, D. E. *Advances in Physical Organic Chemistry*; Richard, J. P. Ed.; Elsevier Academic Press; London, 2005, Vol. 40, pp 247-298.

(18)*Aziridines and Epoxides in Organic Synthesis*; Yudin, K. A. Ed.; Wiley-VCH; Weinheim, 2006.

(19)(a) Posner, G. H.; Rogers, D. Z. *J. Am. Chem. Soc*. **1977**, *99*, 8214−8218. (b) Bellucci, G.; Berti, G.; Ingrosso, G.; Mastrorilli, E. *J. Org. Chem*. **1980**, *45*, 299−303.

(20)(a) Pocker, Y.; Ronald, B. P. *J. Am. Chem. Soc*. **1980**, *102*, 5311−5316. (b) Yagi, H.; Jerina, D. M. *J. Org. Chem*. **2007**, *72*, 9983−9990. (c) Davis, C. E.; Bailey, J. L.; Lockner, J. W.; Coates, R. M. *J. Org. Chem*. **2003**, 68, 75−82. (d) Blumenstein, J. J.; Ukachukwu, V. C.; Mohan, R. S.; Whalen, D. L. *J. Org. Chem*. **1993**, *58*, 924−932.

(21)Reichart, C. *Solvents and Solvent Effects in Organic Chemistry*. 3rd Ed., Wiley-VCH Verlag GmbH & Co. KGaA, Weinheim, 2003. Chap. 5, pp 162−199.

(22)Reichardt, C. *Chem. Rev*. **1994**, *94*, 2319−2358.

(23)Oshima, T.; Asahara, H.; Kubo, E.; Miyamoto, S.; Togaya, K. *Org. Lett*. **2008**, *10*, 2413−2416.

(24)Kita, Y.; Furukawa, A.; Futamura, J.; Higuchi, K.; Ueda, K.; Fujioka, H. *Tetrahedron* **2001**, *57*, 815−825.

(25)(a) Costantino, P.; Crotti, P.; Ferretti, M.; Macchia, F. *J. Org. Chem*. **1982**, *47*, 2917−. (b) Crotti, P.; Ferretti, M.; Macchia, F.; Stoppioni, A. *J. Org. Chem*. **1984**, *49*, 4706−4711. (c) Crotti, P.; Ferretti, M.; Macchia, F.; Stoppioni, A. *J. Org. Chem*. **1986**, *51*, 2759−2766.

(26)Recently, Wang and Tantillo suggested a stepwise reaction pathway for the acid-catalyzed transannular cyclization of **4** based on DFT calculations, (Wang, S. C.; Tantillo, D. J. *J. Org. Chem*. **2007**, *72*, 8394−8401). However, the poor kinetic solvent effects for the reaction of **4** and especially for the present **1** explicitly rule out the intervention of the carbocation intermediate derived from the stepwise S_N1 mechanism.

(27)Kong, J.; White, C. A.; Krylov, A. I.; Sherrill, D.; Adamson, R. D.; Furlani, T. R.; Lee, M. S.; Lee, A. M.; Gwaltney, S. R.; Adams, T. R.; Ochsenfeld, C.; Gilbert, A. T. B.; Kedziora, G. S.; Rassolov, V. A.; Maurice, D. R.; Nair, N.; Shao, Y. H.; Besley, N. A.; Maslen, P. E.; Dombroski, J. P.; Daschel, H.; Zhang, W. M.; Korambath, P. P.; Baker, J.; Byrd, E. F. C.; Van, Voorhis, T.; Oumi, M.; Hirata, S.; Hsu, C. P.; Ishikawa, N.; Florian, J.; Warshel, A.; Johnson, B. G.; Gill, P. M. W.; Head-Gordon, M.; Pople, J. A. *J. Comput. Chem*. **2000**, *21*, 1532−1548.

(28)Asahara, H.; Kubo, E.; Koizumi, T.; Mochizuki, E.; Oshima, T. *Org. Lett*. **2007**, *9*, 3421−3424.

Chapter 3. Consecutive Acid-Catalyzed Rearrangement Reaction of HQ-Epoxides and Cyclobutane-Fused Quinone Epoxide

3-1. Introduction

Thermal and photochemical skeleton rearrangements of strained small rings with multiple bonds and functional groups have attracted much attention from both synthetic and mechanistic viewpoints.[1] Especially, polycyclic ketones bearing high strain energy have great potential to induce a skeletal rearrangement in the presence of acid catalyst.[2] An enormous variety of carbocyclic and heterocyclic medium ring compounds with a wide range of functional groups has been reported to undergo these fascinating processes for modern synthetic chemistry. Transannular cyclization requires a suitable conformation of substarates and prudent selection of functional groups. In this regard, comprehensive knowledge of factors govering reactivity will yield insight into widespread application of transannular reaction.

In Chapter 1 and 2, the author described that the acid-catalyzed rearrangements of polycyclic epoxides to afford the caged diketo alcohol product in quantitative yield.

In this Chapter, the author deals with the consecutive novel skeletal rearrangement to cyclopropane ring opening products and acid-catalyzed rearrangement reaction of cyclobutane-fused quinone epoxides (Scheme 1).

Scheme 1.

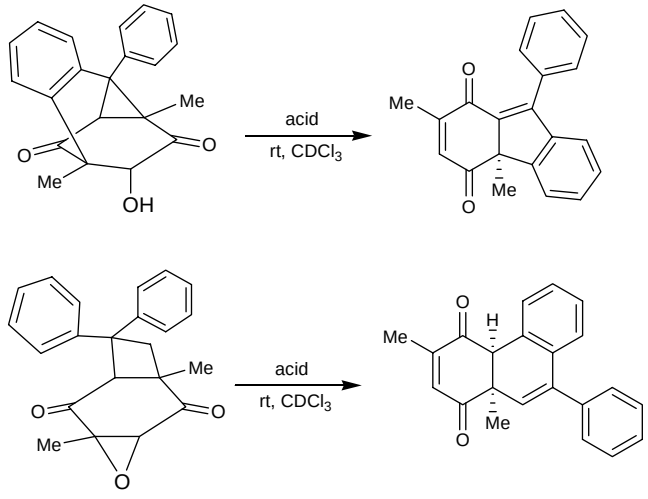

3-2. Results and Discussion

3-2-1. Acid-Catalyzed Reaction of Diketo-Alcohol

CF_3SO_3H catalyzed reactions of HQ-Epoxide **1a** was carried out in $CDCl_3$ at room temperature under the same conditions as BF_3 or $MeSO_3H$ reactions. This protic acid-catalyzed reaction of **1a** gave the cyclopropane ring opened product **3a** and unidentified product **3a'** (Scheme 2).

Scheme 2.

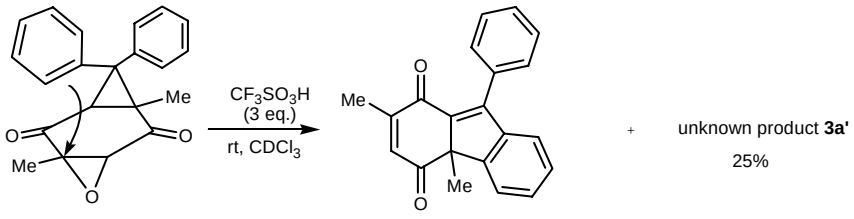

1a **3a** 43%

Next, the author isolated the BF_3-catalyzed reaction product **2a** and investigated the CF_3SO_3H catalyzed reaction (Scheme 3). It is interesting to note that the cyclopropane ring opened product **3a** was isolated selectively. This result means that the compound **3a** was obtained via transannular product **2a** but unknown product **3a'** was formed directly from **1a**.

Scheme 3.

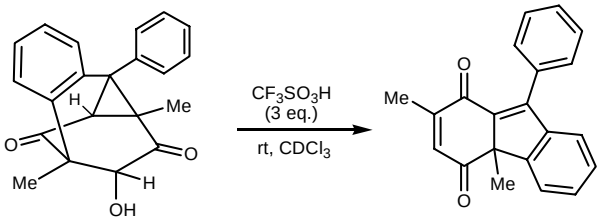

2a **3a** 92%

3-2-2. Acid-Catalyzed reaction of Ethano-Bridged HQ-Epoxide

As discribed in Chapter 1, ethano-bridged HQ-epoxide **1g** underwent the novel consecutive skeltal rearragements. The involved major processes are 1) cyclopropane ring opening, 2) acyl migration reaction, 3) epimerization, 4) ring contration reaction (Scheme 4).

Scheme 4.

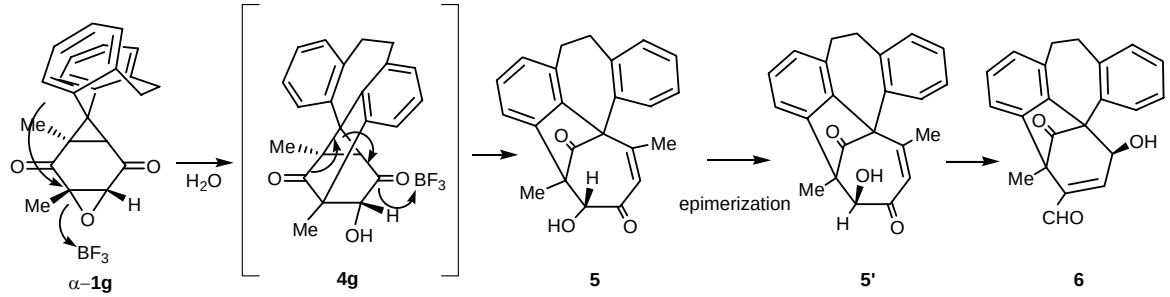

α–**1g** **4g** **5** **5'** **6**

The reactivity was much dependent on the conformational difference of the dibenzocycloheptene ring as experienced by the higher conversion (though shorter reaction time) of β–**1g** compared to the conformational isomer α–**1g** (Table 1). It is very noteworthy

Table 1. Acid-catalysed rearrangement of α/β–**1g** (30 mM) in $CDCl_3$ at 30 °C

sub.	time (h)	conv.[b] (%)	yield[a,b] (%)			
			4	**5**	**5'**	**6**
α–**1g**	16	12	0	28	42	30
β–**1g**	2	85	0	74	21	2

[a] Based on consumed **1**. [b] Determined by ^{1}H NMR.

that the primary product **4g** (not detected) underwent a facile acid-catalyzed acyl migration associated with the cyclopropane ring cleavage.[3] The resulting product **5** was found to undergo the keto-enol tautomerization to be more stable epimer **5'**. The structures of **4f**, **5'** and **6** were confirmed by X-ray crystallographic analyses (Figure 1).[4] Unfortunately, at present, we have no satisfactory mechanistic explanation for the transformation **5'** $\rightarrow$ **6**, although the **5'** is likely to undergo the initial 1,2-migration to the activated carbonyl group and formal loss of one carbon unit.[5]

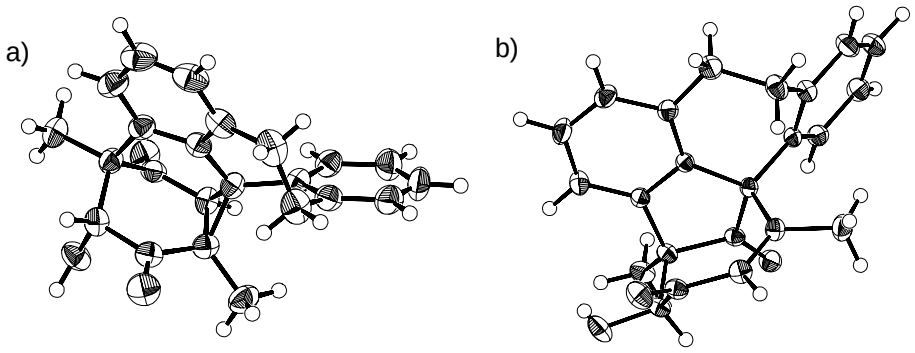

Figure 1. ORTEP drawings of a) **4f** and b) **5'.**

Here, the question is raised on why **4g** undergoes the subsequent cyclopropane ring-opening as well as the acyl migration in contrast to the analogous **4f** (Scheme 5). Only difference between **4f** and **4g** is the substitution pattern of the two quinone Me groups (ie., *para* for **4f** and *meta* for **4g**). Furthermore, it is noted that the similarly *meta*-Me-substituted less strained tricyclic diketo-alchol **4b** do not exhibit such an acyl migration (See Scheme 3 in Chapter 1).

Scheme 5.

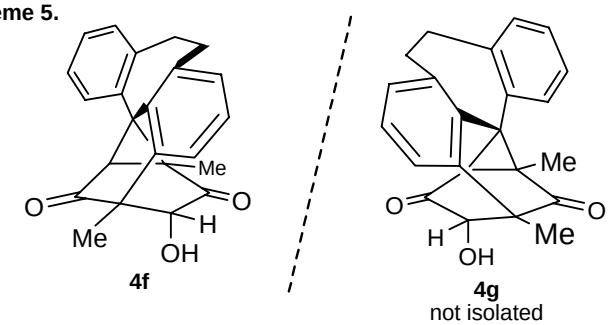

Based on the structural comparison of **4g** with the persistent **4b** and **4f**, we can imagine the several reasons; (1) the **4g** has the less hindered carbonyl group (only substituted by α–OH group) that is needed to be activated by BF_3 for the present cyclopropane ring opening, whereas the relevant carbonyl group of **4f** is well blocked both by the α-Me and α'-OH substitutes, (2) for **4g**, the Me group on cyclopropane ring may accelerate the migration of acyl group by stabilizing the generating positive charge, but this is not the case for **4f**, (3) in contrast to **4f**, compound **4g** forces the considerable coplanarity of ethano-bridged two aromatic nuclei capable of favorably resonating with the cleaved cyclopropane ring. All of these steric and electronic effects would be responsible for the lability of **4g**.

However, the possibility that the transformation of **4g** into **5** occurs through a concerted orbital controlled [σ2s + σ2a] process[6] can not be thoroughly ruled out (Figure 2). In this mechanism, the disrotatory mode of ring-opening (C_2-C_3 σ-bond) involves charge transmittance to the antibonding C_1-C_4 bond. The partially developing positive charge at C_1-carbon atom can be favorably stabilized by the substituted Me group. The stable compound **4f** lacks the corresponding Me group.

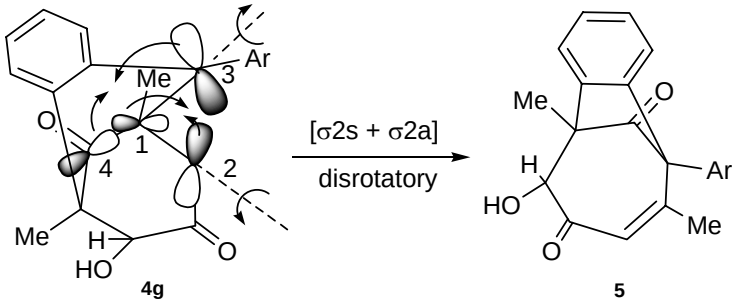

Figure 2. A possible concerted [σ2s + σ2a] pathway for the transformation **4g** → **5**. For simplicity, the ethano-bridge is omitted.

3-2-3. Acid-Catalyzed reaction of Cyclobutane-Fused Quinone Epoxide

Next, the author attempted the skeltal rearrangement of cyclobutane-fused quinone **7**. The reaction of **7** (30 mM) with $BF_3{\cdot}Et_2O$ (3 equiv.) in chloroform at room temperature proceeded rapidly to give tricyclic compound **8** and diphenylethene **9** in yields of 57 and 23%, respectively (Scheme 6). Unlike the acid-catalyzed reaction of homobenzoquinone epoxide **1**,

Scheme 6.

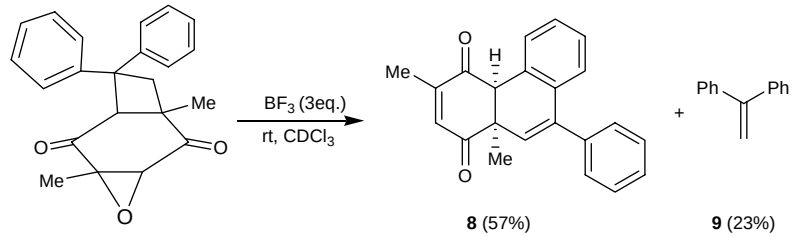

the phenylene-bridged product was not determined in this reaction. Although not presently understood the mechanistic details of this reaction, the author thought that this reaction

proceeded through the *endo*-Ar transannular reaction. Therefore as shown in Scheme 7, the acid-coodinated **7** would produce the bridged intermediate **I** and cyclobutane ring opened intermediate **II**, respectively depending on which oxygen atom (i.e., epoxyde or C=O oxygen

Scheme 7.

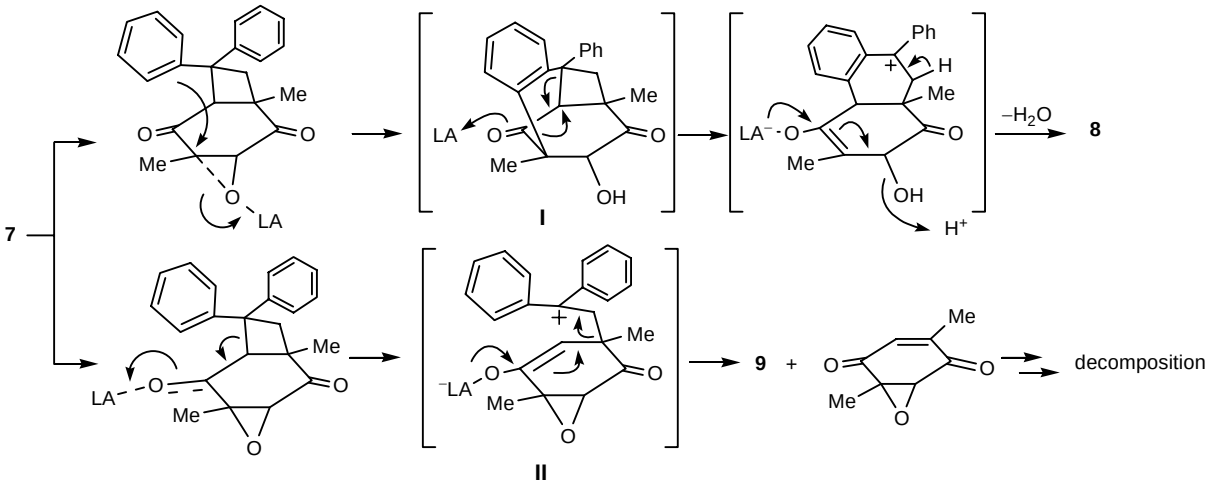

atom) is bound by the Lewis acid. The resulting **I** can perform the cyclobutane ring opening reaction and Ph migration following dehydration to give the tricyclic product **8**. The **II** will provide diphenylethene and quinoepoxide, but quinoepoxide is easily decomposed by acid.

3-3. Conclusion

The author found that the subsequent ring-enlargement by 1,2-acyl migration associated with the incorporated cyclopropane ring-opening, depending on the substitution pattern of the quinone methyl groups. In this Chapter, the author has also investigated the acid-catalyzed rearrangement of cyclobutane-fused quinone epoxide **7**. The compound **7** underwent the novel consecutive skeletal rearrangements. These findings provide the useful information on the rearrangements of polycyclic epoxides and the design of more extended framework compounds.

3-4. Experimental Section

General procedures for the synthesis of homobenzoquinone epoxides. To a mixture of homobenzoquinone (0.5 mmol) and 30% H_2O_2 (0.75 mmol) in DMSO (1 mL) was added dropwisely (10 min) a solution of Bu_4NF (1M solution in THF, 0.5 mmol) at room temperature. After the addition of the reagent the reaction mixture was stirred for 2h. Then, the epoxide **1** was extracted with ethyl acetate (3 mL × 3). The organic layer was washed with water (3 mL × 3) and dried over magnesium sulfate. The solvent was evaporated *in vacuo*. The epoxide **1** was purified by column chromatography on silica gel (benzene as an eluent) and recrystallization from hexane-ether or hexane-benzene. The structures of all epoxides

were deduced from the ^{1}H and ^{13}C NMR, and IR spectra.

General procedures for the synthesis of cyclobutane-fused quinone epoxide. Cyclobutane-fused quinones were synthesized by the [2+2] photocycloaddition of the 2,5-dimethyl *p*-benzoquinone (0.5 mmol) with 1,1-diphenylethene (0.7 mmol). To a mixture of cyclobutane-fused quinone (0.5 mmol) and 30% H_2O_2 (0.75 mmol) in DMSO (1 mL) was added dropwisely (10 min) a solution of Bu_4NF (1M solution in THF, 0.5 mmol) at room temperature. After the addition of the reagent the reaction mixture was stirred for 2h. Then, the epoxide **7** was extracted with ethyl acetate (3 mL × 3). The organic layer was washed with water (3 mL × 3) and dried over magnesium sulfate. The solvent was evaporated *in vacuo*. The epoxide **7** was purified by column chromatography on silica gel (benzene as an eluent) and recrystallization from hexane-ether or hexane-benzene. The structures of all epoxides were deduced from the ^{1}H and ^{13}C NMR, and IR spectra.

General procedures for acid-catalyzed reactions. To a $CDCl_3$ solution (670 μl) of **1** or **7** (0.02 mmol) in a NMR tube was added the requisite amount of acid at room temperature by using a micro syringe. The progress of reaction was monitored by ^{1}H NMR. After a period of requisit time, the reaction solution was transferred into a separate funnel, diluted with chloroform (10 mL) and then washed with water (3 mL × 3). The aqueous layer was extracted with chloroform (5 mL × 2). The combined organic layer was washed with water (3 mL × 3), then dried over calcium chloride. After the evaporation of the solvent *in vacuo*, the residue was submitted for a ^{1}H NMR analysis to determine the product distribution. The column chromatographic treatment of the reaction mixtures on silica gel gave **5**, **5'**, and **6** with a mixture of hexane-ethyl acetate as an elurnt. The structures of all products were deduced from the ^{1}H and ^{13}C NMR, and IR spectra. The structures of **4f**, **5** and **5'** were also confirmed by the X-ray crystallographic analyses.

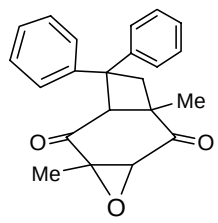

1,5-Dimethyl-8,8-diphenyl-4-oxa-tricyclo[5.2.0.0^{3,5}]nonane-2,6-dione (**7**) : yellow powder; ^{1}H NMR(270 MHz, $CDCl_3$) δ 1.14 (s, 3H), 1.50 (s,3H), 2.50 (d, 1H, *J* = 12.5), 3.30 (s, 1H), 3.80 (dd, 1H, *J* =0.6, 12.5), 4.01(d, 1H, *J* = 0.6), 6.98—7.02 (m, 2H), 7.06—7.25 (m, 4H), 7.32—7.35 (m, 2H); ^{13}C NMR (67.5 MHz, $CDCl_3$) δ 13.7, 16.9, 37.6, 39.7, 49.6, 60.1, 60.3, 127.5, 127.9, 128.2, 128.9, 129.1, 129.5, 138.1, 139.9, 198.1, 200.3.

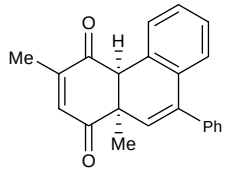

3,10a-Dimethyl-9-phenyl-4a,10a-dihydro-phenanthrene-1,4-dione(8) : white crystal; mp.161.2－162.0°C; ^{1}H NMR(270 MHz, $CDCl_3$) δ 1.38 (s, 3H), 2.03 (d, 3H, *J* = 1.48), 3.89 (s, 1H), 5.76 (s, 1H), 6.61 (d, 1H, *J* = 1.48), 7.05－7.13 (m, 2H), 7.20－7.40 (m, 7H); ^{13}C NMR (67.5 MHz, $CDCl_3$) δ 16.8, 21.4, 50.8, 58.5, 77.1, 126.4, 126.5, 127.8, 128.2, 128.6, 129.0, 129.2, 129.3, 131.3, 132.8, 136.7, 138.8, 140.7, 151.9, 198.1, 200.9.

3-5. Reference and Notes

(1) (a) Paulson, D. R.; Crandall, J. K.; Bunnell, C. A. *J. Org. Chem.* **1970**, *35*, 3708–3714. (b) Jones, M. Jr.,; Hendrick, M. E.; Hardie, J. A. *J. Org. Chem.* **1971**, *36*, 3061–3062. (c) Patrick, T. B.; Haynie, E. C.; Probst, W. J. *J. Org. Chem.* **1972**, *37*, 1553–1556. (d) Sadler, I. H.; Stewart, J. A. G. *J. Chem. Soc., Perkin Trans. 2* **1973**, 278–288. (e) Sugita, H.; Mizuno, K.; Saito, T.; Isagawa, K.; Otsuji, Y. *Tetrahedron Lett.* **1992**, *33*, 2539–2542. (f) Mizuno, K.; Sugita, H.; Kamada, T.; Otsuji, Y. *Chem. Lett.* **1994**, 449–452. (g) Maeda, H.; Hirai, T.; Sugimoto, A.; Mizuno, K. *J. Org. Chem.* **2003**, *68*, 7700–7706.

(2) (a) Finch, Jr., A. M. T.; Vaughan, W. R. *J. Am. Chem. Soc.* **1969**, *91*, 1416–1424; (b) Stork, G.; Grieco, P. A. *J. Am. Chem. Soc.* **1969**, *91*, 2407–2408. (c) Cargill, R. L.; Pond, D. M.; LeGrand, S. O. *J. Org. Chem.* **1970**, *35*, 359–363; (d) Hirao, K.; Taniguchi, M.; Yonemitsu, O.; Flippen, J. L.; Witkop, B. *J. Am. Chem. Soc.* **1979**, 101, 408–414. (e) Iyoda, M.; Kushida, T.; Kitami, S.; Oda, M. *J. Chem. Soc., Chem. Commun.* **1986**, 1049–1050. (f) Paquette, L. A.; Doherty, A. M. *Polyquinane Chemistry*; Springer–Verlag: Berlin, 1987. (g) Fitjer, L.; Majewski, M.; Kanschik, A. *Tetrahedron Lett.* **1988**, *29*, 1263–1264. (h) Yamamoto, H. *Lewis Acids in Organic Synthesis*; Wiley–VCH: Weinheim, 2000.

(3) We could not detect **4g** by ^{1}H NMR, even for shorter reaction times (10 min, 30% conversion) of **1g** under the same conditions. Another possibility that compound **1g** undergoes a prior acyl migration coupled with cyclopropane ring cleavage to give an intermediary dioxocycloheptene epoxide is unlikely, because of its increased heat of formation (by 70.79 kJ/mol on DFT calculation with B3LYP/6-31G*). Incidentally, **4g** and **5** are more stable than **1g** by 76.94 and 80.35 kJ/mol, respectively.

(4) Crystallographic data for the structure of **4f, 5'** and **6** have been deposited with the Cambridge Crystallographic Data Center as supplementary publication number CCDC 650017, 650018 and 650209. Copies of the data can be obtained, free of charge, on application to the CCDC, 12 Union Road, Cambridge CB2 1EZ, UK. Fax: +44-1233-336033. E-mail: deposit@ccdc.cam.ac.uk.

(5) We confirmed that the treatment of isolated **5'** with BF_3 for 12 h under the same conditions provided compound **6** in 96% yield on 52% conversion.

(6) Fukui, K. *Acc. Chem, Res.* **1971**, *4*, 57–64.

Chapter 4. Intramolecular [2+2] Photocycloaddition Reaction of Cyclobutane-Fused Quinone

4-1. Introduction

Intramolecular photochemical [2+2] cycloaddition is one of the most sophisticated methods for the synthesis of strained polycyclic cage compounds.[1] Especially, intramolecular [2+2]-photocycloadditions involving cyclic enones is widely used in organic synthesis as they can lead to cyclobutanes[2], a precursor for the synthesis of natural molecules[3]. The [2+2] photocycloaddition of cyclic enones with alkene has been widely investigated from the mechanistic point of view. A variety of starting molecules bearing the incorporated several π-bond functionaries have been reported to exhibit these fascinating processes.[4] In these photocycloadditions, the geometrical and topological arrangements of the relevant two 2π-components play a crucial role in an efficient cycloaddition of the conformationally restricted substrates.[5] In particular, quinones and their derivatives have attracted the continuous attention in view of the conjugated ring system as well as the suitable structural design of the reacting sites.[6] Accordingly, a number of studies have been made on their intramolecular photocycloadditions.[7]

The author now wishes to report that the photoreaction of variously methyl-substituted 1,4-benzoquinones with 1,1-diphenylethene resulted in the reversible intramolecular [2+2] cycloaddition of the primary 1:1 photoadducts to afford the pentacyclic diones only via the 1,2-addition of *endo*-phenyl ring (Scheme 1).

Scheme 1.

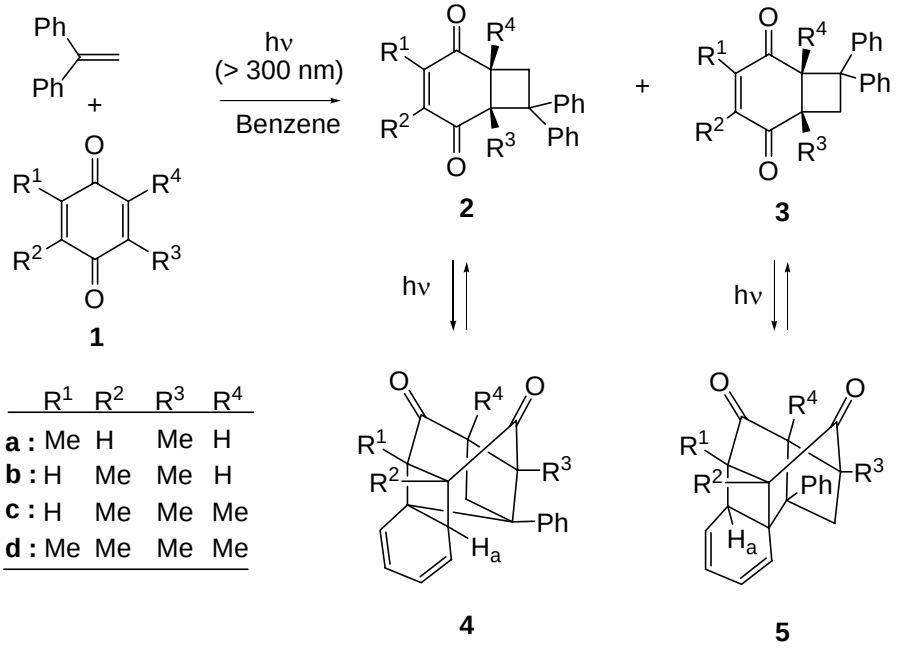

	R^1	R^2	R^3	R^4
a :	Me	H	Me	H
b :	H	Me	Me	H
c :	H	Me	Me	Me
d :	Me	Me	Me	Me

4-2. Results and Discussion

4-2-1. Substitution Patterns of Me-Groups

Irradiation of quinones **1a-d** (30 mM) and 2 equiv. amount of 1,1-diphenylethene in benzene under the argon atmosphere with a high-pressure Hg lamp through a Pyrex filter (λ > 300 nm) provided the regioisomeric mixture of the primary 1:1 photoadducts **2** and **3** along with the respective secondary intramolecular [2+2] cycloadducts **4** and **5** in almost quantitative total yield (Scheme 1 and Table 1).[8] The structures of these products were deduced from their ^{1}H and ^{13}C NMR spectra. The pentacyclic cage compound **5a** was also confirmed by the X-ray crystal analysis (Figure 1).[9] It is clearly demonstrated that the cage compound **5a** includes the diagonal connection of the two cyclobutane rings.[10]

Table 1. Product Distributions in Photoreaction of Quinones **1a-d** with 1,1-Diphenylethene.[a]

entry	compound	irradiation time (h)[c]	yield (%)[b]			
			2	**3**	**4**	**5**
1	**1a**[d]	4	60	20	5	14
2	**1b**[d]	6	30	26	35	8
3	**1c**	1	14	34	42	10
4	**1d**	1	43	–	57	–

[a] Carried out in benzene-d_6 in a NMR tube through a Pyrex filter. [b] Based on quinone used. [c] Irradiateion time for complete consumption of quinones. [d] Trace amount of unidentified products were detected in the ^{1}H NMR spectra of the reaction mixture.

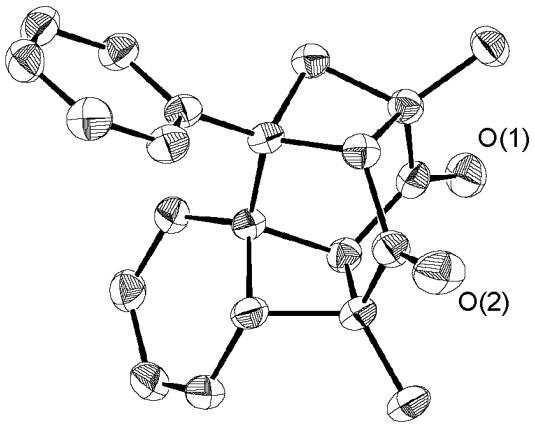

Figure 1. ORTEP drawing of **5a**. For clarity, hydrogen atoms are omitted.

In conformity with this distinctive structure, all cage compounds obtained exhibited no diagnostic NOE effects between the inwardly directed allyl proton (H_a) of fused cyclohexadiene and the inside methylene proton of the original cyclobutane ring.

The polycyclic products **4** and **5** are considered to be formed via a very rare intramolecular [2+2] photoreaction between the excited enedione C=C double bond with the facing

endo-phenyl ring at the 1,2-position.[11] Mechanistically, as in the case of usual [2+2] photocycloaddition of enones,[12] these reactions seem to involve a triplet 1,4-biradical intermediate derived from the spin-inverted excited triplet state of the primary 1:1 adducts, **2** and **3**.

Interestingly, the prolonged irradiation established the photochemical equilibration between the primary and the secondary photoadducts under the complete consumption of the starting quinones as represented for the case of quinone **1d** (Figure 2). This finding apparently indicates

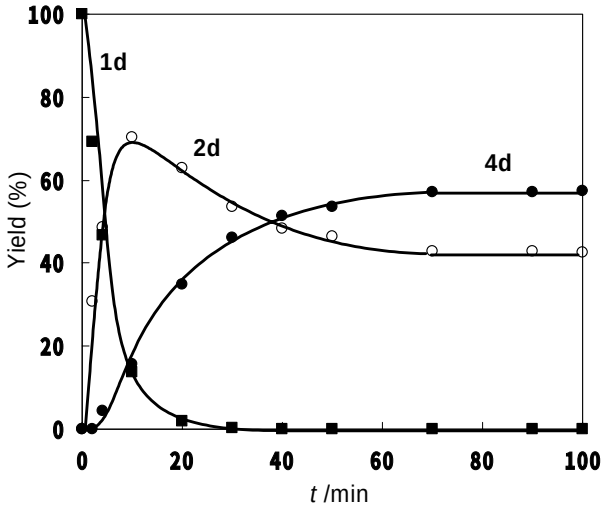

Figure 2. Time-dependent product ratios (%) of **2d** and **4d** in photochemical reaction of quinone **1d** with 1,1-diphenylethene (2 equiv) in benzene-d_6 irradiated in a NMR tube through a Pyrex filter.

the occurrence of [2+2] cycloreversion of the cage compounds (Scheme 1).

To more explicitly know the Me-substituent effects on the photostationary product ratios of cage compounds / bicyclic diones, we have performed the photoequilibration by using the isolated bicyclic diones. As expected, NMR monitoring of the reactions showed the apparent equilibration within 100 min at the photostationary state for all cases tested (Table 2). We also

Table 2. Photostationary equilibrated product ratios (%) of **4** and **5** in reversible photocycloaddition of **2** and **3**.

entry	compound	irradiation time (min)[a]	yield (%)[b]	
			4	**5**
1	**2a**	100	10	–
2	**3a**	60	–	43(44)[b]
3	**2b**	60	67	–
4	**3b**	60	–	31
5	**2c**	60	90	–
6	**2d**(=**3d**)	100	70(>99)[c]	

[a] irradiation in a NMR tube in benzene-d_6 through a Pyrex filter. [b] Value in parenthesis was obtained in the photocycloreversion of **5a**. [c] Value in parenthesis was attained by irradiation of **2c** through a filter (>350 nm).

noted that the irradiation of cage compound led to the identical photoequilibrium as exemplified for **5a** (entry 2). A perusal of Table 2 indicates that the relative ratios (%) of cage

compounds tended to increase for the bicyclic diones in which the *ipso*-carbon of *endo*-phenyl ring combines to the unsubstituted alkenoic carbon atom (entries 2, 3 and 5), but decrease for the bicyclic diones in which the *ipso*-carbon needs to bind to the Me-substituted alkenoic carbon (entries 1 and 4). However, the tetramethyl-substituted **2d**(=**3d**) provided an unexpected intrinsically large amount of cage compound probably because of rather enhanced steric congestion around original cyclobutane ring (entry 6). Thus, the lower ratios of cage compounds can be explained in terms of the more enhanced steric congestion between the *ipso*-carbon of phenyl ring and the substituted Me group.

Why does the present intramolecular photoreaction bring about the diagonal [2+2] cycloaddition of *endo*-phenyl ring? To answer the question, we first made of the conformational analysis of the representative **2d** on the basis of its X-ray crystal structure (Figure 3a). The whole structure of **2d**[13] was found to be considerably twisted in such a way that the *endo*-phenyl ring is inwardly located over the quinone plane. Namely, the cyclobutane ring of **2d** adopts a packered conformation and the *endo*-phenyl ring considerably overhangs the quinone frame (Figure 3b). The spatial distances (broken lines) between the relevant carbon atoms are 3.45 (C(19)-C(26)) and 3.46Å (C(9)-C(8)), respectively. These values are sufficient for the effective photochemical [2+2] cycloaddition.[14]

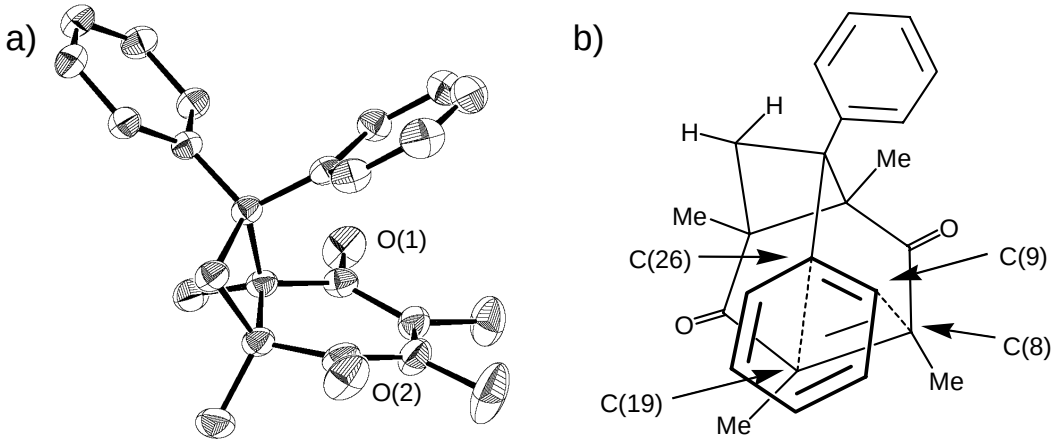

Figure 3. a) ORTEP drawing of **2d**. For clarity, hydrogen atoms are omitted, b) Schematic conformational representation of **2d** showing the favorable topological overlapping of *endo*-phenyl ring and quinone plane for [2+2] photocycloaddition.

Furthermore, the *p*-orbital axis of the aromatic *ipso*-carbon is allowed to favorably overlap with that of the underlying alkenoic carbon atom. These conformational preference would lead to the diagonal conjunction of two cyclobutane rings.

4-2-2. Selective Synthesis of Cage Compound 4

To obtain some information on the photoreversibility in the present intramolecular [2+2] cycloaddition of bicyclic diones, we have measured the absorption spectra of **2d** and **4d** in benzene (Figure 4). It was found that both the **2d** and **4d** have the comparable absorptions in the range of 300–340 nm which are responsible for cycloaddition and cycloreversion.

However, **2d** apparently showed the larger absorption band over 340 nm as compared with **4d**, thus resulting in almost one-way transformation of **2d** to **4d** on longer-wavelength irradiation (>350 nm) (Table 2, entry 6).

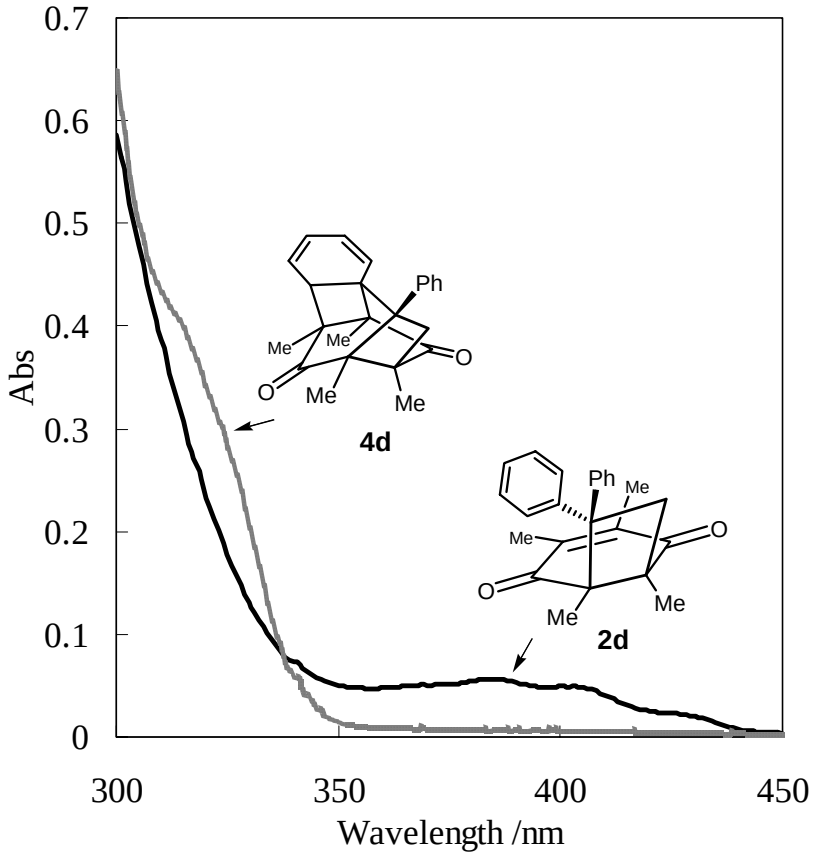

Figure 4. Absorption spectra of compounds **2d** (black line**–**) and **4d** (gray line–) (each in 0.20 mM) in benzene (cell path length 1.0 cm).

As to the photochemical cycloreversion of cyclobutane ring, the conformations of the adjoining π-bond substituents play a role in the efficient bond cleavage.[15] In the case of **4** and **5**, it is likely that the fused cyclohexadiene ring and the two vicinal carbonyl groups are responsible for the regioselective bond fission on account of the favorable excited π-electron donating conjugation with the anti-bonding orbital (σ*) of the cleaved cyclobutane ring.

An attempt was done to determine the triplet energies of cyclobutane-fused quinones **2** and cage compounds **4** by the procedure of Hammond and Saltiel,[16] since **2** and **4** did not emit phosphorescence in rigid glasses. Thus, the photostationary state isomer ratios of **2d**/**4d** were measured in the presence of various sensitizers with triplet energies covering 177-353 kJ/mol in benzene (Table 3). Figure 5 plots the ratio against the triplet energy of the sensitizer. This plot allows us to estimate the triplet energy of **2d** and **4d** as ca. 230 and ca. 200 kJ/mol, respectively. By using triplet sensitizer (9-fluoreneone or benzile), cyclobutane-fused quinone **2** was selectively formed.

Now, the selective synthesis of each compound **2** and **4** has been achieved successfully.

Table 3. Photostationary state isomer ratios in triplet sensitizer irradiation of **2d**.

sensitizer	triplet energy[a] (kJ/mol)	isomer ratio[b]	
		2d	**4d**
anthracene	177	57.8	42.3
acridine	190	66.7	33.3
9-fluorenone	210	100	0
benzile	223	100	0
p-nitroaniline	231	91.0	9.0
2-acetonaphthone	247	66.7	33.3
naphthalene	253	25.6	74.4
phenanthrene	260	19.8	80.2
fluorene	282	20.1	79.9
4'-methylacetophenone	305	26.6	73.4
acetophenone	311	30.0	70.0
acetone	332	30.1	69.9
benzene	353	30.0	70.0

[a] S. L. Murov, "Handbook of Photochemistry," Marcel Dekker, New York (1973). [b] Determined by ^{1}H NMR.

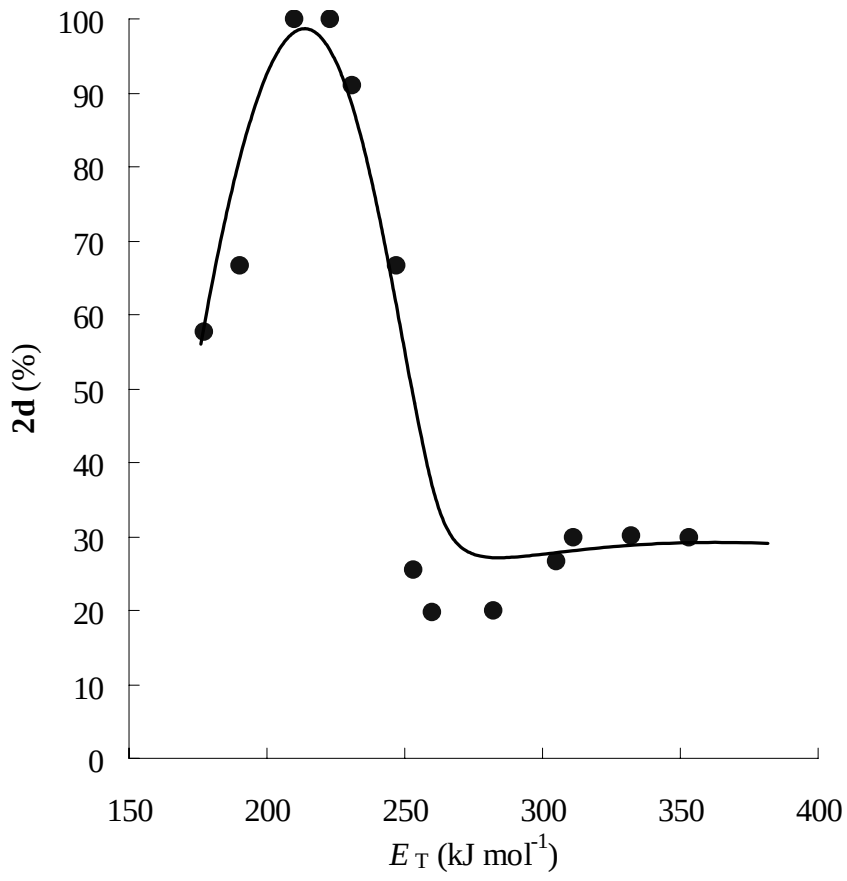

Figure 3. Hammpmd-Saltiel plot of triplet sensitized isomerization of **1d**.

4-2-3. Substituents Effect on Intramolecular [2+2] Photocycloaddition Reaction

To gain further information on the mechanistic property of intramolecular [2+2] photcycloaddition reaction, the author investigated the aromatic ring substituents effect on the photoreaction of variously *m*- and *p*-substituted diarylcyclobutane-fused quinone **1d-m** (Scheme 2).

Scheme 2.

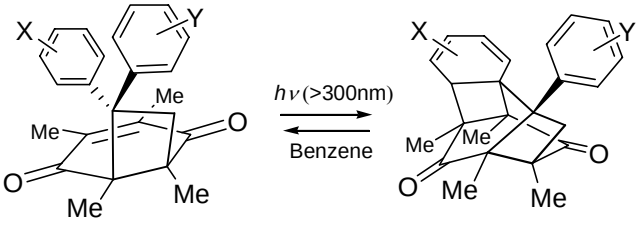

2d-m **4d-m**

	X	Y		X	Y
d	H	H	**i**	*p*-Me	*p*-Me
e	*p*-CF_3	H	**j**	*p*-OMe	*p*-OMe
f	H	*p*-CF_3	**k**	*p*-OMe	H
g	*p*-F	*p*-F	**l**	H	*p*-OMe
h	*p*-Cl	*p*-Cl	**m**	*m*-OMe	H

The quantum yield for the photocycloaddition reaction of variously substituted cyclobutane-fused quinone **2d-m** to cage compound **4d-m** were deteremined in benzene at their low conversion (<10%). Here, it should be noted that the quantum yields increased with increasing electron-donating power of the substituent on phenyl ring (except *endo-p*OMe entry 8). Although not presently understood the mechanistic explanation for such substituents effect, now it is under consideration.

Table 4. Photostationary equilibrated product ratios (**2** : **4**) in reversible photocycloaddition of **2**.

Entry	Compd.	X	Y	Irradiation time (min)	Ratio[a] **2** : **4**	$\Phi_{(\mathbf{2}\rightarrow\mathbf{4})}$
1	**2d**	H	H	100	30:70	0.043
2	**2e**	*p*-CF_3	H	240	18:82	0.029
3	**2f**	H	*p*-CF_3	180	29:71	0.032
4	**2g**	*p*-F	*p*-F	300	23:77	0.032
5	**2h**	*p*-Cl	*p*-Cl	100	50:50	0.030
6	**2i**	*p*-Me	*p*-Me	100	20:80	0.049
7	**2j**	*p*-OMe	*p*-OMe	120	13:87	0.103
8	**2k**	*p*-OMe	H	300	9:91	0.037
9	**2l**[b]	H	*p*-OMe	-	-	-
10	**2m**	*m*-OMe	H	100	17:83	0.15

[a] Irradiated in a NMR tube in benzene-d_6 through a Pyrex filter.[b] Unfortunately, it was not isolated in pure.

4-3. Conclusion

In summary, the primary [2+2] photocycloadducts of variously Me-substituted 1,4-benzoquinones with 1,1-diphenylethene underwent the reversible intramolecular [2+2] photocycloaddition to provide pentacyclotetradeca-10,12-diene-2,7-diones. The cage skeleton was characterized by very rare diagonal conjunction of two facing cyclobutane rings. The geometrical features of these reactions were interpreted in terms of the conformational preference which allowed the proximity of the relevant 2π components.

4-4. Experimental Section

Preparative Photoreaction of Quinones with 1,1-diphenylethene. Typical experimental procedure is described for the case of *p*-xyloquinone (**1a**). A solution of *p*-xyloquinone **1a** (1.0 g, 7.4 mmol) and 1,1-diphenylethene (2.58 ml, 14.8 mmol) in benzene (20 mL) was irradiated in a Pyrex tube with a filtered light (> 300 nm) at room temperature under an argon atmosphere for 40 h. After removal of solvent *in vacuo*, the reaction mixture was submitted for ^{1}H NMR to determine the product distributions. Column chromatographic treatment of the reaction mixture on silica gel successively gave recovered 1,1-diphenylethene, **2a** (1.78 g, 76 %), **3a** (0.33 g, 14 %), **4a** (trace) and **5a** (trace) with a mixture of ethyl acetate (5~20 % by volume) and hexane as eluent. The compounds **4** and **5** were separately prepared by irradiation (>300 nm) of a solution of **2** and **3** in a NMR tube (benzene-d_6) (*vide infra*). The structures of compounds **2-5** were deduced from the ^{1}H-NMR, ^{13}C-NMR, IR spectra as well as elemental analysis as shown below.

Reversible Photoisomerization of 2 and 3 into 4 and 5. General procedure is described for the case of **2**. A solution of **2** (0.02 mmol) in benzene-d_6 (670 μl) was irradiated in a NMR tube with a filtered light (> 300 nm). The ^{1}H-NMR monitoring of the reaction revealed the photoequilibration within 100 min for all the primary [2+2] photocycloadducts **2** and **3**.

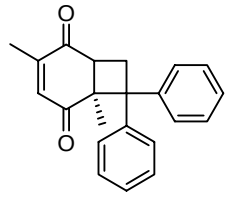

1,4-Dimethyl-8,8-diphenyl-bicyclo[4.2.0]oct-3-ene-2,5-dione(2a) : mp 80.9-82.5 °C (from hexane-chloroform); ^{1}H NMR (270 MHz, $CDCl_3$) δ 1.51 (s, 3H), 1.72 (d, 3H, *J*= 1.48), 2.84 (dd, 1H, *J*= 2.14, 10.4), 3.21 (dd, 1H, *J*= 10.4, 12.5), 3.56 (dd, 1H, *J*= 1.48, 12.5), 6.21 (q, 1H, *J*= 1.48), 7.04-7.19 (m, 6H), 7.24-7.36 (m, 4H); ^{13}C NMR (270MHz, $CDCl_3$) δ 16.6, 22.8, 33.4, 47.1, 56.2, 59.2, 126.1, 126.5, 127.0, 127.5, 128.1, 128.2, 128.5, 139.2, 141.5, 145.3, 150.7, 200.3, 200.5; IR (KBr): 1669, 1616, 1495, 1439, 1375, 1360, 1325, 1294, 1225 cm^{-1}. Anal. Calcd for $C_{22}H_{20}O_2$: C, 83.51; H, 6.37%. Found: C, 83.51; H, 6.29%.

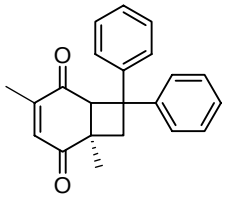

1,4-Dimethyl-7,7-diphenyl-bicyclo[4.2.0]oct-3-ene-2,5-dione(3a): mp 126.5-127.3 °C (from hexane-chloroform); ^{1}H NMR (270 MHz, $CDCl_3$) δ 1.37 (s, 3H), 1.62 (d, 3H, *J*= 1.32), 2.55 (d, 1H, *J*= 12.5), 3.71 (d, 1H, *J*= 12.5), 4.10 (s, 1H), 6.27 (q, 1H, *J*= 1.32), 7.05-7.20 (m, 6H), 7.29-7.40 (m, 4H); ^{13}C NMR (270MHz, $CDCl_3$) δ 16.1, 26.3, 42.45, 45.6, 53.8, 61.0, 126.2, 127.5, 128.3, 138.0, 149.9, 151.8, 198.2, 202.7; IR (KBr): 1669, 1616, 1495, 1439, 1375, 1360, 1325, 1294, 1225 cm^{-1}. Anal. Calcd for $C_{22}H_{20}O_2$: C, 83.51; H, 6.37%. Found: C, 83.39; H, 6.40%.

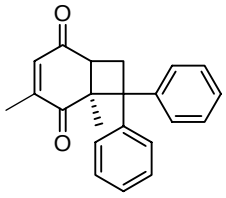

1,3-Dimethyl-8,8-diphenyl-bicyclo[4.2.0]oct-3-ene-2,5-dione(2b): mp 106.7-107.4 °C (from hexane-chloroform); ^{1}H NMR (270 MHz, $CDCl_3$) δ 1.55 (s, 3H), 1.67 (d, 3H, *J*= 1.40), 2.85 (dd, 1H, *J* = 1.98, 10.7), 3.19 (dd, 1H, *J*= 10.7, 12.5), 3.55 (dd, 1H, *J* =1.98, 12.5), 6.28(q, 1H, *J* = 1.40), 7.01-7.18 (m, 6H), 7.23-7.35 (m, 4H); ^{13}C NMR (270MHz, $CDCl_3$) δ 16.6, 23.0, 33.0, 47.7, 55.2, 59.4, 126.1, 126.5, 126.8, 127.6, 128.1, 128.3, 138.7, 141.7, 145.6, 151.4, 199.7, 201.1; IR (KBr): 1661, 1618, 1579, 1493, 1464, 1446, 1376, 1315, 1267 cm^{-1}.

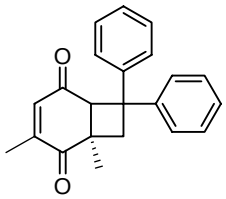

1,3-Dimethyl-7,7-diphenyl-bicyclo[4.2.0]oct-3-ene-2,5-dione(3b): mp 127.1-128.0 °C (from hexane-chloroform); ^{1}H NMR (270 MHz, $CDCl_3$) δ 1.37 (s, 3H), 1.74 (d, 3H, *J*= 1.48), 2.56 (d, 1H, *J* = 12.5), 3.75 (d, 1H, *J*= 12.5), 4.05 (s, 1H), 6.20(q, 1H, *J* = 1.48), 7.03-7.21 (m, 6H), 7.26-7.39 (m, 4H); ^{13}C NMR (270MHz, $CDCl_3$) δ 16.7, 26.6, 42.8, 45.0, 54.0, 61.6, 126.0, 126.1, 126.6, 127.8, 127.6, 128.5, 139.3, 140.3, 150.0, 150.4, 197.1, 203.2; IR (KBr): 1679, 1659, 1609, 1578, 1492, 1454, 1444, 1375, 1314, 1296, 1274 cm^{-1}.

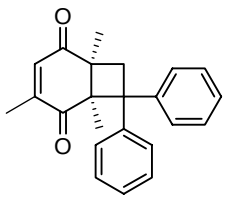

1,3,6-Trimethyl-8,8-diphenyl-bicyclo[4.2.0]oct-3-ene-2,5-dione(2c) : mp 118.7-119.9 °C (from hexane-chloroform); ^{1}H NMR (270 MHz, $CDCl_3$) δ 1.21 (s, 3H), 1.41 (s, 3H), 1.65 (d, 3H, *J* = 1.48), 2.72 (d, 1H, *J*= 12.0), 3.76 (d, 1H, *J*= 12.0), 6.25(q, 1H, *J* = 1.48), 7.01-7.15 (m, 6H), 7.22-7.32 (m, 4H); ^{13}C NMR (270MHz, $CDCl_3$) δ 16.5, 18.1, 21.6, 39.5, 49.0, 58.4, 58.5, 126.0, 126.4, 126.9, 127.6, 128.0, 128.2, 137.5, 141.6, 145.8, 150.9, 201.6, 203.4; IR (KBr): 1663, 1626, 1597, 1579, 1493, 1463, 1446, 1375, 1349, 1298, 1251, 1221 cm^{-1}. Anal. Calcd for $C_{22}H_{20}O_2$: C, 83.60; H, 6.71%. Found: C,83.46; H,6.56%.

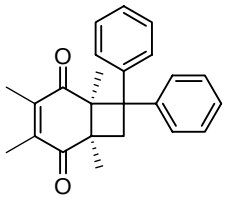

1,3,4,6-Tetramethyl-7,7-diphenyl-bicyclo[4.2.0]oct-3-ene-2,5-dione(2d=3d): mp 116.1-117.0 °C (from hexane-chloroform); ^{1}H NMR (270 MHz, $CDCl_3$) δ 1.20 (s, 3H), 1.43 (s, 3H), 1.64 (d, 3H, *J* = 1.07), 1.72 (d, 3H, *J*= 1.07), 2.71 (d, 1H, *J*= 12.0), 3.73 (d, 1H, *J*= 12.0), 6.98-7.15 (m, 4H), 7.20-7.34 (m, 6H); ^{13}C NMR (270MHz, $CDCl_3$) δ 13.0, 13.0, 18.3, 21.8, 39.9, 47.9, 58.3, 58.4, 125.9, 126.2, 126.9, 127.5, 128.0, 141.8, 145.7, 145.9, 146.8, 200.2, 203.1; IR (KBr): 1655, 1618, 1598, 1580, 1492, 1463, 1446, 1373, 1331, 1271, 1236 cm^{-1}.

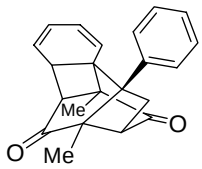

9,13-dimethyl-12-phenyl-pentacyclo[8.2.2.0^{1,6}.0^{7,13}.0^{9,12}]tetradeca-2,4-diene-8,14-dione (4a): ^{1}H NMR (270 MHz, $CDCl_3$) δ 1.34 (s, 3H), 1.79 (s, 3H), 2.44 (d, 1H, *J*= 11.0), 2.84 (d, 1H, *J*= 7.58), 3.08 (dd, 1H, *J*= 7.58, 11.0), 3.15 (m, 1H), 3.29 (m, 1H), 5.32 (m, 1H), 5.71-5.78 (m, 2H), 5.81-5.87 (m, 1H), 6.94-6.97 (m, 2H), 7.23-7.29 (m, 1H), 7.32-7.38 (m, 2H).

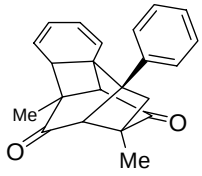

7,10-dimethyl-12-phenyl-pentacyclo[8.2.2.0^{1,6}.0^{7,13}.0^{9,12}]tetradeca-2,4-diene-8,14-dione (5a): ^{1}H NMR (270 MHz, $CDCl_3$) δ 1.27 (s, 3H), 1.30 (s, 3H), 2.56 (d, 1H, *J*= 10.7), 2.66 (d, 1H, *J*= 10.7), 3.04 (m, 1H), 3.31 (s, 1H), 3.63 (s, 1H), 5.56-5.61 (m, 1H), 5.72-5.76 (m, 1H), 5.82-5.88 (m, 1H), 5.84-5.98 (m, 1H), 7.05-7.09 (m, 2H), 7.22-7.29 (m, 1H), 7.33-7.38 (m, 1H); ^{13}C NMR (270MHz, $CDCl_3$) δ 12.6, 18.3, 41.2, 44.6, 46.4, 47.3, 53.1, 57.6, 57.8, 64.6, 122.8, 123.3, 124.6, 125.4, 126.3, 126.6, 128.4, 142.4, 207.5, 208.9.

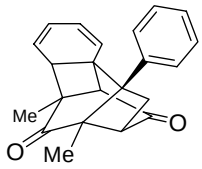

7,9-dimethyl-12-phenyl-pentacyclo[8.2.2.0^{1,6}.0^{7,13}.0^{9,12}]tetradeca-2,4-diene-8,14-dione (4b): ^{1}H NMR (270 MHz, $CDCl_3$) δ 1.32(s, 3H), 1.35 (s, 3H), 2.57 (dd, 1H, *J*= 1.90, 11.0), 2.76 (dd, 1H, *J*= 1.90, 7.58), 3.12 (dd, 1H, *J*= 7.58, 11.0), 3.22 (m, 1H), 3.63 (s, 1H), 5.55-5.63 (m, 2H), 5.73-5.79 (m, 1H), 5.90-5.97 (m, 1H), 6.91-6.95 (m, 2H), 7.23-7.29 (m, 1H), 7.31-7.37 (m, 2H); ^{13}C NMR (270MHz, $CDCl_3$) δ 12.9, 14.2, 22.4, 33.6, 45.6, 52.1, 53.8, 57.0, 63.3, 123.5, 124.4, 125.0, 125.4, 127.0, 127.3, 128.2, 139.9, 206.5, 210.6.

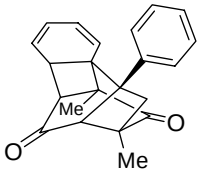

10,13-dimethyl-12-phenyl-pentacyclo[8.2.2.0^{1,6}.0^{7,13}.0^{9,12}]tetradeca-2,4-diene-8,14-dione (5b): ^{1}H NMR (270 MHz, $CDCl_3$) δ 1.29(s, 3H), 1.78 (s, 3H), 2.53 (s, 1H), 2.53 (s, 1H), 3.05 (d, 1H), 3.11 (dd, 1H), 3.27 (dd, 1H), 5.49 (m, 1H), 5.73-5.79 (m, 1H), 5.72-5.73 (m, 2H), 5.92-5.98 (m, 1H), 7.07-7.12 (m, 2H), 7.23-7.29 (m, 1H), 7.34-7.39 (m, 2H); ^{13}C NMR (270MHz, $CDCl_3$) δ 14.1, 18.5, 41.0, 41.2, 48.7, 52.5, 52.7, 54.7, 56.8, 64.5, 120.5, 124.8, 126.7, 126.9, 127.0, 127.4, 128.4, 142.9, 207.2, 208.0.

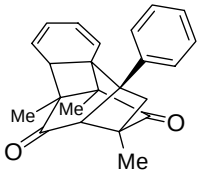

7,9,10-trimethyl-12-phenyl-pentacyclo[8.2.2.0^{1,6}.0^{7,13}.0^{9,12}]tetradeca-2,4-diene-8,14-dione (4c): ^{1}H NMR (270 MHz, $CDCl_3$) δ 1.08 (s, 3H), 1.20 (s, 3H), 1.32 (s, 3H), 2.61 (d, 1H, *J*= 10.9), 2.69 (d, 1H, *J*= 10.9), 3.27 (m, 1H), 3.65 (s,1H), 5.52 (dd, 1H, *J*= 0.82, 9.73), 5.61 (dd, 1H, *J*= 3.38, 9.73), 5.74 (dd, 1H, *J*= 5.44, 9.73), 5.89-5.96 (m, 1H), 6.90-7.09 (m, 3H); ^{13}C NMR (270MHz, $CDCl_3$) δ 11.7, 12.8, 13.4, 39.8, 45.1, 47.0, 50.7, 54.4, 54.8, 56.7, 63.1, 123.6, 124.4, 125.4, 126.9, 127.7, 128.1, 140.0, 207.6, 211.1.

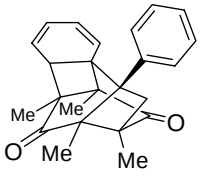

7,9,10,13-tetramethyl-12-phenyl-pentacyclo[8.2.2.0^{1,6}.0^{7,13}.0^{9,12}]tetradeca-2,4-diene-8,14-dione (4d): ^{1}H NMR (270 MHz, $CDCl_3$) δ 0.99 (s, 3H), 1.14 (s, 3H), 1.15 (s, 3H), 1.76 (s, 3H), 1.94 (d, 1H, *J*= 10.9), 2.09 (d, 1H, *J*= 10.9), 3.07 (m, 1H), 5.17-5.24 (m, 1H), 5.26-5.34 (m, 1H), 5.38-5.45 (m, 1H), 6.64-6.67 (m, 2H), 6.90-7.09 (m, 3H); ^{13}C NMR (270MHz, $CDCl_3$) δ 7.74, 11.4, 11.9, 13.5, 38.8, 43.5, 50.9, 51.7, 53.4, 54.0, 56.3, 63.0, 120.6, 120.9, 125.3, 125.7, 126.3, 126.9, 128.0, 140.6, 208.7, 210.7; IR (KBr): 1655, 1618, 1598, 1580, 1492, 1463, 1446, 1373, 1331, 1271, 1236 cm^{-1}.

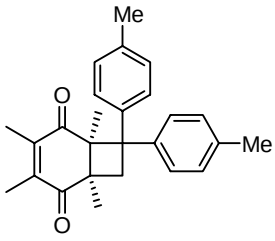

1,3,4,6-tetramethyl-7,7-di*p*-tolylbicyclo[4.2.0]oct-3-ene-2,5-dione (2i); ^{1}H NMR (270 MHz, $CDCl_3$) δ 1.18 (s, 3H), 1.40 (s, 3H), 1.65 (q, 3H, *J* = 0.99 Hz), 1.74 (q, 3H, *J* = 0.99 Hz), 2.14 (s, 3H), 2.25 (s, 3H), 2.67 (d, 1H, *J* = 11.9 Hz), 3.66 (d, 1H, *J* = 11.9 Hz), 6.85 (d, 2H, *J* = 8.24 Hz), 7.05 (d, 2H, *J* = 5.94 Hz), 7.08 (d, 2H, *J* = 5.94 Hz), 7.18 (d, 2H, *J* = 8.24 Hz); ^{13}C NMR (67.5 MHz, $CDCl_3$) δ 13.0, 13.1, 18.2, 20.8, 21.0, 21.7, 39.8, 47.9, 57.8, 58.1, 126.7, 127.3, 128.6, 128.6, 135.3, 135.6, 139.1, 143.2, 145.6, 146.7, 200.4, 203.2; IR (KBr): 3317, 3020, 2987, 2959, 2922, 2872, 2731, 2361, 1905, 1795, 1655, 1618, 1510, 1468, 1447, 1377, 1335, 1324, 1279, 1251, 1237, 1197, 1162, 1142, 1114 cm^{-1}; *Anal* Calcd for $C_{26}H_{28}O_2$: C, 83.83; H, 7.58, Found : C, 83.59; H, 7.61.

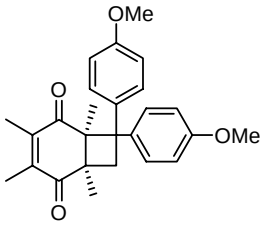

7,7-bis(4-methoxyphenyl)-1,3,4,6-tetramethylbicyclo[4.2.0]oct-3-ene-2,5-dione (2j); mp. 96.4-97.2 ^{o}C (from chloroform / *n*-hexane); ^{1}H NMR (270 MHz, $CDCl_3$) δ 1.18 (s, 3H), 1.39 (s, 3H), 1.69 (q, 3H, *J* = 0.99 Hz), 1.75 (q, 3H, *J* = 0.99 Hz), 2.65 (d, 1H, *J* = 12.4 Hz), 3.64 (d, 1H, *J* = 12.4 Hz), 3.66 (s, 3H), 3.74 (s, 3H), 6.60 (d, 2H, *J* = 8.90 Hz), 6.80 (d, 2H, *J* = 8.90 Hz), 7.10 (d, 2H, *J* = 8.90 Hz), 7.21 (d, 2H, *J* = 8.90 Hz); ^{13}C NMR (67.5 MHz, $CDCl_3$) δ 13.0, 13.2, 18.2, 21.6, 21.8, 39.8, 47.8, 55.2, 57.2, 58.1, 113.1, 113.3, 127.8, 128.6, 134.2, 138.6, 145.8, 146.6, 157.4, 157.5, 200.5, 203.2; IR (KBr): 3433, 2997, 2981, 2958, 2830, 2044, 1672, 1654, 1606, 1578, 1512, 1463, 1378, 1335, 1296, 1248, 1190, 1179, 1112 cm^{-1}; *Anal* Calcd for $C_{26}H_{28}O_4$: C, 77.20; H, 6.98, Found: C, 77.13; H, 6.98.

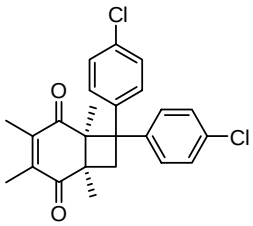

7,7-bis(4-chlorophenyl)-1,3,4,6-tetramethylbicyclo[4.2.0]oct-3-ene-2,5-dione (2h); ^{1}H NMR (270 MHz, $CDCl_3$) δ 1.17 (s, 3H), 1.37 (s, 3H), 1.70 (q, 3H, *J* = 1.15 Hz), 1.75 (q, 3H, *J* = 1.15 Hz), 2.63 (d, 1H, *J* = 12.0 Hz), 3.64 (d, 1H, *J* = 12.0 Hz), 7.02 (d, 2H, *J* = 6.76 Hz), 7.10 (d, 2H, *J* = 9.07 Hz), 7.20-7.23 (m, 4H); ^{13}C NMR (67.5 MHz, $CDCl_3$) δ 13.0, 13.3, 18.4, 21.6, 39.4, 47.9, 57.4, 57.9, 128.1, 128.2, 128.3, 128.9, 132.1, 132.5, 139.8, 143.9, 146.3, 146.7, 199.8, 202.7; IR (KBr): 3423, 2989, 2966, 2873, 2361, 1658, 1615, 1492, 1467, 1404, 1374, 1334, 1281, 1235, 1094, 1065 cm^{-1}; *Anal* Calcd for $C_{24}H_{22}Cl_2O_2$: C, 69.74; H, 5.25; Cl, 17.15, Found : C, 69.45; H, 5.25; Cl, 17.31.

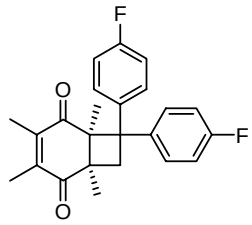

7,7-bis(4-fluorophenyl)-1,3,4,6-tetramethylbicyclo[4.2.0]oct-3-ene-2,5-dione (2g); ^{1}H NMR (270 MHz, $CDCl_3$) δ 1.20 (s, 3H), 1.40 (s, 3H), 1.71 (q, 3H, *J* = 1.32 Hz), 1.76 (q, 3H, *J* = 1.32 Hz), 2.67 (d, 1H, *J* = 12.2 Hz), 3.68 (d, 1H, *J* = 12.2 Hz), 6.73-6.80 (m, 2H), 6.93-7.00 (m, 2H), 7.13-7.20 (m, 2H), 7.23-7.30 (m, 2H); ^{13}C NMR (67.5 MHz, $CDCl_3$) δ 12.7, 13.1, 18.3, 21.5, 39.7, 47.7, 57.2, 57.9, 114.8 (*J* = 21.2), 115.0 (*J* = 21.2), 128.5 (*J* = 7.82), 129.4 (*J* = 7.82), 139.6 (*J* = 289.4), 139.6 (*J* = 289.9), 146.3, 146.7, 159.3, 162.9, 200.1, 202.9; IR (KBr): 3423, 2989, 2966, 2873, 2361, 1658, 1615, 1492, 1467, 1404, 1374, 1334, 1281, 1235, 1094, 1065 cm^{-1}.

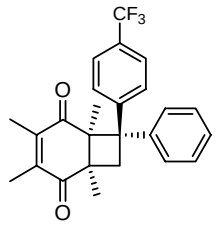

***endo*-(1R,6S,7S)-1,3,4,6-tetramethyl-7-phenyl-7-(4-(trifluoromethyl)phenyl)bicyclo[4.2.0]oct-3-ene-2,5-dione (2e)**; ^{1}H NMR (270 MHz, $CDCl_3$) δ 1.21 (s, 3H), 1.44 (s, 3H), 1.66 (q, 3H, *J* = 0.98 Hz), 1.74 (q, 3H, *J* = 0.98 Hz), 2.76 (d, 1H, *J* = 12.2 Hz), 3.74 (d, 1H, *J* = 12.2 Hz), 7.13-7.18 (m, 1H), 7.26-7.39 (m, 8H); ^{13}C NMR (67.5 MHz, $CDCl_3$) δ 12.8, 13.0, 18.3, 21.5, 39.6, 48.0, 58.3, 58.3, 124.8, 124.9, 126.4, 127.0, 128.1, 128.3, 128.8, 145.1, 146.2, 146.3, 146.9, 199.9, 203.1; IR (KBr): 3317, 3057, 2987, 2959, 2873, 1933, 1672, 1656, 1617, 1600, 1494, 1469, 1445, 1410, 1380, 1333, 1272, 1237, 1208, 1173, 1109 cm^{-1}; *Anal* Calcd for $C_{25}H_{23}F_3O_2$: C, 72.8; H, 5.62; F, 13.82, Found : C, 72.62; H, 5.61; F, 13.99.

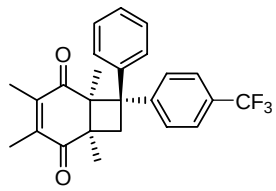

***exo*-(1R,6S,7S)-1,3,4,6-tetramethyl-7-phenyl-7-(4-(trifluoromethyl)phenyl)bicyclo[4.2.0]oct-3-ene-2,5-dione (2f)**; ^{1}H NMR (270 MHz, $CDCl_3$) δ 1.13 (s, 3H), 1.34 (s, 3H), 1.58 (q, 3H, *J* = 0.99 Hz), 1.66 (q, 3H, *J* = 0.99 Hz), 2.62 (d, 1H, *J* = 11.9 Hz), 3.69 (d, 1H, *J* = 11.9 Hz), 6.91-7.05 (m, 3H), 7.10-7.15 (m, 2H), 7.36 (d, 2H, *J* = 8.24 Hz), 7.45 (d, 2H, *J* = 8.24 Hz); ^{13}C NMR (67.5 MHz, $CDCl_3$) δ 12.8, 13.0, 18.2, 21.6, 39.6, 47.8, 58.1, 58.1, 125.1, 125.1, 126.7, 127.4, 127.6, 128.2, 140.8, 146.1, 146.1, 149.9, 200.0, 202.8; IR (KBr): 3317, 3057, 2987, 2959, 2873, 1933, 1672, 1656, 1617, 1600, 1494, 1469, 1445, 1410, 1380, 1333, 1272, 1237, 1208, 1173, 1109 cm^{-1}; *Anal* Calcd for $C_{25}H_{23}F_3O_2$: C, 72.8; H, 5.62; F, 13.82, Found : C, 72.53; H, 5.56; F, 14.00.

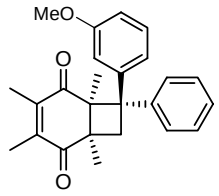

***endo*-(1R,6S,7S)-1,3,4,6-tetramethyl-7-phenyl-7-(3-methoxyphenyl)bicyclo[4.2.0]oct-3-ene-2,5-dione (2m)**; ^{1}H NMR (270 MHz, $CDCl_3$) δ 1.19 (s, 3H), 1.42 (s, 3H), 1.67 (q, 3H, *J* = 0.99 Hz), 1.74 (q, 3H, *J* = 0.99 Hz), 2.71 (d, 1H, *J* = 12.0 Hz), 3.68 (d, 1H, *J* = 12.0 Hz), 3.69 (s, 3H), 6.51-6.55 (m, 1H), 6.74-6.81 (m, 2H), 6.95-6.98 (m, 1H), 7.01-7.16 (m, 1H), 7.23-7.33 (m, 4H); ^{13}C NMR (67.5 MHz, $CDCl_3$) δ 13.0, 13.0, 18.2, 21.8, 40.1, 47.9, 55.0, 58.2, 58.3, 112.2, 113.3, 120.0, 125.9, 126.9, 127.9, 129.0, 143.4, 145.4, 145.7, 146.6, 159.0, 200.1, 203.0; IR (KBr): 3317, 3057, 2987, 2959, 2873, 1933, 1672, 1656, 1617, 1600, 1494, 1469, 1445, 1410, 1380, 1333, 1272, 1237, 1208, 1173, 1109 cm^{-1}.

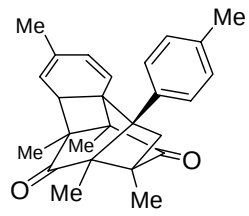

3,7,9,10,13-pentamethyl-12-tolyl-pentacyclo[8.2.2.0^{1,6}.0^{7,13}.0^{9,12}]tetradeca-2,4-diene-8,14-dione (4i); ^{1}H NMR (270 MHz, $CDCl_3$) δ 1.06 (s, 3H), 1.11 (s, 3H), 1.21 (s, 3H), 1.56 (s, 3H), 1.62 (dd, 3H, *J* = 2.47, 1.48 Hz), 2.32 (s, 3H), 2.47 (d, 1H, *J* = 10.8 Hz), 2.60 (d, 1H, *J* = 10.8 Hz), 3.22 (m, 1H), 5.24-5.28 (m, 2H), 5.63 (d, 1H, *J* = 9.89 Hz), 6.88 (d, 2H, *J* = 7.90 Hz), 7.13 (d, 2H, *J* = 7.90 Hz).

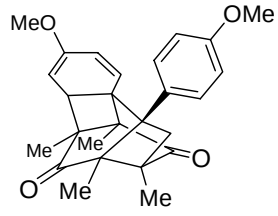

3-methoxy-7,9,10,13-tetramethyl-12-anysyl-pentacyclo[8.2.2.0^{1,6}.0^{7,13}.0^{9,12}]tetradeca-2,4-diene-8,14-dione (4j);^{1}H NMR (270 MHz, $CDCl_3$) δ 1.07 (s, 3H), 1.12 (s, 3H), 1.22 (s, 3H), 1.59 (s, 3H), 2.46 (d, 1H, *J* = 10.9 Hz), 2.61 (d, 1H, *J* = 10.9 Hz), 3.36 (d, 1H, *J* = 3.63 Hz), 3.50 (s, 3H), 3.79 (s, 3H), 4.40 (dd, 1H, *J* = 3.63, 1.98 Hz), 5.36 (d, 1H, *J* = 10.2 Hz), 5.63 (dd, 1H, *J* = 1.98, 10.2 Hz), 6.86 (d, 2H, *J* = 8.90 Hz), 6.93 (d, 2H, *J* = 8.90 Hz); ^{13}C NMR (67.5 MHz, $CDCl_3$) δ 7.48, 11.5, 11.7, 13.4, 38.9, 43.1, 51.0, 53.6, 53.8, 54.3, 55.2, 55.5, 61.7, 113.6, 123.9, 127.1, 129.1, 132.7, 153.7, 158.3, 209.2, 211.3;

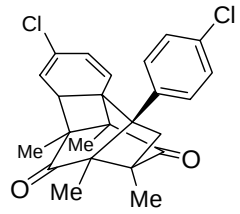

3-chloro-7,9,10,13-tetramethyl-12-(4-chlorophenyl)-pentacyclo[8.2.2.0^{1,6}.0^{7,13}.0^{9,12}]tetradeca-2,4-diene-8,14-dione (4h); ^{1}H NMR (270 MHz, $CDCl_3$) δ 1.08 (s, 3H), 1.13 (s, 3H), 1.22 (s, 3H), 1.61 (s, 3H), 2.48 (d, 1H, *J* = 11.0 Hz), 2.62 (d, 1H, *J* = 11.0 Hz), 3.27 (d, 1H, *J* = 3.80 Hz), 5.34 (d, 1H, *J* = 10.1 Hz), 5.66 (dd, 1H, *J* = 3.80, 1.48 Hz), 5.72 (dd, 1H, *J* = 10.1, 1.48 Hz), 6.91 (d, 2H, *J* = 8.57 Hz), 7.33 (d, 2H, *J* = 8.57 Hz); ^{13}C NMR (67.5 MHz, $CDCl_3$) δ 7.84, 11.3, 11.8, 13.5, 38.6, 44.6, 50.1, 51.1, 53.4, 54.0, 56.2, 62.9, 120.1, 123.9, 128.2, 128.8, 129.0, 129.8, 133.1, 138.6, 207.6, 209.5.

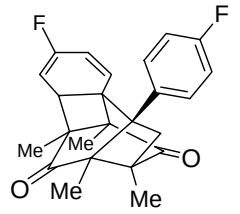

3-fluoro-7,9,10,13-tetramethyl-12-(4-fluorophenyl)-pentacyclo[8.2.2.0^{1,6}.0^{7,13}.0^{9,12}]tetradeca-2,4-diene-8,14-dione (4h); ^{1}H NMR (270 MHz, $CDCl_3$) δ 1.08 (s, 3H), 1.13 (s, 3H), 1.22 (s, 3H), 1.61 (s, 3H), 2.48 (d, 1H, *J* = 11.0 Hz), 2.62 (d, 1H, *J* = 11.0 Hz), 3.27 (d, 1H, *J* = 3.80 Hz), 5.34 (d, 1H, *J* = 10.1 Hz), 5.66 (dd, 1H, *J* = 3.80, 1.48 Hz), 5.72 (dd, 1H, *J* = 10.1, 1.48 Hz), 6.91 (d, 2H, *J* = 8.57 Hz), 7.33 (d, 2H, *J* = 8.57 Hz); ^{13}C NMR (67.5 MHz, $CDCl_3$) δ 7.84, 11.3, 11.8, 13.5, 38.6, 44.6, 50.1, 51.1, 53.4, 54.0, 56.2, 62.9, 120.1, 123.9, 128.2, 128.8, 129.0, 129.8, 133.1, 138.6, 207.6, 209.5.

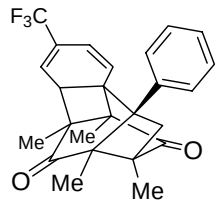

7,9,10,13-tetramethyl-3-trifluoromethyl--12-phenyl-pentacyclo[8.2.2.0^{1,6}.0^{7,13}.0^{9,12}]tetradeca-2,4-diene-8,14-dione (4e); ^{1}H NMR (270 MHz, $CDCl_3$) δ 1.09 (s, 3H), 1.17 (s, 3H), 1.25 (s, 3H), 1.55 (s, 3H), 2.53 (d, 1H, *J* = 10.9 Hz), 2.68 (d, 1H, *J* = 10.9 Hz), 3.32-3.35 (m, 1H), 5.50 (dd, 1H, *J* = 9.89, 0.99 Hz), 5.87 (d, 1H, *J* = 0.99 Hz), 6.17-6.19 (m, 1H), 6.96-6.99 (m, 2H), 7.25-7.39 (m, 3H); ^{13}C NMR (67.5 MHz, $CDCl_3$) δ 7.74, 11.1, 11.7, 13.4, 38.7, 42.6, 50.9, 51.4, 53.5, 54.2, 56.5, 63.3, 121.6, 124.0, 124.6, 127.1, 127.2, 127.8, 128.4, 140.1, 207.8, 209.7.

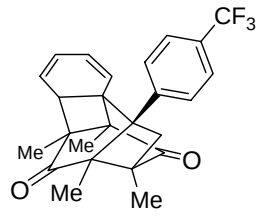

7,9,10,13-tetramethyl-12-(4-trifuluoromethylphenyl)-pentacyclo [8.2.2.0^{1,6}.0^{7,13}.0^{9,12}]tetradeca-2,4-diene-8,14-dione (4f); ^{1}H NMR (270 MHz, $CDCl_3$) δ 1.09 (s, 3H), 1.15 (s, 3H), 1.23 (s, 3H), 1.66 (s, 3H), 2.53 (d, 1H, *J* = 10.9 Hz), 2.63 (d, 1H, *J* = 10.9 Hz), 3.23 (m, 1H), 5.22 (m, 1H), 5.62-5.67 (m, 1H), 5.72-5.83 (m, 2H), 7.12 (d, 2H, *J* = 8.24 Hz), 7.60 (d, 2H, *J* = 8.24 Hz).

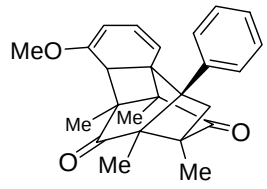

2-methoxy-7,9,10,13-tetramethyl-12-phenyl-pentacyclo[8.2.2.0^{1,6} .0^{7,13}.0^{9,12}]tetradeca-2,4-diene-8,14-dione (4m); ^{1}H NMR (270 MHz, $CDCl_3$) δ 1.07 (s, 3H), 1.11 (s, 3H), 1.14 (s, 3H), 1.61 (s, 3H), 2.51 (d, 1H, *J* = 10.9 Hz), 2.63 (d, 1H, *J* = 10.9 Hz), 3.29 (m, 1H), 3.53 (s, 3H), 4.76 (d, 1H, *J* = 6.59 Hz), 4.98 (d, 1H, *J* = 9.56 Hz), 5.81 (dd, 1H, *J* = 6.59, 9.56 Hz), 7.01 (d, 2H, *J* = 6.92 Hz), 7.24-7.34 (m, 3H); ^{13}C NMR (67.5 MHz, $CDCl_3$) δ 10.4, 11.1, 11.8, 13.4, 39.0, 44.4, 51.5, 53.4, 54.1, 54.2, 54.7, 56.1, 62.3, 94.5, 113.5, 126.8, 127.2, 128.1, 128.1, 140.7, 157.3, 209.1, 210.7

X-ray Crystal Structure Determination of 2d: $C_{24}H_{24}O_2$, M = 344.45, monoclinic, space group $P2_1/c$ with *a* = 9.0060(4), *b* = 15.4309(6), *c* = 14.1258(6) Å, β = 103.187(1)^{o}, *V* = 1911.3(1) Å ^{3}, *Z* = 4, *Dcalc* = 1.197 g/cm^3, *R* = 0.090 and *Rw* = 0.180 for 4362 reflections with *I*>2.0σ(*I*).

X-ray Crystal Structure Determination of 2i: $C_{26}H_{28}O_2$, M = 372.51, monoclinic, space group $P2_1/c$ with *a* = 8.7765(4), *b* = 19.7514(8), *c* = 12.5870(6) Å, β = 101.484(1)^{o}, *V* = 2138.2(2) Å ^{3}, *Z* = 4, *Dcalc* = 1.157 g/cm^3, *R* = 0.129 and *Rw* = 0.187 for 4904 reflections with *I*>2.0σ(*I*).

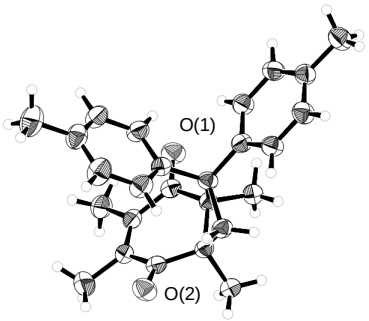

Figure 4. ORTEP drawing of **2i**.

X-ray Crystal Structure Determination of 4d: $C_{24}H_{24}O_2$, M = 344.45, monoclinic, space group $P2_1/a$ with a = 9.1018(2), b = 16.3061(3), c = 12.8443(2) Å, β = 104.4717(8)°, V = 1845.81(6) Å ^{3}, Z = 4, $Dcalc$ = 1.157 g/cm^3, R = 0.198 and Rw = 0.214 for 1886 reflections with $I>2.0\sigma(I)$.

X-ray Crystal Structure Determination of 2f: $C_{25}H_{23}O_2$, M = 412.45, orthorhombic, space group $P2_12_12_1$ with a = 16.8434(3), b = 8.5049(2), c = 14.6979(3) Å, V = 2105.5(1) Å ^{3}, Z = 4, $Dcalc$ = 1.301 g/cm^3, R = 0.169 and Rw = 0.160 for 2303 reflections with $I>2.0\sigma(I)$.

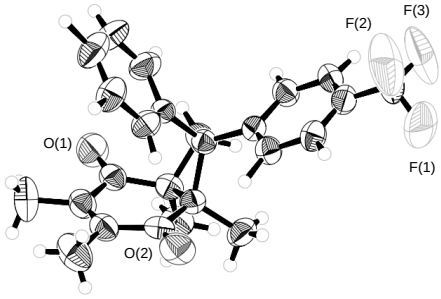

Figure 5. ORTEP drawing of **2f**.

X-ray Crystal Structure Determination of 2g: $C_{24}H_{22}F_2O_2$, M = 380.43, monoclinic, space group $P2_1/n$ with a = 14.2181(3), b = 8.3439(2), c = 17.9660(3) Å, β = 111.8375(7)°, V = 1978.44(6) Å ^{3}, Z = 4, $Dcalc$ = 1.277 g/cm^3, R = 0.065 and Rw = 0.1402 for 3831 reflections with $I>2.0\sigma(I)$.

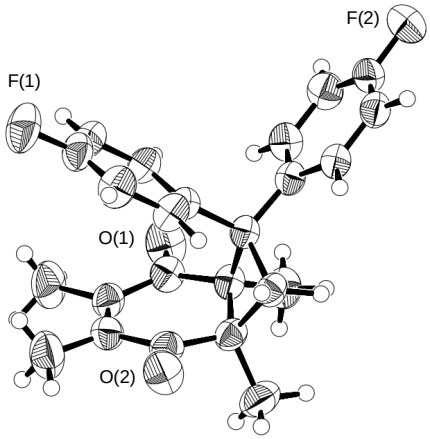

Figure 6. ORTEP drawing of **2g**.

X-ray Crystal Structure Determination of 2k: $C_{25}H_{26}O_3$, M = 380.43, monoclinic, space group P-1 with *a* = 8.2764(2), *b* = 21.2146(5), *c* = 10.8897(3) Å, β = 96.284(2)°, *V* = 1900.54(8) Å ^{3}, *Z* = 4, *Dcalc* = 1.329 g/cm^3, *R* = 0.0603 and *Rw* = 0.1404 for 3762 reflections with *I*>2.0σ(*I*).

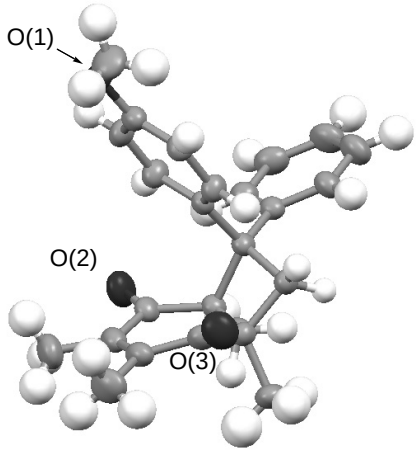

Figure 7. ORTEP drawing of **2k**.

X-ray Crystal Structure Determination of 2j: $C_{26}H_{28}O_4$, M = 404.50, monoclinic, space group $P2_1/a$ with *a* = 9.9518(3), *b* = 13.4718(4), *c* = 17.0032(5) Å, β = 104.4754(14)°, *V* = 2207.24(11) Å ^{3}, *Z* = 4, *Dcalc* = 1.217 g/cm^3, *R* = 0.0717 and *Rw* = 0.2299 for 4228 reflections with *I*>2.0σ(*I*).

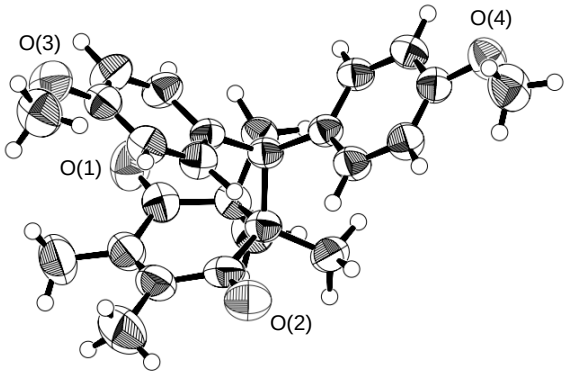

Figure 8. ORTEP drawing of **2j**.

X-ray Crystal Structure Determination of 4g: $C_{26}H_{28}O_4$, M = 404.50, monoclinic, space group $P2_1/a$ with a = 9.9518(3), b = 13.4718(4), c = 17.0032(5) Å, β = 104.4754(14)°, V = 2207.24(11) Å ^{3}, Z = 4, $Dcalc$ = 1.217 g/cm^3, R = 0.0717 and Rw = 0.2299 for 4228 reflections with I>2.0σ(I).

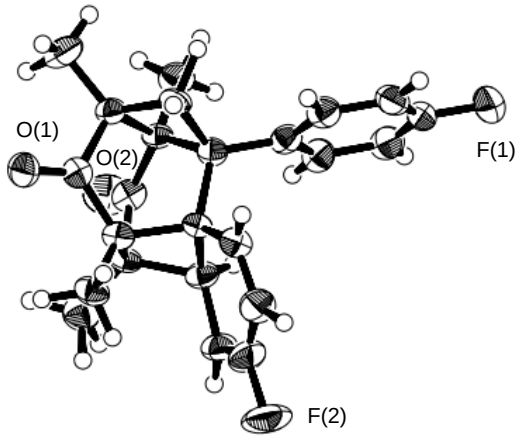

Figure 9. ORTEP drawing of **4g**.

X-ray Crystal Structure Determination of α-2m: $C_{25}H_{26}O_3$, M = 374.48, monoclinic, space group $P2_1/a$ with a = 13.4860(3), b = 10.2260(4), c = 14.9480(5) Å, β = 90.3660(14)°, V = 2061.4(11) Å ^{3}, Z = 4, $Dcalc$ = 1.207 g/cm^3, R = 0.1227 and Rw = 0.4403 for 3938 reflections with I>2.0σ(I).

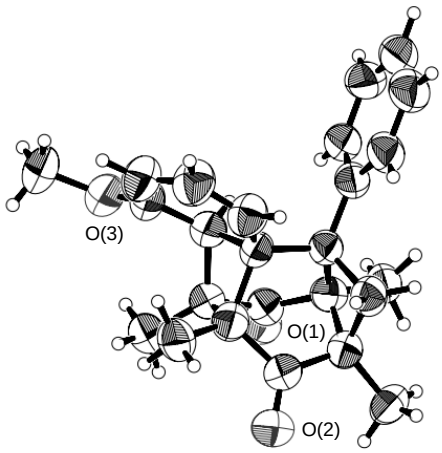

Figure 10. ORTEP drawing of **α-2m.**

X-ray Crystal Structure Determination of β-2m: $C_{25}H_{26}O_3$, M = 374.48, monoclinic, space group $P2_1/a$ with a = 13.4664(3), b = 10.2169(2), c = 14.998(3) Å, β = 90.7449(13)°, V = 2059.44(11) Å ^{3}, Z = 4, $Dcalc$ = 1.208 g/cm^3, R = 0.0491 and Rw = 0.1720 for 3675 reflections with $I>2.0\sigma(I)$.

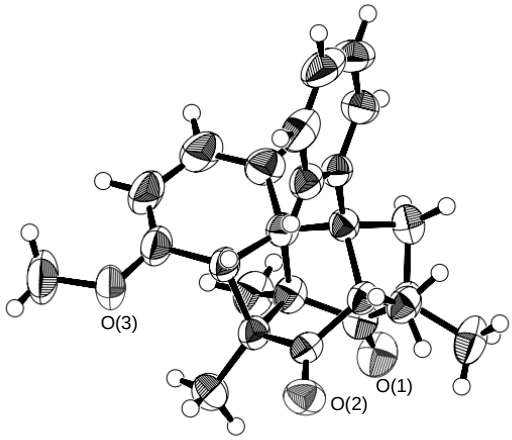

Figure 11. ORTEP drawing of **β-2m.**

4-5. Reference and Notes

(1) (a) Jones, G.; Becker, W. G.; Chiang, S.-H. *J. Am. Chem. Soc*. **1983**, *105*, 1269–1276. (b) Behr, J.; Braun, R.; Grimme, S.; Kummer, M.; Martin, H.-D.; Mayer, B.; Rubin, M.B.; Ruck, C. *Eur. J. Org. Chem*. **1998**, 2339–2348. (c)Laurenti, D.; Santelli-Rouvier, C.; Pèpe, G.; Santelli, M. *J. Org. Chem.* **2000**, *65*, 6418–6422. (d) Koizumi, T,; Harada, K.; Asahara, H.; Mochizuki, E.; Kokubo, K.; Oshima, T. *J. Org. Chem*. **2005**, *70*, 8364–8371.

(2) Crimmins, M. T. *Chem. Rev.* **1988**, *88*, 1453–1473.

(3) (a) Fleck, M.; Bach, T. *Angew. Chem*. **2008**, *47*, 6189–6191. (b) Shipe, W. D.; Sorensen, E. J. *J. Am. Chem. Soc*. **2006**, *128*, 7025−7035. (c) Lo, P. C.-K.; Snapper, M. L. *Org. Lett.* **2001**, *3*, 2819–2821.

(4) (a) Nishimura, J.; Nakamura, Y.; Hayashida, Y.; Kudo, T. *Acc. Chem. Res*. **2000**, *33*. 679–686. (b) Faure, S.; Blanc, P.-L. S.; Piva, Olivier. *Tetrahedron Lett.* **1999**, *40*, 6001–6004. (c) Vassilikogiannakis, G.; Hatzimarinaki, M.; Orfanopoulos, M. *J. Org. Chem.* **2000**, *65*, 8180–8187. (d) Hoffmann, N. *Tetrahedron*, **2002**, *58*, 7933–7941.

(5) (a) Mattay, J. *Tetahedron*. **1985**, *41*, 2405–2417. (b)Yoshimi, Y.; Konishi, S.; Maeda, H.; Mizuno, K. *Tetrahedron Lett.* **2001**, *42*, 3475–3477. (c) Maeda, H.; Waseda, S.; Mizuno, K. *Chem. Lett.* **2000**, 1238–1239.

(6) (a) Kokubo, K.; Nakajima, Y.; Iijima, K.; Yamaguchi, H.; Kawamoto, T.; Oshima, T. *J. Org. Chem.* **2000**, *65*, 3371–3378. (b) Braun, M.; Christl, M.; Peters, E.M.; Peters, K. *J. Chem. Soc., Perkin Trans. 1*. **1999**, 2813–2820. (c) Bosch, E.; Hubig, S.M.; Lindeman, S.V.; Kochi, J. K. *J. Org. Chem.* **1998**, *63*, 592–601. (d) Kokubo, K.; Masaki, T.; Oshima, T. *Org. Lett.* **2000**, *2*, 1979–1981. (e) Kokubo, K.;

Kawahara, K.; Takatani, T.; Moriwaki, H.; Kawamoto, T.; Oshima, T. *Org. Lett.* **2000**, *2*, 559–562.

(7) (a) Barborak, J. C.; Watts, L.; Pettit, R. *J. Am. Chem.Soc.* **1966**, *88*, 1328–1329 (b) Fessner, W.-D.; Rodriguez, M. *Angew. Chem., Int. Ed.* **1991**, *30*, 1020–1022. (c) Nair, M. S.; Sudhir, U.; Joly, S.; Rath, N. P.; *Tetrahedron*. **1999**, *55*, 7653–7660. (d) Wladislaw, B.; Marzorati, L.; Campos, I. P. A.; Viertler, H. *J. Chem. Soc., Perkin Trans. 2*. **1992**, *2*, 475–477. (e) Iwamoto, H.; Takuwa, A.; Hamada, K.; Fujiwara, R. *J. Chem. Soc., Perkin Trans. 1*. **1999**, 575–582. (f) Appel, W. K.; Greenhough, T. J.; Scheffer, J. R.; Trotter, J.; Walsh, L. *J. Am. Chem. Soc.* **1980**, *102*, 1158–1160. (g) Appel, W. K.; Greenhough, T. J.; Scheffer, J. R.; Trotter, J.; Walsh, L. *J. Am.Chem.Soc.* **1980**, *102*, 1160–1161.

(8) We could not find any appreciable CT absorption due to the quinone-ethene complexation over practical 330 nm in view of the essential superimposition of UV spectrum of **1a** (10 mM in benzene; λ_{shol} = 350 nm (ε = 134), λ_{max} = 427 (25.3) and 443 (25.7), and λ_{shol} = 470 (15.6)) in the absence and the presence of 10 equivalent of ethene. This implies that the possible CT complex plays a less important role in the present [2+2] photocycloaddition.

(9) Crystallographic data for the compound **5a** have been deposited with the Cambridge Crystallographic Data Centre as supplementary publication number CCDC 615010. Copies of the data can be obtained, free of charge, on application to CCDC, 12 Union Road, Cambridge CB2 1EZ, UK (fax: +44(0)-1223-336033 or e-mail: deposit@ccdc.cam.ac.uk).

(10) Recently, Xu et al. reported that the irradiation of chloranil with variously *p*-substituted 1,1-diphenylethene gave the pentacyclic cage compounds with orthogonally connected two cyclobutane rings in markedly contrast to our pentacyclic cage compounds; see *J. Org. Chem.* **2000**, *65*, 30–40.

(11) (a) Crimmins, M. T.; Pace, J. M.; Nantermet, P. G.; Kim-Meade, A. S.; Thomas, J. B.; Watterson, S. H.; Wagman, A. S. *J. Am. Chem. Soc*. **2000**, *122*, 8453–8463. (b) Ferrer, L. O.; Margaretha, P. *Chem. Commun.* **2001**, 481–482. (c) Chen, C.; Chang, V.; Cai, X.; Duesler, E.; Mariano, P. S. *J. Am. Chem. Soc*. **2001**, *123*, 6433–6434.

(12) (a) Wagner, P. J.; *Tetrahedron Lett*. **2002**, *43*, 3569–3571. (b) Kokubo, K.; Yamaguchi, H.; Kawamoto, T,.; Oshima, T. *J. Am. Chem.Soc.* **2002**, *124*, 8912–8921. (c) Hei, X.-M.; Song, Q.-H.; Li, X.-B.; Tang, W.-J.; Wang, H.-B.; Guo, Q.-X. *J. Org. Chem.* **2005**, *70*, 2522–2527. (d) Aoyama, H.; Arata, Y.; Omote, Y. *J. Chem. Soc. Commun.* **1990**, 736–737.

(13) Crystallographic data for the compound **2d** have been deposited with the Cambridge Crystallographic Data Centre as supplementary publication number CCDC 615011. Copies of the data can be obtained, free of charge, on application to CCDC, 12 Union Road, Cambridge CB2 1EZ, UK (fax: +44(0)-1223-336033 or e-mail: deposit@ccdc.cam.ac.uk).

(14) Kohmoto, S.; Ono, Y.; Masu, H.; Yamaguchi, K.; Kishikawa, K.; Yamamoto, M. *Org. Lett.* **2001**, *3*, 4153–4155.

(15) (a) Miranda, M. A.; Izquierdo, M. A. *Chem. Comm.* **2003**, 364–365. (b) Okada, K.; Hisamitsu, K.; Mukai, T. *Tetrahedron Lett.* **1981**, *22*, 1251–1254. (c) Masnovi, J. M.; Kochi, J. K. *J. Am. Chem.Soc.* **1985**, *107*, 6781–6788. (d) Yonezawa, N.; Yamashita, T.; Kanoe, T.; Saigo, K.; Hasegawa, M. *Ind. Eng. Chem. Prod. Res.* **1985**, *24*, 593–598.

(16)(a) Hammond, G. S.; Saltiel, J. *J. Am. Chem.Soc.* **1963**, *85*, 2516–2617. (b) Hammond, G. S.; Saltiel, J.; Lamola, A. A.; Turro, N. J.; Bradshaw, J. S.; Cowan, D. O.; Counsell, R. C.; Vogt, V.; Dalton, C. *J. Am. Chem.Soc.* **1964**, *86*, 3197–3217.

Conclusions

This thesis deals with the acid- and photo-reaction of small-membered ring fused quinone derivatives comprised of the following points, (1) remote π-Aryl participation reaction of Homobenzoquinone epoxide, (2) a prominent role of oxirane Walsh orbital, (3) rearrnagement reaction of cyclobutane-fused quinone. The author hopes that this basic work described in this thesis contributes to the further development of synthesis of novel carbon skeletons, which are difficult to produce by conventional methods.

In chapter 1, the acid-catalyzed rearrangement of homobenzoquinone epoxides possessing *endo*-aromatic ring displayed a new synthesis of polycyclic compounds involving a regioselective oxirane ring-opening and a crucial transannular cyclization. Additionally, based on the kinetics and conformational effects in acid-catalysed reactions of the present homobenzoquinone epoxides, the author has found that the π-aryl participated electron-donating interaction with the vacant oxirane Walsh orbital plays a prominent role in the epoxide ring-opening. Moreover, the dual pathway for *p,p'*-dichloro substituted homobenzoquinone epoxide is likely to prove that the acid-catalyzed ring-opening of diarylhomobenzoquinone epoxides occurs via a concerted manner involving a very rare remote (δ-located) π-aryl participated transition state. These findings will provide very useful insights into the mechanistic understanding of the acid-catalyzed ring-opening of epoxides.

In chapter 2, the author has performed a kinetic study of the BF_3-catalyzed ring-opening reactions of *endo*/*exo* *m*- and *p*-substituted diarylhomobenzoquinone epoxides. These reactions proceeded through two types of S_E2-Ar transannular cyclizations to give tricyclic diketo-alcohols and cyclohexadienone spiro-linked tricyclic diketo-alcohols, respectively. The rates were significantly accelerated by the through-space π-aryl participation of electron-donating *endo*-aromatic rings, but negligibly influenced by the through-bond

electronic effects of *exo*-aromatic rings. The Hammett treatment using modified site-dependent substituent parameters σ^{ipso} and σ^{ortho} indicated that the *ipso*/*ortho* dihapto(η^2) π-aryl participation occurs for the *endo*-aryl groups. Kinetics substituent effects of these reactions were compared with those of the analogous acid-catalyzed transannular cyclization of the cyclobutene-fused diarylhomobenzoquinones. It was found that the present epoxides exhibit the η^2 π-aryl participation with the 1.6-times more effective contribution at the *ipso*-position, whereas the cyclobutene-fused homologues with almost comparable *ipso*/*ortho* contribution. These results were interpreted in terms of the geometrical features of the π–electron accepting vacant orbital of oxirane and cyclobutene ring. The physicochemical information obtained in the present study will provide a very important insight into the understanding of the π-aryl participation as well as the mechanistic aspects in the acid-catalyzed ring-opening reaction of epoxides.

In chapter 3, the author found that the subsequent ring-enlargement by 1,2-acyl migration associated with the incorporated cyclopropane ring-opening reaction, depending on the substitution pattern of the quinone methyl groups. The author has also investigated the acid-catalyzed rearrangement of cyclobutane-fused quinone epoxide. This compound underwent the novel consecutive skeletal rearrangements. These findings provide the useful information on the rearrangements of polycyclic epoxides and the design of more extended framework compounds.

In chapter 4, the primary [2+2] photocycloadducts of variously Me-substituted 1,4-benzoquinones with 1,1-diphenylethene underwent the reversible intramolecular [2+2] photocycloaddition to provide pentacyclotetradeca-10,12-diene-2,7-diones. The cage skeleton was characterized by very rare diagonal conjunction of two facing cyclobutane rings. The geometrical features of these reactions were interpreted in terms of the conformational preference which allowed the proximity of the relevant 2π components.

List of Publications

1. "Two Conformers of 10,11-dihydro-5*H*-dibenzo[*a*,*d*]cycloheptene spiro-linked with homobenzoquinone epoxide"
   Haruyasu Asahara, Takuya Koizumi, Eiko Mochizuki, and Takumi Oshima
   Acta Cryst. C., **2006**, *62*, 136–138.

2. "Conformational Analysis in Reversible Intramolecular [2+2] Photocycloaddition of Diphenylbicyclo[4.2.0]oct-3-ene-2,5-diones"
   Haruyasu Asahara, Eiko Mochizuki and Takumi Oshima
   Tetrahedron Lett., **2006**, *47*, 7881–7884.

3. "Acid-Catalyzed Rearrangement of Aryl-Substituted Homobenzoquinone Epoxides"
   Haruyasu Asahara, Emi Kubo, Kyoko Togaya, Takuya Koizumi, Eiko Mochizuki, and Takumi Oshima
   Org. Lett., **2007**, *9*, 3421–3424.

4. "Mechanistic evidence for the remote π-aryl participation in acid-catalyzed ring opening of homobenzoquinone epoxides"
   Takumi Oshima, Haruyasu Asahara, Takuya Koizumi, and Saki Miyamoto
   Chem. Commun., **2008**, *15*, 1804–1806.

5. "Conformational Effects in Acid-Mediated Ring Opening of Epoxides: A Prominent Role of the Oxirane Walsh Orbital"
   Takumi Oshima, Haruyasu Asahara, Emi Kubo, Saki Miyamoto, and Kyoko Togaya
   Org. Lett., **2008**, *10*, 2413–2416.

6. "Kinetic Evidence for Dihapto (η^2) π-Aryl Participation in Acid-Catalyzed Ring-Opening of Diarylhomobenzoquinone Epoxides"
   Haruyasu Asahara, Kohta Saito, Naohiko Ikuma, and Takumi Oshima
   J. Org. Chem., **2010**, *75*, 733–740.

7. "Substituent Effect on Intramolecular [2+2] Photocycloaddition of Cyclobutane-Fused Quinone"
   Haruyasu Asahara, Naohiko Ikuma, Kei Ohkubo, Shunichi Fukuzumi, and Takumi Oshima
   in preparation

(**List of Supplementary Publications**)

1. "Acid-Catalyzed Transannular Cyclization of 3a*H*-Cyclopentene [8] annulene-1,4-(5*H*,9a*H*)-diones and Some Proposed Mechanisms"
   Takuya Koizumi, Kenji Harada, Haruyasu Asahara, Eiko Mochizuki, Ken Kokubo and Takumi Oshima
   J. Org. Chem., **2005**, *70*, 8364–8371

Acknowledgement

The author would like to express his sincerest gratitude to Professor Takumi Oshima, Department of Applied Chemistry, Graduate School of Engineering, Osaka University, for his continuous guidance throughout this work.

The author is indebted to Associated professor Masashi Hamaguchi retired last year for his hearty encouragement.

The author also wishes to thanks to Dr. Ken Kokubo, Dr. Naohiko Ikuma, Dr. Takuya Koizumi and Mr. Taijiro Higashi for their helpful comments and suggestions.

The author also wishes to thank to Dr. Eiko Mochizuki and Dr. Nobuko Kanahisa for her performance of X-ray crystal structure analysis and valuable comments.

Moreover, the author grateful acknowledgement to Ms. Emi Kubo, Ms. Saki Miyamoto, Ms. Kyoko Togaya and Mr. Kohta Saito for their helpful collaboration in the course of experiments. Further, the author also wishes to thank all the members of the research group of Professor Takumi Oshima and for their hearty supports, helpful advises, and friendship.

Thanks are also due to Miss Kanako Mori and her family, and the author’s friend of ballroom dance club of Osaka University and many ballroom dancers, for their hearty supports and kind friendships.

Finally, the author is deeply grateful to his family for their continuous and heartfelt supports and encouragement.

Haruyasu Asahara